

2-9-2010

# Development of novel fluorescent sensors for the detection of functional and bio-interesting small molecules and metal ions

Wei Jiang

Follow this and additional works at: [https://digitalrepository.unm.edu/chem\\_etds](https://digitalrepository.unm.edu/chem_etds)

---

## Recommended Citation

Jiang, Wei. "Development of novel fluorescent sensors for the detection of functional and bio-interesting small molecules and metal ions." (2010). [https://digitalrepository.unm.edu/chem\\_etds/4](https://digitalrepository.unm.edu/chem_etds/4)

This Dissertation is brought to you for free and open access by the Electronic Theses and Dissertations at UNM Digital Repository. It has been accepted for inclusion in Chemistry ETDs by an authorized administrator of UNM Digital Repository. For more information, please contact [disc@unm.edu](mailto:disc@unm.edu).

Wei Jiang

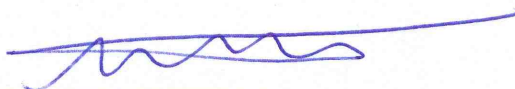
*Candidate*

Chemistry & Chemical Biology

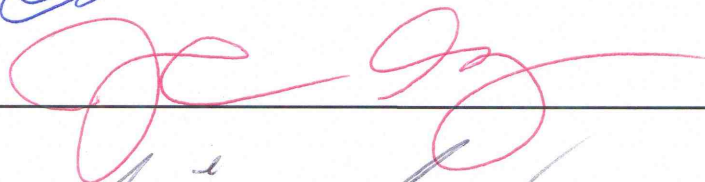
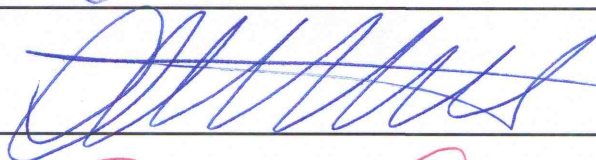
*Department*

This dissertation is approved, and it is acceptable in quality and form for publication:

*Approved by the Dissertation Committee:*



, Chairperson



**DEVELOPMENT OF NOVEL FLUORESCENT SENSORS FOR  
THE DETECTION OF FUNCTIONAL AND BIO-INTERESTING  
SMALL MOLECULES AND METAL IONS**

**BY**

**WEI JIANG**

B.S., Applied chemistry, Jilin University, 2002  
M.S., Polymer chemistry and physics, Jilin University, 2005

DISSERTATION

Submitted in Partial Fulfillment of the  
Requirements for the Degree of

**Doctor of Philosophy  
Chemistry**

The University of New Mexico  
Albuquerque, New Mexico

**December, 2009**

© 2009, Wei Jiang

## **DEDICATION**

To

My Parents, Fushun Jiang and Baomei Wang

And

My Wife, Fanny Lin

## ACKNOWLEDGEMENTS

My first thoughts in this section necessarily go to my advisor, Professor Wei Wang. I will never find the words to thank him for his guidance and support on me. His broad knowledge, ingenious creativity and diligence philosophy benefit me all the time and lead me onto a right road of doing research. His patience and exciting encouragement give me great confidence to finish my Ph.D. study. It's my fortune to have such an amazing experience of exploring chemistry with a truly capable "teacher".

Also, I owe big gratitude to all my committee members, Professor Patrick S. Mariano, Professor Changjian Feng and Professor John Grey for their precious time and patience in evaluating the manuscript and sent feedbacks with valuable suggestions.

Great gratitude goes to the ex-members in Wang's group. Since I joined the group as a rookie of organic chemistry, Dr. Jian Wang, Dr. Hao Li, Dr. Liansuo Zu and Dr. Hexin Xie gave me continuous help and useful advice both in experiments and my living. Even after they left, I still miss the memorable times we five guys sat along the fume hoods.

I would also like to collectively thank all the current group members for making our lab a great working environment. Dr. Shilei Zhang and Dr. Yinan Zhang are very experienced organic chemists and have strong ability of solving experimental problems. Xixi Song, Chenguan Yu, Xinshuai Zhang, Yuan Liu, Sihan Zhao and Yanteng Cao are all highly motivated and hard working. I wish them successes in the future.

Very, very special respect goes to the teammates of our soccer club, CSSC. Playing soccer with those nice guys on every Saturday has been an indispensable relaxation and gave me lots of fun. Min Wang, you are my best partner on the field. Lao Zhang, you are a respecting captain, a real soccer player.

Last and foremost I would like to thank my family for their endless and unconditional supports. My parents, Fushun Jiang and Baomei Wang, provided me a loving home when I were in China. Through my childhood they endow the deepest love and solicitude to me. When I suffered from difficulties and felt confused to my future, they always stood behind me and backed me up; when I made mistakes, they never blame me to my face but encourage me to make it up. My wife, Fanny Lin, is such a caring wife and bosom friend of me. How luck I were to meet her in my life! I enjoyed every wonderful meal she prepared and every humorous story she shared with me. She gives me the confidence of trying my best to build up our happy family.

**DEVELOPMENT OF NOVEL FLUORESCENT SENSORS FOR  
THE DETECTION OF FUNCTIONAL AND BIO-INTERESTING  
SMALL MOLECULES AND METAL IONS**

**BY**

**WEI JIANG**

ABSTRACT OF DISSERTATION

Submitted in Partial Fulfillment of the  
Requirements for the Degree of

**Doctor of Philosophy  
Chemistry**

The University of New Mexico  
Albuquerque, New Mexico

**December, 2009**



# **Development of Novel Fluorescent Sensors For the Detection and Specific Recognition of Small Molecules and Metal Ions**

By

**Wei Jiang**

B.S., Applied chemistry, Jilin University, 2002

M.S., Polymer chemistry and physics, Jilin University, 2005

Ph.D, Chemistry, University of New Mexico, 2009

## **ABSTRACT**

As one important kind of sensitive analytical technology, fluorescence method is widely applied in environmental science, materials, medicine pharmacy and nowadays much popularly in cellular biological science, which requires the development of diverse fluorescent sensors to meet various analytical and researching demands. During my Ph.D. study, my work focuses on the development of novel fluorescent sensors for the detection and specific recognition of functional and bio-interesting small molecules and metal ions, and the contents are described in this dissertation using three sections.

In the first part, novel fluorescent sensors for the specific recognition of bio-toxic thiophenols have been developed based on ICT and PET mechanism separately. These sensors were designed with an 2,4-dinitrobenzenesulfonamide as the recognition moiety and consequently are able to differentiate thiophenols from bio-active aliphatic thiols

such as cysteine in neutral aqueous solution due to their different  $pK_a$  values. Moreover, the sensor constructed on NBD fluorophore has a long-wavelength emission ( $> 500$  nm) and were employed as the first fluorescent sensor to detect selenocysteine, a special amine acid in body, without interference with other amino acids including similar cysteine.

In the second part, we have made our efforts on the detection of explosive peroxides and discovered a highly sensitive and selective fluorescent sensor for peroxy acids. This sensor took advantage of the ring-open mechanism so as to achieve complete “on-off” switch in the recognition process. Significant fluorescence signals were observed upon addition of peroxy acids while other peroxides and ROS couldn't make influence on the sensor.

In the third part, we turned our attention to the bio-interesting metal ions. A turn-on fluorescent sensor has been developed for the detection of bio-active  $Zn^{2+}$  with based on PET mechanism. This sensor is highly selective for  $Zn^{2+}$  and showed no response to numerous metal ions such as  $K^+$ ,  $Ca^{2+}$ ,  $Mg^{2+}$ ,  $Fe^{3+}$ ,  $Cu^{2+}$ ,  $Co^{2+}$ ,  $Cd^{2+}$ , etc. Moreover, we successfully designed an unprecedented chemodosimeter for the detection of highly toxic  $Hg^{2+}$  in the aqueous solution, which came from a unique  $Hg^{2+}$  facilitated desulfurization–lactonization cascade reaction by transforming a weakly fluorescent precursor to a highly fluorescent coumarin derivative.

## Table of Contents

Acknowledgements.....	v
Abstract.....	viii
Table of Contents.....	x
List of Abbreviations .....	xv
Table of Figures.....	xviii
List of Schemes.....	xxiii
<b>Chapter 1: Introduction .....</b>	<b>1</b>
1.1. Background.....	1
1.2. Key Concept for Fluorescent Sensors.....	2
1.2.1. Fluorescence and its generation.....	2
1.2.2. Effects of other de-excitation processes of excited molecules .....	5
1.2.3. Common features of fluorescent sensors.....	7
1.3. Design Principles of Fluorescent Sensors.....	9
1.3.1. Photoinduced electron transfer.....	9
1.3.2. Photoinduced charge transfer.....	11
1.3.3. Excimer and exciplex formation.....	14
1.3.4. Fluorescence resonance energy transfer.....	15
1.4. Commonly used organic dyes as Fluorophores.....	17
1.5. Summary .....	20
1.6. Reference .....	21

<b>Chapter 2: Development of Fluorescent Sensors for Thiols and Selenols</b> .....	26
2.1. Design of Fluorescent Sensor Based on NBD Fluorophore for the Discrimination of Thiophenols and Aliphatic Thiols.....	26
2.1.1. Background and significance.....	26
2.1.2. Design plan.....	29
2.1.3. Synthesis.....	32
2.1.4. Results and discussion.....	33
2.1.4.1. The sensitivity towards thiophenol and aliphatic cysteine.....	33
2.1.4.2. The specificity for thiophenols.....	36
2.1.4.3. The effect of pH on the fluorescence intensity and reactivity.....	38
2.1.5. Conclusion.....	39
2.2. Design of Fluorescent Sensor Based on PET Mechanism for the Discrimination of Thiophenols and Aliphatic Thiols.....	39
2.2.1. Design plan.....	39
2.2.2. Synthesis.....	41
2.2.3. Results and discussion.....	42
2.2.3.1. Dual functionality of DNS moiety.....	42
2.2.3.2 Sensitivity and selectivity.....	44
2.2.3.3. The effect of pH on the fluorescence intensity and reactivity.....	46
2.2.4. Conclusion.....	47
2.3. Fluorescent Sensor for Selenocysteine and Selenoproteins.....	47
2.3.1. Background and significance.....	47
2.3.2. Design plan.....	49

2.3.3. Results and discussion.....	51
2.3.3.1. The sensitivity towards selenocysteine.....	51
2.3.3.2. The specificity towards selenocysteine.....	53
2.3.4. Conclusion.....	54
2.4. Experimental Section.....	56
2.5. Reference.....	66
<b>Chapter 3: Development of Sensors for the Detection of Peroxy Acids: Easy Tools for Explosive Peroxides.....</b>	<b>72</b>
3.1. Introduction.....	72
3.2. Design Plan.....	74
3.3. Results and Discussion.....	76
3.3.1. Synthesis and confirmation of the configuration.....	76
3.3.2 Fluorescence response towards peroxides and ROS.....	78
3.3.3. Examination of sensitivity and reactivity.....	80
3.3.4. The effect of thiourea substituent group on the fluorescence intensity and reactivity.....	82
3.3.5. The effect of pH on the fluorescence intensity and reactivity.....	83
3.4. Summary.....	85
3.5. Experimental Section.....	86
3.6. References.....	91

## **Chapter 4: Development of Fluorescent Sensors for the Detection of Bio-interesting**

<b>Metal Ions</b> .....	95
4.1. Background and Significance.....	95
4.2. Development of Fluorescent Sensor for Zinc Ion.....	96
4.2.1. Introduction.....	96
4.2.2. Design Plan.....	99
4.2.3. Synthesis.....	101
4.2.4. Results and Discussion.....	102
4.2.4.1. Fluorescent properties and response towards Zn <sup>2+</sup> .....	102
4.2.4.2. Examination of selectivity.....	106
4.2.4.3. Kinetic analysis of the complex formation with Zn <sup>2+</sup> .....	107
4.2.5. Conclusion.....	108
4.3. Development of Fluorescent Sensor for Mercury Ion.....	108
4.3.1. Introduction.....	108
4.3.1.1. Sources of Mercury contamination and bioaccumulation.....	109
4.3.1.2. Consequences mercury toxicity for human health.....	111
4.3.1.3. Fluorescent detection of mercury.....	111
4.3.2. Research design.....	114
4.3.2.1. Design of first model.....	114
4.3.2.2. Problems and solutions.....	114
4.3.2.3. New designed model.....	115
4.3.3. Synthesis.....	117

4.3.4. Results and discussion.....	118
4.3.4.1. Fluorescent property and response towards Hg <sup>2+</sup> .....	118
4.3.4.2. Kinetic analysis.....	119
4.3.4.3. Examination of selectivity.....	121
4.3.4.4. The effect of pH on the stability and reactivity.....	122
4.3.5. Conclusion.....	123
4.4. Experiment Data.....	124
4.5. References.....	134

## List of Abbreviations

$[\alpha]_D$	specific rotation at wavelength of sodium D line
Ac	acetyl, acetate
Bn	benzyl
Boc	<i>t</i> -butoxycarbonyl
<i>n</i> BuLi	<i>n</i> -butyllithium
Bz	benzoyl
°C	degrees Celsius
calcd.	calculated
CAN	ceric ammonium nitrate
Cbz	benzyloxycarbonyl
CDCl <sub>3</sub>	deuterated chloroform
$\delta$	chemical shift
DMAP	4-dimethylaminopyridine
DME	dimethoxyethane
DMF	<i>N,N</i> -dimethylformamide
DMSO	dimethyl sulfoxide
D <sub>2</sub> O	deuterated water
dr	diastereomeric ratio
ee	enantiomeric excess
ESI	electrospray ionization
EtOAc	ethyl acetate



EtOH	ethanol
EWG	electron withdrawing group
g	gram(s)
h	hour(s)
HPLC	high performance liquid chromatography
HRMS	high resolution mass spectra
Hz	hertz
IR	infrared (spectroscopy)
<i>J</i>	coupling constant
$\lambda$	wavelength
lit.	literature
M	molar
<i>m</i>	meta
<i>m</i> CPBA	<i>meta</i> -Chloroperoxybenzoic acid
Me	methyl
MeCN	acetonitrile
mg	milligram(s)
MHz	megahertz
min	minute(s)
mL	milliliter
mmol	millimole
mp	melting point
MsCl	methanesulfonyl Chloride

NBS	<i>N</i> -bromosuccinimide
NMR	nuclear magnetic resonance
<i>p</i>	para
PCC	pyridinium chlorochromate
Pd	palladium
Ph	phenyl
PMP	4-methoxyphenyl
ppm	parts per million
<i>i</i> -PrOH	isopropyl alcohol
rac	racemic
rt	room temperature
TEA	triethylamine
TFA	trifluoroacetic acid
TFAA	trifluoroacetic anhydride
THF	tetrahydrofuran
TLC	thin layer chromatography
TMEDA	<i>N,N,N',N'</i> -tetramethylethylenediamine
TMG	1,1,3,3-tetramethylguanidine
TMS	trimethylsilyl
TS	Transition State
TsOH	<i>p</i> -toluenesulfonic acid
μL	microliter

## List of Figures

<b>Chapter 1: Introduction</b> .....	1
<b>Figure 1.1</b> Jablonski Diagram .....	3
<b>Figure 1.2.</b> Possible de-excitation pathways of excited molecules.....	6
<b>Figure 1.3.</b> Various parameters influencing the emission of fluorescence.....	7
<b>Figure 1.4.</b> Operating principle of analyte-responsive auxochrome–spacer–receptor systems.....	8
<b>Figure 1.5.</b> PET mechanism: (a) reductive PET; (b) oxidative PET.....	10
<b>Figure 1.6.</b> Examples of electron donors and acceptors in excited states.....	11
<b>Figure 1.7.</b> Schematic drawing of sensors based on PET mechanism.....	12
<b>Figure 1.8.</b> PCT mechanism and sensor examples: (a) analyte interact with the donor group; (b) analyte interact with acceptor group.....	13
<b>Figure 1.9.</b> Schematic drawing of sensor based on excimer/exciple formation....	15
<b>Figure 1.10.</b> FRET mechanism.....	16
<b>Figure 1.11.</b> A FRET sensor for Hg <sup>2+</sup> .....	17
<b>Figure 1.12.</b> Schematic drawing of commonly used heterocyclic dyes.....	19
<b>Chapter 2: Development of Fluorescent Sensors for Thiols and Selenols</b> .....	26
<b>Figure 2.1.</b> Schematic drawing of common thiols.....	27
<b>Figure 2.2.</b> Zhu’s sensor for thiols based on HTM quenching mechanism.....	27
<b>Figure 2.3.</b> Reduction of the <b>DSSA<sub>AI</sub></b> probe by various thiols.....	28
<b>Figure 2.4.</b> pH dependent behavior of <b>DSSA</b> .....	28

<b>Figure 2.5.</b> Change of fluorescence properties of NBD induced by 4-substituents.	31
<b>Figure 2.6.</b> Proposed mechanism for sensor <b>1</b> .	32
<b>Figure 2.7.</b> Emission time profile of sensor <b>1</b> towards thiophenol.	34
<b>Figure 2.8.</b> Effect of thiophenol concentration on the absorption and fluorescence emission of sensor <b>1</b> .	35
<b>Figure 2.9.</b> Emission time profile of sensor <b>1</b> towards cysteine.	36
<b>Figure 2.10.</b> The selectivity of sensor <b>1</b> towards thiols and other nucleophiles.	37
<b>Figure 2.11.</b> Effect of pH on the fluorescence response of sensor <b>1</b> ( $2 \times 10^{-5}$ M) towards thiophenol at $\lambda_{\text{ex}} = 465$ nm and $\lambda_{\text{em}} = 555$ nm.	38
<b>Figure 2.12.</b> Proposed mechanism for sensor <b>3</b> .	41
<b>Figure 2.13.</b> Emission time profile of sensor <b>3</b> towards thiophenol.	43
<b>Figure 2.14.</b> Structure and fluorescence response of the benzoxazole derivative <b>3'</b> towards thiophenol.	44
<b>Figure 2.15.</b> Effect of thiophenol concentration on the fluorescence emission of sensor <b>3</b> .	45
<b>Figure 2.16.</b> Fluorescence response of 2 $\mu\text{M}$ sensor <b>3</b> towards various nucleophilic reagents.	46
<b>Figure 2.17.</b> Effect of pH on the fluorescence response of probe <b>3</b> (2 $\mu\text{M}$ ) towards thiophenol.	47
<b>Figure 2.18.</b> Proposed mechanism of sensor <b>1</b> for the detection of selenocysteine.	51
<b>Figure 2.19.</b> Emission time profile of sensor <b>1</b> towards selenocysteine.	52
<b>Figure 2.20.</b> Fluorescence response of the sensor <b>1</b> ( $2 \times 10^{-5}$ M) towards selenolcysteine generated from (CysSe) <sub>2</sub> and dithiothreitol (DTT).	53

<b>Figure 2.21.</b> The selectivity of sensor <b>1</b> towards SeCys and bio-thiols.....	54
<b>Figure 2.22.</b> Effect of DTT on the fluorescent response of sensor <b>1</b> towards selenocysteine.....	64
<b>Chapter 3: Development of Sensors for the Detection of Peroxy Acids: Easy Tools for Explosive Peroxides.....</b>	<b>72</b>
<b>Figure 3.1.</b> Photographs of (a) Spain bombings in 2004, and (b) London bombings in 2005.....	72
<b>Figure 3.2.</b> Sensor for the detection of BPO and PAA.....	75
<b>Figure 3.3.</b> Proposed mechanism for sensor <b>1a</b> .....	76
<b>Figure 3.4.</b> X-ray crystal structure of compound <b>1a</b> .....	77
<b>Figure 3.5.</b> Selectivity of probe <b>1a</b> towards various peroxides in H <sub>2</sub> O.....	79
<b>Figure 3.6.</b> Selectivity of probe <b>1a</b> toward various peroxides in methanol.....	80
<b>Figure 3.7.</b> Fluorescence excitation ( $\lambda_{em} = 550$ nm) and emission ( $\lambda_{ex} = 530$ nm) response of 1 $\mu$ M sensor <b>1a</b> towards various concentration of <i>m</i> CPBA.....	81
<b>Figure 3.8.</b> Proposed structure of final product <b>3</b> .....	81
<b>Figure 3.9.</b> Reactivity of probe <b>1a, 1b, 1c</b> (final 1 $\mu$ M) towards <i>m</i> CPBA.....	82
<b>Figure 3.10.</b> Reactivity of probe <b>1d</b> (final 1 $\mu$ M) towards for <i>m</i> CPBA.....	83
<b>Figure 3.11.</b> Effect of pH on the fluorescence response of probe <b>1a</b> (1 $\mu$ M) towards towards <i>m</i> CPBA.....	84
<b>Chapter 4: Development of Fluorescent Sensors for the Detection of Bio-interesting Metal Ions.....</b>	<b>95</b>

<b>Figure 4.1.</b> Schematic drawing of quinoline-based sensors.....	97
<b>Figure 4.2.</b> Schematic drawing of fluorescein-based sensors developed by Lippard's group.....	98
<b>Figure 4.3.</b> Design of Zn <sup>2+</sup> sensor <b>1</b> and <b>2</b> .....	100
<b>Figure 4.4.</b> Effect of Zn <sup>2+</sup> concentration on the fluorescence of sensor <b>1</b> .....	102
<b>Figure 4.5.</b> Emission spectra ( $\lambda_{\text{ex}} = 470 \text{ nm}$ ) of sensor <b>1</b> in a range concentration of $0-1.4 \times 10^{-5} \text{ M}$ after addition of the same amounts of Zn <sup>2+</sup> at room temperature in phosphate buffer (pH 7.3).....	103
<b>Figure 4.6.</b> Plot of the concentration of Zn <sup>2+</sup> vs. $\Delta I$ .....	103
<b>Figure 4.7.</b> Effect of Zn <sup>2+</sup> concentration on the absorption of sensor <b>1</b> .....	104
<b>Figure 4.8.</b> Proposed binding model of <b>1</b> with Zn <sup>2+</sup> .....	105
<b>Figure 4.9.</b> Fluorescence response of sensor <b>2</b> towards Zn <sup>2+</sup> .....	105
<b>Figure 4.10.</b> The selectivity of sensor <b>1</b> towards various metal ions.....	106
<b>Figure 4.11.</b> Job's plot of <b>1</b> and Zn <sup>2+</sup> .....	107
<b>Figure 4.12.</b> Amount of atmospheric mercury deposited at Wyoming's Upper Fremont Glacier over the last 270 years.....	109
<b>Figure 4.13.</b> Examples of fluorescent sensors for Hg <sup>2+</sup> based on ligand binding..	113
<b>Figure 4.14.</b> Examples of fluorescent sensors for Hg <sup>2+</sup> based on other principles..	113
<b>Figure 4.15.</b> Design principle of sensor <b>6</b> for Hg <sup>2+</sup> .....	114
<b>Figure 4.16.</b> Design of Hg <sup>2+</sup> facilitated facile desulfurization–actonization fluorescent chemodosimeter.....	116
<b>Figure 4.17.</b> Fluorescence response ( $\lambda_{\text{ex}} = 430 \text{ nm}$ ) and plot (emission collected at $480 \text{ nm}$ ) of the $5 \mu\text{M}$ sensor <b>7</b> towards Hg <sup>2+</sup> .....	119

<b>Figure 4.18.</b> Reaction time profile of sensor <b>7</b> (5 $\mu\text{M}$ , $\lambda_{\text{ex}} = 430 \text{ nm}$ ) towards $\text{Hg}^{2+}$ (2.5 $\mu\text{M}$ ) in pH 6.0 phosphate buffer (I = 0.05 M).....	120
<b>Figure 4.19.</b> UV response of the 5 $\mu\text{M}$ sensor <b>7</b> towards $\text{Hg}^{2+}$ .....	120
<b>Figure 4.20.</b> Job's plot of sensor <b>7</b> and $\text{Hg}^{2+}$ .....	121
<b>Figure 4.21.</b> Fluorescence response of the 5 $\mu\text{M}$ sensor <b>7</b> upon addition of $\text{Hg}^{2+}$ (5 $\mu\text{M}$ ) and various other metal cations (10 $\mu\text{M}$ each).....	122
<b>Figure 4.22.</b> Effect of pH on the stability of sensor <b>7</b> (5 $\mu\text{M}$ ) and its fluorescence response on $\text{Hg}^{2+}$ .....	123

## List of Schemes

<b>Chapter 1: Introduction</b> .....	1
<b>Scheme 1.1.</b> Quantum yield and lifetime of some aromatic hydrocabons .....	5
<b>Scheme 1.2.</b> Examples of commonly used orgnic dyes.....	18
<b>Chapter 2: Development of Fluorescent Sensors for Thiols and Selenols</b> .....	26
<b>Scheme 2.1.</b> Cleavage of 2,4-dinitrobenzenesulfonamide by a thiol.....	30
<b>Scheme 2.2.</b> Synthesis of sensor <b>1</b> .....	33
<b>Scheme 2.3.</b> Synthesis of Sensor <b>3</b> .....	42
<b>Scheme 2.4.</b> Some reactions catalyzed by selenocysteine-containing enzymes.....	48
<b>Scheme 2.5.</b> Generation of selenocysteine from (CysSe) <sub>2</sub> .....	51
<b>Chapter 3: Development of Sensors for the Detection of Peroxy Acids: Easy Tools for Explosive Peroxides</b> .....	72
<b>Scheme 3.1.</b> Synthesis of sensor <b>1a</b> .....	76
<b>Chapter 4: Development of Fluorescent Sensors for the Detection of Bio-interesting Metal Ions</b> .....	95
<b>Scheme 4.1.</b> Synthesis of (a) sensor <b>1</b> , and (b) sensor <b>2</b> .....	101
<b>Scheme 4.2.</b> Synthesis of sensor <b>7</b> .....	117



# Chapter 1

## Introduction

### 1.1 Background

Ubiquitous recognition and interaction events and processes in chemistry, biology, material and environmental science generally occur at molecular levels. We can not feel them, or even see and smell them. In order to study these important events and control the process, researchers need to readily transform the information into detectable signals. An effective method is monitoring the change in “light” signal, such as highly sensitive fluorescence.<sup>1-8</sup> Fluorescent sensors are built on the basis of “call-and-response” since their signals can be switched between two distinguishable states by environmental stimuli. Moreover, by careful design, it can selectively bind with analyte of interest over other potential interfering candidates, cause the change in one or more properties of the system such as redox potentials, absorption, fluorescence excitation and emission intensity and/or wavelength, etc. The advantages of molecular fluorescence or luminescence for sensing and switching can be summarized<sup>7,8</sup> as high sensitivity of detection down to single molecules,<sup>9-14</sup> “on-off” switchability, feasibility of human-molecule communication, subnanometer spatial resolution with submicron visualization<sup>15-19</sup> and submillisecond temporal resolution<sup>20</sup> etc.

In spite of important advantages and intensive interests in fluorescent sensors, the field with systematic investigation started on the synthesis of metal ions receptors

only after the development of the supramolecular chemistry by the pioneering works of Pedersen, Cram and Lehn, etc.<sup>21</sup> At the same time, the advancement of photochemistry afforded the basis for designing systems in which changes in absorbance and/or fluorescence bands could signal analyte complexation. Since then significant progress has been made for the rational design of fluorescent indicators.<sup>22-26</sup> In recent years, accompanied with the flourishing booms and demand of biological and life science, great efforts have gone into the development of fluorescence sensors for the imaging of bio-interesting molecules and metal ions with highly selective and sensitive, even high-speed spatial analysis of cells.<sup>27</sup> Progress in instrumentation has considerably improved the sensitivity of fluorescence detection. Advanced fluorescence microscopy techniques allow detection at single molecule level, which opens up new opportunities for the development of fluorescence-based methods or assays in material sciences, environmental science, biotechnology and the pharmaceutical industry. Thus, researchers have been dedicated to this field and explored a vast number of fluorescent probes<sup>28-32</sup> for various targeting molecules and ions with broad emission wavelengths, functionality, working concentration and pH range as tools to meet diversified detection aims in different kinds of scientific research areas.

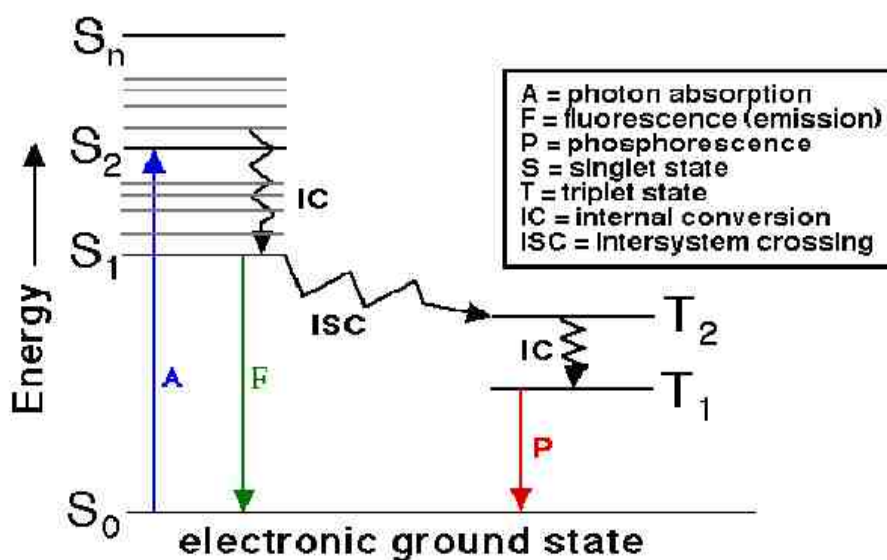
## **1.2. Key Concepts for Fluorescent Sensors**

### **1.2.1. Fluorescence and its generation (Joblonski diagram).**

Once a molecule has absorbed energy in the form of electromagnetic radiation, it

jumps from the ground state to the singlet excited state. Then there are many ways by which it can return to the ground state (the statistically most common energy state for room temperature chemical species). With respect to fluorescence, if the photon emission occurs between states of the same spin state (e.g. from  $S_1$  to  $S_0$ ), this is termed “fluorescence”. If the spin state of the initial and final energy levels are different (e.g. from  $T_1$  to  $S_0$ ), the emission is called “phosphorescence” (Figure 1.1).

**Figure 1.1.** Jablonski diagram.



Fluorescence emission:  $S_1 \rightarrow S_0 + h\nu$ , here  $h\nu$  is a generic term for photon energy with  $h =$  Planck's constant and  $\nu =$  frequency of light. (The specific frequencies of exciting and emitted light are dependent on the particular system). State  $S_0$  is called the ground state of the fluorophore (fluorescent molecule) and  $S_1$  is its first (electronically) excited state. The “Stokes shift” ( $h\nu_{ex} - h\nu_{em}$ ) is the gap


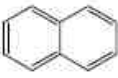
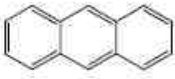
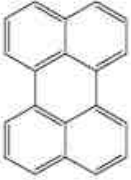


between the maximum of the first absorption band and the maximum of the fluorescence emission spectrum (expressed in wave numbers). The fluorescence “lifetime” refers to the average time the molecule stays in its excited state before emitting a photon.

The fluorescence “quantum yield” gives the efficiency of the fluorescence process. It is the fraction of excited molecules that return to the ground state  $S_0$  with emission of fluorescence photons. In other words, the fluorescence quantum yield is the ratio of the number of emitted photons (over the whole duration of the decay) to the number of absorbed photons. The measurement of “absolute” quantum yield is critical and requires special equipment.<sup>33</sup> However, for routine work one is often satisfied with determining the “relative” quantum yields. The fluorescence efficiency of an unknown molecule is then related to that of a standard by the equation:

$$\Phi_{F(X)} = (A_s / A_x) (F_x / F_s) (n_x / n_s)^2 \Phi_{F(S)}$$

Where  $\Phi_F$  is the fluorescence quantum yield,  $A$  is the absorbance at the excitation wavelength,  $F$  is the area under the corrected emission curve (expressed in number of photons) and  $n$  is the refractive index of the solvents used. Subscripts  $s$  and  $x$  refer to the standard and the unknown molecules respectively. Scheme 1.1 introduces the quantum yield and lifetime of some aromatic hydrocabons. The maximum fluorescence quantum yield is 1.0 (100%); every photon absorbed results in a photon emitted. Compounds with quantum yields of 0.01 are still considered quite fluorescent.

**Scheme 1.1.** Quantum yield and lifetime of some aromatic hydrocabons.

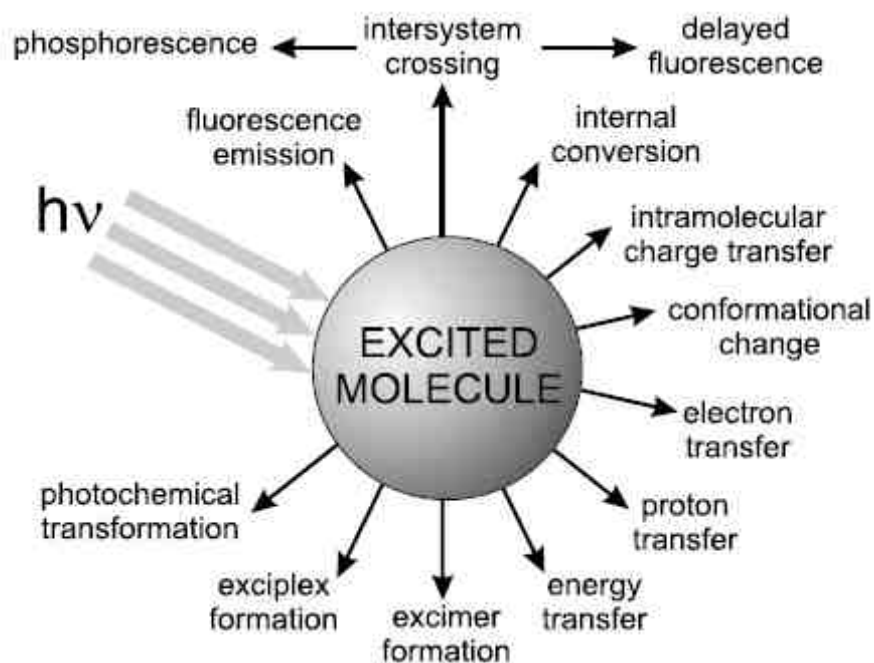
<i>Compound</i>	<i>Formula</i>	<i>Solvent (temp.)</i>	$\Phi_F$	$\tau_S$ (ns)
Benzene		Ethanol (293 K) EPA <sup>a)</sup> (77 K)	0.04	31
Naphthalene		Ethanol (293 K) Cyclohexane (293 K) EPA (77 K)	0.21 0.19	2.7 96
Anthracene		Ethanol (293 K) Cyclohexane (293 K) EPA (77 K)	0.27 0.30	5.1 5.24
Perylene		n-Hexane Cyclohexane (293 K)	0.98 0.78	6
Pyrene		Ethanol (293 K) Cyclohexane (293 K)	0.65 0.65	410 450
Phenanthrene		Ethanol (293 K) n-Heptane (293 K) EPA (77 K) Polymer film	0.13 0.16 0.12	0.60

### 1.2.2. Fluorescence and other de-excitation processes of excited molecules

Once a molecule is excited by absorption of a photon, it can return to the ground state with emission of fluorescence, but many other pathways for de-excitation are also possible (Figure 1.2): internal conversion (IC, i.e. direct return to the ground state without emission of fluorescence), intersystem crossing (ISC, possibly followed by emission of phosphorescence), intramolecular charge transfer and conformational change. Interactions in the excited state with other molecules may also compete with de-excitation: electron transfer, proton transfer, energy transfer, excimer or exciplex

formation.

**Figure 1.2.** Possible de-excitation pathways of excited molecules.



These de-excitation pathways may compete with fluorescence emission if they take place on a time-scale comparable with the average time (lifetime) during which the molecules stay in the excited state. This average time represents the experimental time window for observation of dynamic processes. The characteristics of fluorescence (spectrum, quantum yield, life time), which are affected by any excited state process involving interactions of the excited molecule with its close environment, can then provide information on such a microenvironment. It should be noted that some excited-state processes (conformational change, electron transfer, proton transfer, energy transfer, excimer or exciplex formation) may lead to a fluorescent species whose emission can superimpose that of the initially excited molecule. Such

an emission should be distinguished from the ‘primary’ fluorescence arising from the excited molecule.

The success of fluorescence as an investigative tool in studying the structure and dynamics of matter or living systems arises from the high sensitivity of fluorometric techniques, the specificity of fluorescence characteristics due to the microenvironment of the emitting molecule, and the ability of the latter to provide spatial and temporal information. Figure 1.3 showed the physical and chemical parameters that characterize the microenvironment and can thus affect the fluorescence characteristics of a molecule.

**Figure 1.3.** Various parameters influencing the emission of fluorescence.

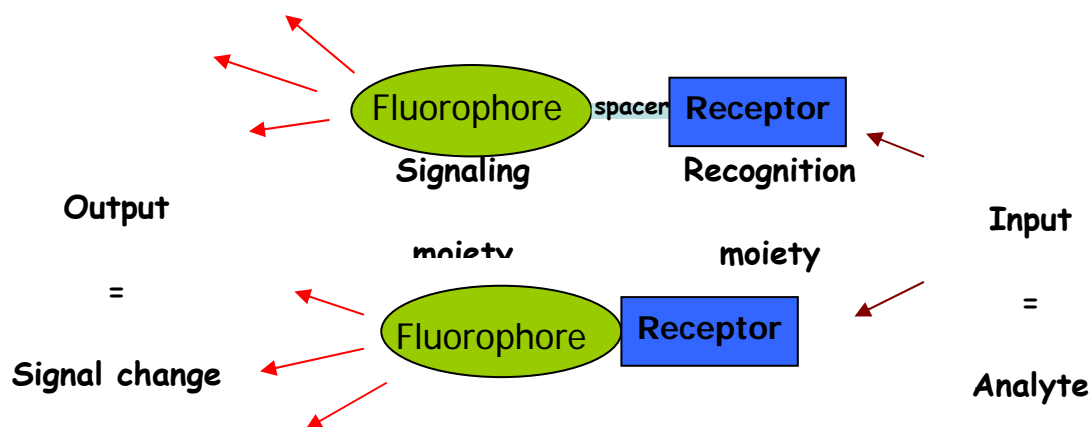


### 1.2.3. Common Features of Fluorescent Sensors

As a consequence of the strong influence of the surrounding medium on

fluorescence emission, fluorescent molecules are currently used as sensors for the investigation of physicochemical, biochemical and biological systems. Supramolecular chemistry and molecular recognition chemistry are at the heart of tailor-making or optimizing the chemical selectivity and sensitivity of fluorescent molecular sensing devices. Besides that, the tuning of the signaling features is predominantly connected to dye architecture and photophysics. To be able to control and tune both properties as independently as possible, a composite constitution of the reporter molecule is chosen in most cases.<sup>34-36</sup>

**Figure 1.4.** Operating principle of analyte-responsive auxochrome–spacer–receptor systems.



As is schematically depicted in Figure 1.4, the common molecular fluorescent probe consists of an auxochrome as the key component for generating the fluorescence signal (also called signaling moiety or fluorophore) and an analyte-responsive receptor (recognition moiety), both of which are linked by a spacer. Depending on the underlying photophysical mechanism, the spacer can be saturated to



disconnect the electron systems of chromophore and binding unit or unsaturated to couple these electronic subsystems. In the design of such sensors, attention should be paid to both recognition and signaling moieties. The recognition event, which takes place at the receptor moiety and accordingly perturb its topology and characters, is transduced through spacer to the signaling moiety and consequently affects its photophysical characteristics.

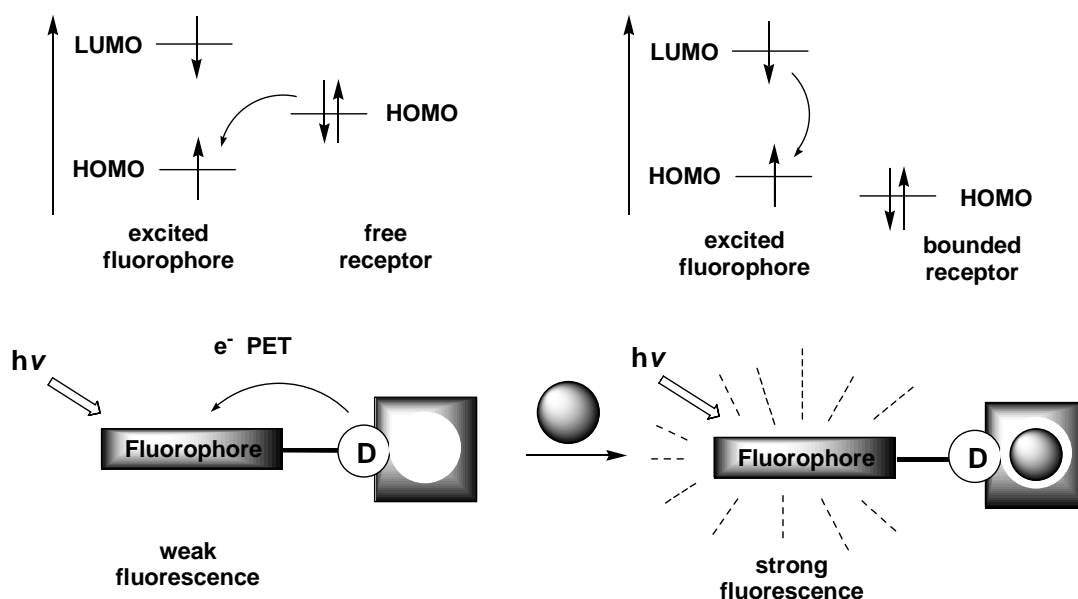
### **1.3. Design Principles of Fluorescent Sensors**

#### **1.3.1. Photoinduced Electron Transfer.**

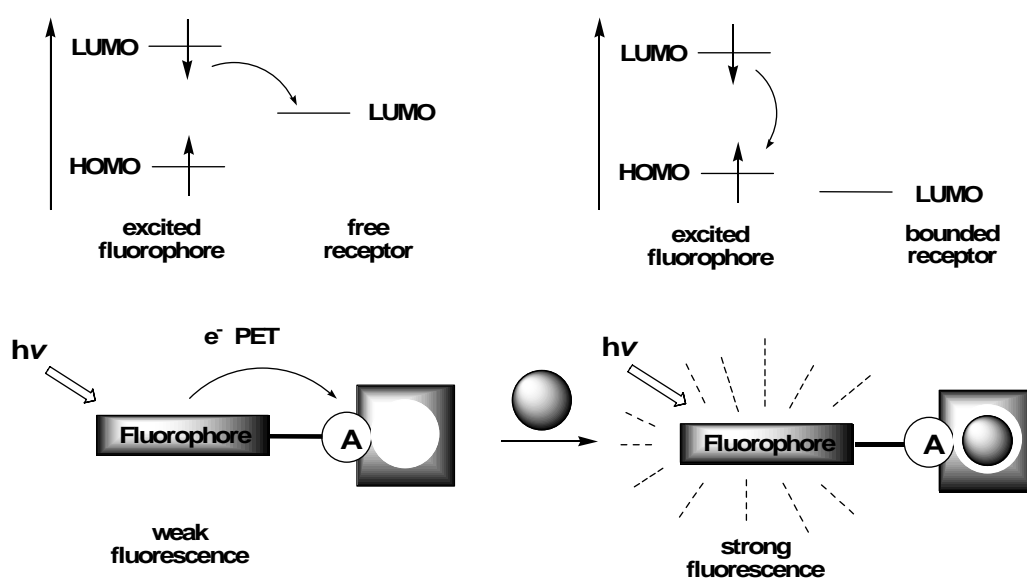
Photoinduced electron transfer (PET) process based on frontier orbital theory is most extensively employed in the design of fluorescent probes for the analyte recognition. In this case, the binding unit (receptor) and the signaling unit (fluorophore) are usually separated by a short spacer or perpendicular to each other, electronically disconnecting the p electron systems of receptor and fluorophore (Figure 1.5). Normally, when a free fluorophore is exposed to a light of certain frequency, an electron is promoted from HOMO to LUMO, and the subsequent decay back to HOMO produces fluorescence emission. However, the existence of “quencher” is able to disturb this sequent process. According to the electronic characteristics of the quencher, ET process can be divided into two types: reductive electron transfer and oxidative electron transfer process. In the unbounded state, after excitation, a fast electron transfer (from the HOMO of reductive quencher to the LUMO of fluorophore or from the LUMO of fluorophore to the LUMO of oxidative

quencher) will quench the fluorescence of the system. However, analyte binding at the receptor moiety modulates the redox potential of the quencher and slows down (or completely ‘switches off’) the ET process so as to revive fluorescence emission. Representative examples of donor and acceptor molecules are given in Figure 1.6.

**Figure 1.5.** PET mechanism: (a) reductive PET; (b) oxidative PET.

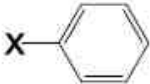



(a) Reductive PET.



(b) Oxidative PET

**Figure 1.6.** Examples of electron donors and acceptors in excited states.

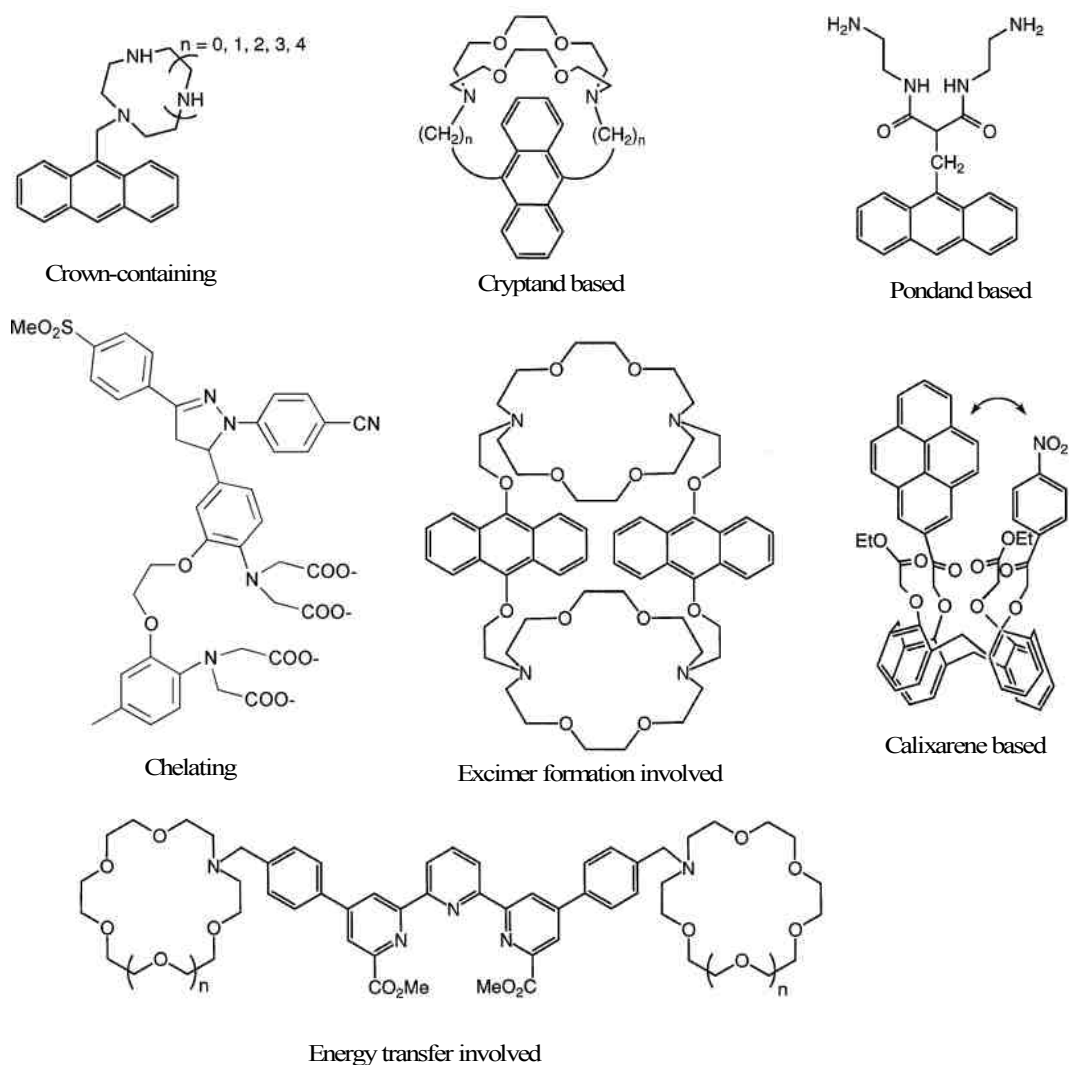
electron donors D*	electron acceptors A*
 <p>X = H-, (CH<sub>3</sub>)<sub>2</sub>N-, CH<sub>3</sub>-O-, HS- naphthalene, anthracene, phenanthrene, pyrene, perylene</p>	 <p>Y = -C≡N, -C(=O)-R, -N=O 9,10-dicyanoanthracene</p>

Typically, there are many fluorescent sensors for the detection of metal ions designed based on PET mechanism called fluoroionophores. The recognition moiety (ionophore) is linked to the fluorophore via a spacer. Ionophore moiety is responsible for the selective binding with metal ions give rise to the changes in fluorescence characteristics of the fluorophore moiety upon binding (Figure 1.7).<sup>37</sup>

### 1.3.2. Photoinduced Charge Transfer.

When a fluorophore contains an electron-donating group (often an amino group) conjugated to an electron-withdrawing group, it undergoes intramolecular charge transfer from the donor to the acceptor upon excitation by light. The consequent change in dipole moment results in a Stokes shift that depends on the microenvironment of the fluorophore. It can thus be anticipated that analytes in close interaction with the donor or the acceptor moiety will change the photophysical properties of the fluorophore by affecting the efficiency of intramolecular charge transfer.<sup>38</sup>

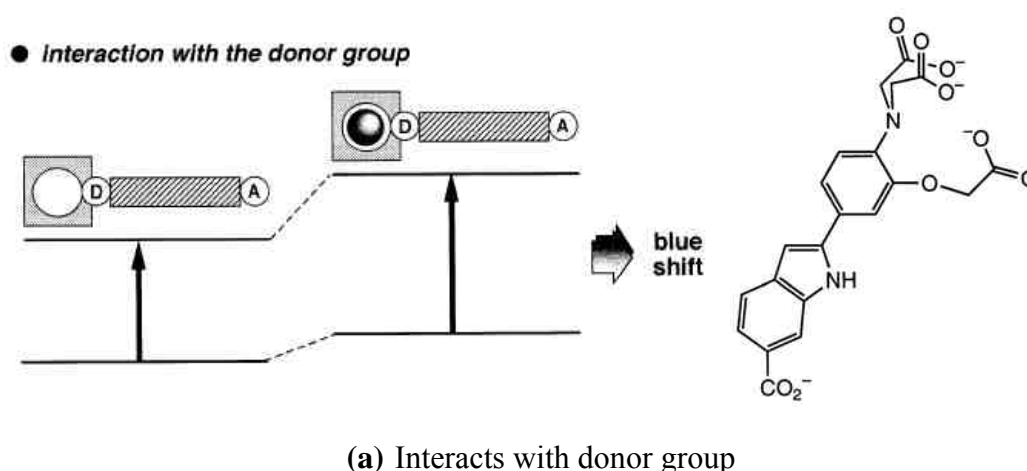
**Figure 1.7.** Schematic drawing of ion sensors based on PET mechanism.

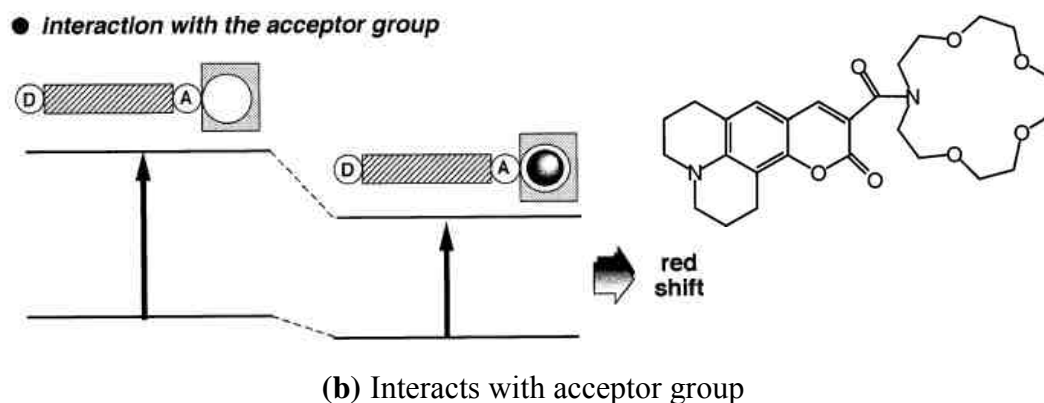


When a group (like an amino group) playing the role of an electron donor within the fluorophore interacts with an analyte, the latter reduces the electron-donating character of this group; owing to the resulting reduction of conjugation, a blue shift of the absorption spectrum is expected together with a decrease of the extinction coefficient. Conversely, an analyte interacting with the acceptor group enhances the electron-withdrawing character of this group; the absorption spectrum is thus red-shifted and the molar absorption coefficient is increased. The fluorescence spectra

in principle shift in the same direction as those of the absorption spectra. In addition to these shifts, changes in quantum yields and lifetimes are often observed. All these photophysical effects are obviously dependent on the characteristics of the analytes, and selectivity of these effects is expected. The photophysical changes upon analytes binding can also be described in terms of charge dipole interaction. Let us consider only the case where the dipole moment in the excited state is larger than that in the ground state. Then, when the analyte interacts with the donor group, the excited state is more strongly destabilized by the cation than the ground state, and a blue shift of the absorption and emission spectra is expected (however the fluorescence spectrum undergoes only a slight blue shift in most cases). Conversely, when the analyte interacts with the acceptor group, the excited state is more stabilized by the cation than the ground state, and this leads to a red shift of the absorption and emission spectra (Figure 1.8).<sup>39</sup>

**Figure 1.8.** PCT mechanism and sensor examples: (a) an analyte interacts with the donor group; (b) an analyte interacts with acceptor group.





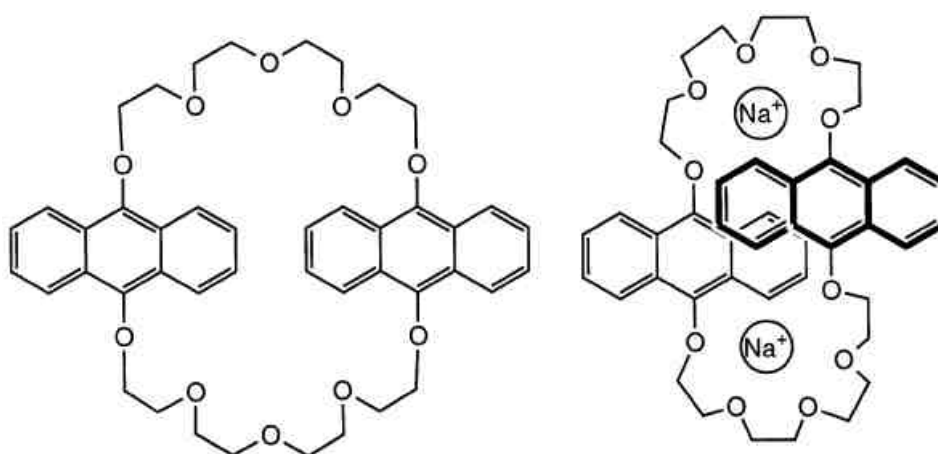
### 1.3.3. Excimer and Exciplex Formation.

Several fluorophores like anthracene and pyrene can form excimer (excited dimer) when an excited molecule can come in close approach to another one during the lifetime of the excited state. Dual fluorescence is then observed with a monomer band and, at longer wavelengths, a structureless broad band due to excimer formation. The ratio of the fluorescence intensities corresponds to monomer and excimer emission on molecular mobility and ‘microviscosity’. When a fluorescent probe contains two fluorophores whose mutual distance is affected by analyte (usually metal cation) complexation, recognition of this analyte can be monitored by the monomer/excimer fluorescence–intensity ratio.<sup>40</sup> Cation binding may favor or hinder excimer formation. In any case, such a ratiometric method allowing self-calibration measurement is of great interest for practical applications.

For example, the bisanthracene-crown ether exhibits a fluorescence spectrum composed of the characteristic monomer and excimer bands (Figure 1.9). It was demonstrated to form a 1:2 complex with  $\text{Na}^+$  in MeOH and  $\text{CH}_3\text{CN}$  with a positive cooperative effect. Gradual addition of sodium perchlorate to the solution induces a

decrease in the monomer band and an increase in the excimer band. Complexation is indeed expected to bring closer together the two anthracene units which favors excimer formation.

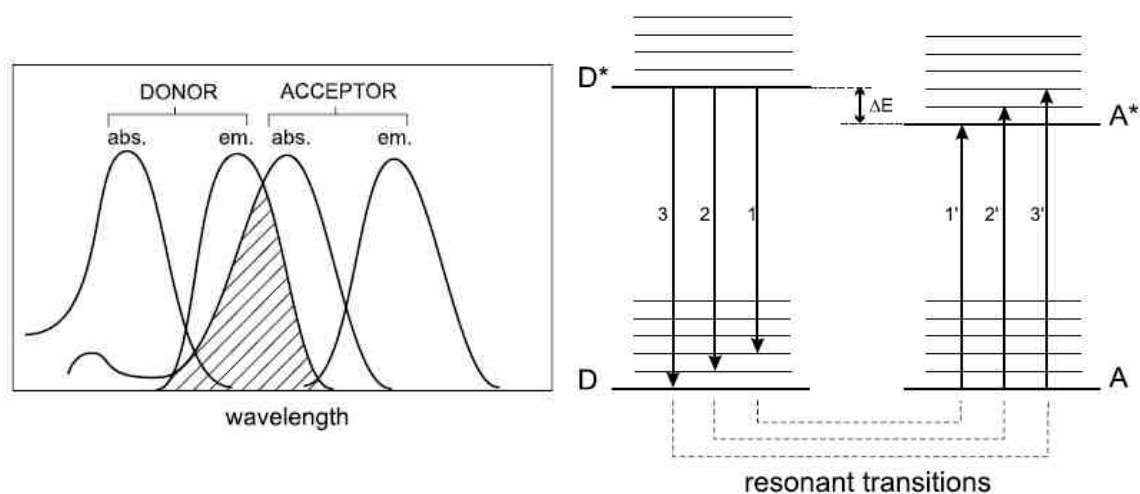
**Figure 1.9.** Schematic drawing of sensor based on excimer/exciplep formation.



#### 1.3.4. Fluorescence Resonance Energy Transfer.

Non-radiative transfer of excitation energy requires some interaction between a donor molecule and an acceptor molecule, and it can occur if the emission spectrum of the donor overlaps the absorption spectrum of the acceptor, so that several vibronic transitions in the donor have practically the same energy as the corresponding transitions in the acceptor. Such transitions are dipole-dipole coupled (see Figure 1.10) in resonance. This mechanism is termed "Förster resonance energy transfer" (FRET). When both chromophores are fluorescent, the term "fluorescence resonance energy transfer" is often used instead, although the energy is not actually transferred by fluorescence.<sup>41</sup>

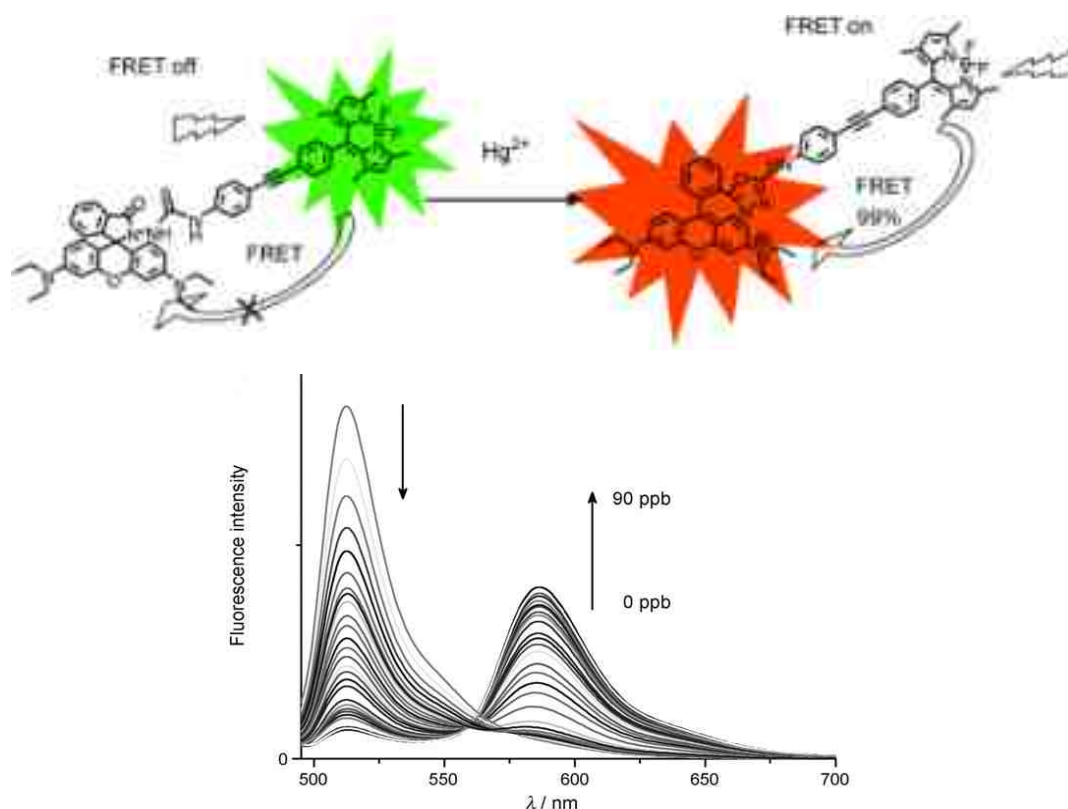
**Figure 1.10.** FRET mechanism.



A typical example is like the FRET fluorescent probe for  $\text{Hg}^{2+}$  developed by Qian's group in 2008 (Figure 1.11).<sup>42</sup> In this probe, a leuco-rhodamine derivative was chosen as a sensitive and selective chemosensor for  $\text{Hg}^{2+}$  ions since the highly efficient ring-opening reaction induced by  $\text{Hg}^{2+}$  generates the long-wavelength rhodamine fluorophore which can act as the energy acceptor. BODIPY was chosen as the energy donor because its intense fluorescence is insensitive to environmental factors and its fluorescence spectrum matches well with the absorption spectrum of rhodamine. As the result, an  $\text{Hg}^{2+}$ -induced process can change the emission maximum of the system from 514 nm (the characteristic peak of BODIPY) to 589 nm (the characteristic peak of rhodamine).



**Figure 1.11.** A FRET sensor for  $\text{Hg}^{2+}$ .



#### 1.4. Commonly Used Organic Dyes as Fluorophores

As we know, fluorescence detections have been used in a wide range of studies on various analytes relate to chemical, biological and material science. The number of established fluorescent probes is large, and there are also many newer systems available. Therefore, there is a strong need for fluorophores that can meet particular applications. Nowadays, commonly used organic dyes including compounds with emission from the ultraviolet to the near-infrared in the electromagnetic spectrum were synthesized, and even more candidates have been or could be developed and modified to improve their characters such as water solubility, quantum yield and emission wavelength, etc (Scheme 1.2).

**Scheme 1.2.** Examples of commonly used organic dyes.

<b>Probe</b>	<b>Ex (nm)</b>	<b>Em (nm)</b>	<b>Notes</b>
Hydroxycoumarin	325	386	Succinimidyl ester
Aminocoumarin	350	445	Succinimidyl ester
Methoxycoumarin	360	410	Succinimidyl ester
Cascade Blue	(375);401	423	Hydrazide
Pacific Blue	403	455	Maleimide
Pacific Orange	403	551	
Lucifer yellow	425	528	
NBD	466	539	NBD-X
R-Phycoerythrin (PE)	480;565	578	
PE-Cy5 conjugates	480;565;650	670	aka Cychrome, R670, Tri-Color, Quantum Red
PE-Cy7 conjugates	480;565;743	767	
Red 613	480;565	613	PE-Texas Red
PerCP	490	675	Peridinin chlorophyll protein
TruRed	490,675	695	PerCP-Cy5.5 conjugate
FluorX	494	520	(GE Healthcare)
Fluorescein	495	519	FITC; pH sensitive
BODIPY-FL	503	512	
TRITC	547	572	TRITC
X-Rhodamine	570	576	XRITC
Lissamine Rhodamine B	570	590	
Texas Red	589	615	Sulfonyl chloride
Allophycocyanin (APC)	650	660	
APC-Cy7 conjugates	650;755	767	PharRed

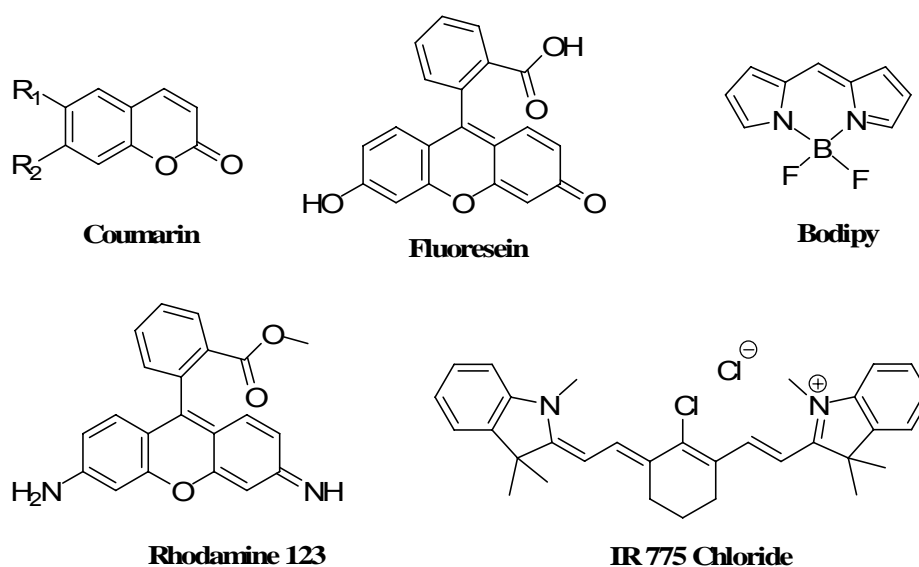
In spite of the diversity of organic dyes, they can be classified into two categories.

The first class is polyaromatic hydrocarbons (eg. anthracene and pyrene). Although

widely used, they have drawbacks such as poor water solubility, short emission wavelength (emission usually less than 500 nm) so that not suitable to in vivo study. Therefore, the other type, polyaromatic heterocycles, are more extensively explored and developed. Representative examples in this class include coumarin, fluorescein, rhodamine, bodipy, and cyanine etc (Figure 1.12).

Besides organic dyes, some inorganic compounds like uranyl ion ( $UO_2^{2+}$ ), lanthanide ions (e.g.  $Eu^{3+}$ ,  $Tb^{3+}$ ), doped glasses (e.g. with Nd, Mn, Ce, Sn, Cu, Ag), crystals (ZnS, CdS, ZnSe, CdSe, GaS, GaP,  $Al_2O_3/Cr^{3+}$  (ruby), etc, can also act as the fluorophore for the design of fluorescent sensors.

**Figure 1.12.** Schematic drawing of commonly used heterocyclic dyes.



## 1.5. Summary

Using fluorescence techniques to detect bio-interesting molecules and ions have drawn increasing interest to many researchers including chemists, biologists, clinical biochemists and environmentalists. Therefore, considerable efforts are being made to develop selective fluorescent sensors in order to reach all sorts of researching aims. In the following chapters of my dissertation, I will detail my efforts towards design, synthesis of highly efficient fluorescent sensor and their applications. Chapter **2** focuses on fluorescent sensors for selectively recognizing thiols and selenols. In chapter **3** I describe a turn-on sensor which can specifically detect zinc ions. And chapter **4** reports the development a highly selective mercury ion sensor with a novel recognition mechanism.

## 1.6. Reference

1. Lehn, J. M. *Angew. Chem., Int. Ed. Engl.* **1988**, 27, 89.
2. Lehn, J. M. *Angew. Chem., Int. Ed. Engl.* **1990**, 29, 1304.
3. Lehn, J. M. *Supramolecular Chemistry*; VCH: Weinheim, **1995**.
4. Balzani, V. in *Supramolecular Photochemistry*, V. Balzani (Ed.), Reidel, Dordrecht, **1987**.
5. Balzani, V. and Scandola, F. *Supramolecular Photochemistry*; Ellis-Horwood limited: Chichester, **1991**.
6. Balzani, V.; Credi, A.; Scandola, F. in *Transition Metals in Supramolecular Chemistry*; Fabbrizzi, L., Poggi, A., (Eds.); Kluwer: Dordrecht, **1994**.
7. Bryan, A. J.; de Silva, A. P.; de Silva, S. A.; Rupasinghe, R. A. D. D. and Sandanayake, K. R. A. S. *Biosensors* **1989**, 4, 169.
8. Bissell, R. A.; de Silva, A. P.; Gunaratne, H. Q. N.; Lynch, P. L. M.; Maguire, G.E. M.; Sandanayake, K. R. A. S. *Chem. Soc. Rev.* **1992**, 21, 187.
9. Xie, X. S. *Acc. Chem. Res.* **1996**, 29, 598.
10. Goodwin, P. M.; Ambrose, W. P. and Keller, R. A. *Acc. Chem. Res.* **1996**, 29, 607.
11. Orrit, M. and Bernard, J. *Phys. Rev. Lett.* **1990**, 65, 2716.
12. Mets, U. and Rigler, R. *J. Fluoresc.* **1994**, 4, 259.
13. (a) Moerner, W. E. and Basche, T. *Angew. Chem., Int. Ed. Engl.* **1993**, 32, 457. (b) Moerner, W. E. *Acc. Chem. Res.* **1996**, 29, 563.
14. Yeung, E. S. *Acc. Chem. Res.* **1994**, 27, 209.

15. Dixon, A. J. and Benham, G. S. *Int. Lab.* **1988** (4), 38.
16. Tan, W.; Shi, Z. Y. and Kopelman, R. *Anal. Chem.* **1992**, *64*, 2985.
17. Tan, W.; Shi, Z. Y.; Smith, S.; Birnbaum, D. and Kopelman, R. *Science* **1992**, 258, 778.
18. Sharp, S. L.; Warmack, R. J.; Goudonnet, J. P.; Lee, I. and Ferrell, T. L. *Acc. Chem. Res.* **1993**, *26*, 377.
19. Lewis, A. and Lieberman, K. *Anal. Chem.* **1991**, *63*, 625A. (a) Xie, X. S. *Acc. Chem. Res.* **1996**, *29*, 598.
20. Czarnik, A. W. *Fluorescent Chemosensors for Ion and Molecule Recognition*. A. C.: Washington, **1992**.
21. (a) Malmstrom, B. G. *Nobel Lectures, Chemistry 1981-199*, World Scientific, London, UK, **1992**, 411. (b) Izatt, R. M. and Bradshaw, J. S. *J. Incl. Phenom. Mol. Recognit. Chem. The Pedersen memorial issue.* **1992**, *12*, 1.
22. Valeur B. and Leray, I. *Coord. Chem. Rev.* **2000**, *205*, 3.
23. Wang, S.; Shen, W.; Feng Y. L. and Tian, H. *Chem. Commun.* **2006**, 1497.
24. Callan, J. F.; De Silva P. and Magri, D. C. *Tetrahedron* **2005**, *61*, 8551.
25. Xu, S.; Chen K. C. and Tian, H. *J. Mater. Chem.* **2005**, *15*, 2676.
26. Bell J. W. and Hext, N. M. *Chem. Soc. Rev.* **2004**, *33*, 589.
27. Irvine, D. J.; Purbhoo, M. A.; Krosggaard M. and Davis, M. M. *Nature* **2002**, *419*, 845.
28. Czarnik, A.W. (Ed.), *Fluorescent Chemosensors for Ion and Molecule Recognition*, ACS Symposium Series 358, American Chemical Society,

Washington, DC, **1993**.

29. Lakowicz J.R. (Ed.), *Probe Design and Chemical Sensing, Topics in Fluorescence Spectroscopy, vol. 4*, Plenum, New York, **1994**.
30. Valeur, B. and Bardez, E. *Chem. Br.* **1995**, *31*, 216.
31. Fabbrizzi, L. and Poggi, A. *Chem. Soc. Rev.* **1995**, *24*, 197.
32. Desvergne, J. P. and Czarnik, A.W. *Chemosensors of Ion and Molecule Recognition, NATO ASI Series*, Kluwer, Dordrecht, **1997**.
33. (a) Parker, C. A. and Rees, W. T. *Analyst* **1960**, *85*, 587. (b) Demas, J. N. and Crosby, G. A. *J. Phys. Chem.* **1971**, *75*, 991. (c) Miller, J. N. (Ed.), *Standards for Fluorescence Spectrometry*, Chapman and Hall: London, **1981**.
34. de Silva, A. P.; Gunaratne, H. Q. N.; Gunnlaugsson, T.; Huxley, A. J. M.; McCoy, C. P.; Rademacher, J. T. and Rice, T. E. *Chem. Rev.* **1997**, *97*, 1515.
35. de Silva, A. P.; Fox, D. B.; Moody, T. S. and Weir, S. M. *Trends Biotechnol.*, **2001**, *19*, 29.
36. Beer, P. D. and Gale, P. A. *Angew. Chem., Int. Ed. Engl.* **2001**, *40*, 486.
37. (a) Fabbrizzi, L.; Lichelli, M.; Pallavicini, P.; Sacchi, D. and Taglietti, A. *Analyst* **1996**, *121*, 1763. (b) Bergonzi, R.; Fabbrizzi, L.; Lichelli, M. and Mangano, C. *Coord. Chem. Rev.* **1998**, *170*, 31. (c) Akkaya, E.U.; Huston, M.E. and Czarnik, A.W. *J. Am. Chem. Soc.* **1990**, *112*, 3590. (d) de Silva, A.P.; Gunaratne, H.Q.N. and Gunnlaugsson, T. *Chem. Commun.* **1996**, 1967. (e) Fabbrizzi, L.; Lichelli, M.; Pallavicini, P.; Perotti, A. and Sacchi, D. *Angew. Chem. Int. Ed. Engl.* **1994**, *33*, 1975. (f) Fabbrizzi, L.; Lichelli, M.; Pallavicini, P.; Perotti, A.; Taglietti, A. and

- Sacchi, D. *Chem. Eur. J.* **1996**, *2*, 167. (g) Aoki, I.; Sakaki, T. and Shinkai, S. *J. Chem. Soc. Chem. Commun.* **1992**, 730. (h) Fages, F.; Desvergne, J. P.; Bouas-Laurent, H.; Lehn, J. M.; Konopelski, J. P.; Marsau, P.; Barrans, Y. *J. Chem. Soc. Chem. Commun.* **1990**, 655. (i) Fages, F.; Desvergne, J. P.; Kampke, K.; Bouas-Laurent, H.; Lehn, J. M.; Meyer, M. and Albrecht-Gary, A. M. *J. Am. Chem. Soc.* **1993**, *115*, 3658. (j) de Silva, A.P.; Gunaratne, H.Q.N.; Rice, T.E. and Stewart, S. *J. Chem. Soc. Chem. Commun.* **1997**, 1891.
38. (a) Valeur, B. in *Molecular Luminescence Spectroscopy, Part 3*, Wiley, Schulman, S.G. (Ed.), New York, **1993**, p. 25. (b) Valeur, B.; Bourson, J. and Pouget, J. in *Fluorescent Chemosensors for Ion and Molecule Recognition, ACS Symposium Series 538*, A.W. Czarnik (Ed.), American Chemical Society, Washington, DC, **1993**, 25. (c) Rettig, W. and Lapouyade, R. *Probe design and chemical sensing, Topics in Fluorescence Spectroscopy, vol. 4*, Lakowicz, J.R. (Ed.), Plenum, New York, **1994**, 109. (d) Valeur, B.; Badaoui, F.; Bardez, E.; Bourson, J.; Boutin, P.; Chatelain, A.; Devol, I.; Larrey, B.; Lefèvre, J. P. and Soulet, A. in *Chemosensors of Ion and Molecule Recognition, NATO ASI Series*, Desvergne, J. P.; Czarnik, A.W. (Eds.), Kluwer, Dordrecht, **1997**, 195. (e) Löhr, H. G. and Vögtle, F. *Acc. Chem. Res.* **1985**, *18*, 65 and Refs. cited therein.
39. (a) Haugland, R.P. *Handbook of Fluorescent Probes and Research Chemicals, Molecular Probes, Inc, Eugene, OR, USA*. (b) Ohki, A.; Lu, J. P.; Hallman, J. L.; Huang, X. and Bartsch, R.A. *Anal. Chem.* **1995**, *67*, 2405.
40. (a) Bouas-Laurent, H.; Castellán, A.; Daney, M.; Desvergne, J. P.; Guinand, G.;



- Marsau, P. and Riffaud, M. H. *J. Am. Chem. Soc.* **1986**, *108*, 315. (b) Marquis, D. and Desvergne, J. P. *Chem. Phys. Lett.* **1994**, *230*, 131. (c) Marquis, D.; Desvergne, J. P. and Bouas-Laurent, H. *J. Org. Chem.* **1995**, *60*, 7984.
41. (a) Förster T. *Ann. Physik.* **1948**, *437*, 55. (b) Joseph R. Lakowicz, *Principles of Fluorescence Spectroscopy*, 2nd edition, Plenum, **1999**.
42. Zhang, X. L.; Xiao, Y. and Qian, X. H. *Angew. Chem. Int. Ed. Engl.* **2008**, *47*, 8025.

## Chapter 2

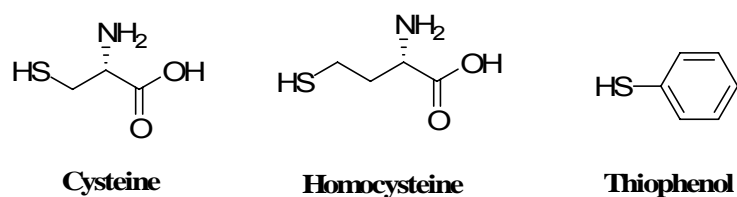
### Development of Fluorescent Sensors for Thiols and Selenols

#### 2.1. Design of Fluorescent Sensor Based on NBD Fluorophore for the Discrimination of Thiophenols and Aliphatic Thiols

##### 2.1.1. Background and significance.

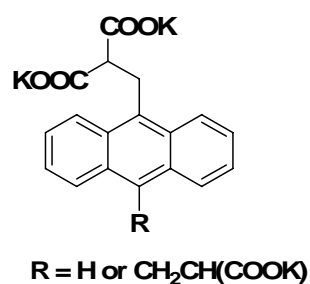
The development of highly sensitive and selective detection techniques for the discrimination of relevant biologically active and toxic molecules is of considerable importance in the fields of chemical, biological, and environmental sciences. Thiols (Figure 2.1) are an important class of molecules in biological systems and chemical science. Aliphatic thiols are found in several biologically important molecules including cysteine,<sup>1</sup> homocysteine,<sup>2</sup> and glutathione,<sup>3</sup> which are associated with a wide range of biological functions. While thiophenols, in spite of their broad synthetic utility,<sup>4</sup> are a class of highly toxic and pollutant compounds. The study of the toxicity of thiols in fish reveals that the median lethal dose (LC<sub>50</sub>) values range from 0.01 to 0.4 mM.<sup>5</sup> Generally, thiophenols are more toxic than aliphatic alcohols.<sup>6</sup> Symptoms of exposure include a burning sensation, coughing, wheezing, laryngitis, shortness of breath, headache, nausea, and vomiting through targeting of the central nervous system, kidney, and liver.<sup>7</sup> In a worst-case scenario, they can result in death. The main sources of the production of toxic and pollutant thiophenols include oil and coal refineries,<sup>8</sup> the plastics and rubber industry,<sup>9</sup> and waste-deposit landfills.<sup>10</sup>

**Figure 2.1.** Schematic drawing of common thiols.



A variety of examination methods<sup>11</sup> including sensitive fluorescent probes have been reported,<sup>12-14</sup> but most of them only focused on detecting thiol-containing amino acids and peptides (usually bio-active aliphatic thiols). For example, Zhu and coworker developed an anthracene-based complex as a turn-on fluorescent sensor for the detection of cysteine and homocysteine (Figure 2.2). In this sensor, anthracene was used as a fluorescence signaling moiety and the carboxylate groups acted as binding sites for Cu<sup>2+</sup> to form a complex. In the thiol-free state, the fluorescence of the complex was quenched by Cu<sup>2+</sup>. However, thiol-containing amino acids and peptides can coordinate preferentially to Cu<sup>2+</sup> compared to the sensor and recover the fluorescence from the sensor.

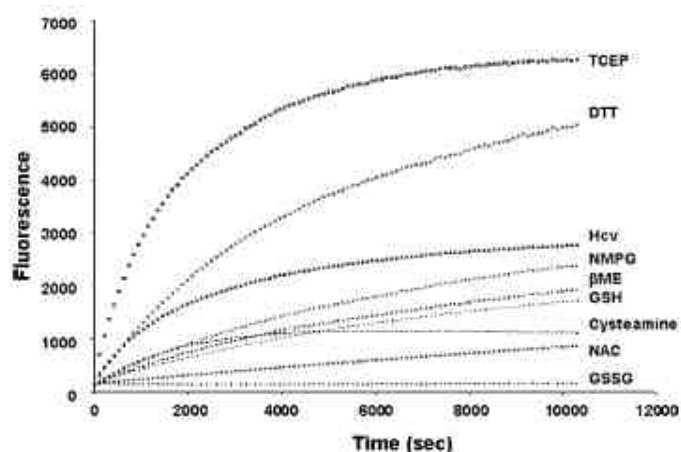
**Figure 2.2.** Zhu's sensor for thiols based on HTM quenching mechanism.



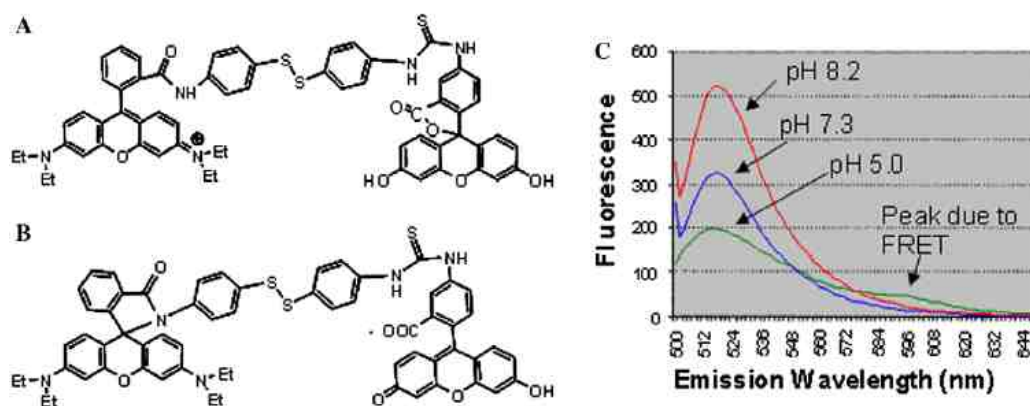
Using dithiol as receptor for thiols is another popular method. Daniel S. Sem's

group developed probe **DSSA** to detect bio-active thiols both in vitro and in vivo (Figure 2.3). **DSSA** was constructed by two fluorophore, fluorescein and rhodamine, connected which is a dithiol linker which also worked as the receptor (Figure 2.4). Its fluorescence behavior was highly pH-dependent and exhibited some FRET phenomena at weak acidic condition. **DSSA** will give obvious fluorescence increase upon addition of DTT (dithiothreitol) and GSH (glutathione) due to the removal of rhodamine as the fluorescence quencher or the acceptor in FRET process.<sup>15</sup>

**Figure 2.3.** Reduction of the **DSSA<sub>AI</sub>** probe by various thiols.



**Figure 2.4.** pH dependent behavior of **DSSA**.



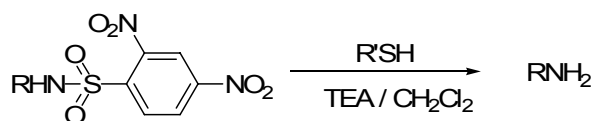
For available fluorescent sensors, examination revealed that most of them suffer from poor selectivity toward aliphatic thiols and thiophenols or even didn't make a study of comparing these two types of thiol-species. Accordingly, a fluorescent reagent that enables thiophenols and aliphatic thiols to be selectively differentiated is needed. It is fully realized that the design of such fluorescent reagents is a challenging task because of the similar chemical profiles of aliphatic thiols and thiophenols. If a probe is very sensitive to aliphatic thiols, it is not possibly inert to thiophenols. Then the differentiation between these two species will become difficult. To the best of our knowledge, such a probe has not been described before. Herein, we want to explore some probes using fluorescence sensing technique for the highly sensitive and selective detection and recognition of thiophenols and aliphatic thiols.

### **2.1.2. Design plan.**

For the successfully design of an aimed fluorescent probe, the most import things are choosing an effective receptor (recognition moiety) as well as rationally connecting it with a proper fluorophore. It is well known that the strongly electron-withdrawing 2,4-dinitrobenzenesulfonyl (DNS) group has been used for the protection of an amino group.<sup>16</sup> The resulting sulfonamide can be readily cleaved by a thiolate anion, derived from a thiol under basic conditions through an aromatic nucleophilic substitution ( $S_NAr$ ) process in organic solvents (Scheme 2.1). This mechanism underlines the importance of the nucleophilic thiolate, which is an essentially reactive form for the reaction. In the aqueous solution, the  $pK_a$  value of

thiophenols is around 6.5, whereas that of aliphatic thiols is about 8.5. Therefore, in a neutral reaction medium (for example, pH 7.3), the high degree of dissociation of thiophenols results in the predominant generation of the corresponding thiolate, which can effectively react with 2,4-dinitrobenzenesulfonamide. However, under the same reaction conditions, the aliphatic thiols remain as a less reactive neutral form and thus the cleavage of the sulfonamide is much slower. This DNS group will make the differentiation of thiophenols from aliphatic thiols feasible, so we chose it as the recognition moiety for our probe.

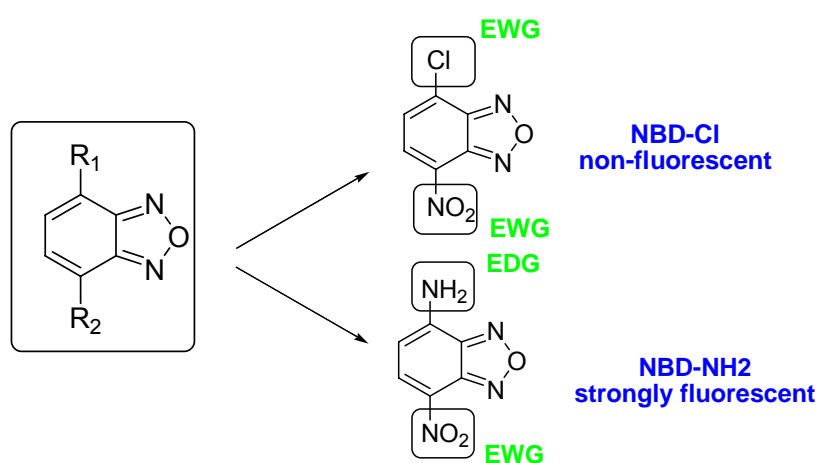
**Scheme 2.1.** Cleavage of 2,4-dinitrobenzenesulfonamide by a thiol.



Then the next problem is what kind of fluorophore we should employ and how to construct the whole probe molecule. We know that manipulating the electronic features of the substituent groups on a fluorophore may lead to significant change in its fluorescence emission profile, through either intramolecular charge transfer (ICT)<sup>17</sup> or photoinduced electron transfer (PET) pathways.<sup>18</sup> The design of the PET-based fluorescent sensor is relatively easier because the efficiency of the PET process can be predicted. Nevertheless, the ICT type of fluorescent reagents can afford high sensitivity due to their quite low intrinsic fluorescence. A typical example is the nonfluorescent probe 4-chloro-7-nitro-benzofurazan (NBD-Cl) as a result of two

electron-withdrawing groups (EWGs; 4-chloro and 7-nitro), which features pull-pull system and blocks the ICT process. However, the substitution of the “Cl” atom by an amino moiety as electron-donating group (EDG) could change it to push-push system and result in a dramatic increase in fluorescence (Figure 2.5).<sup>19</sup>

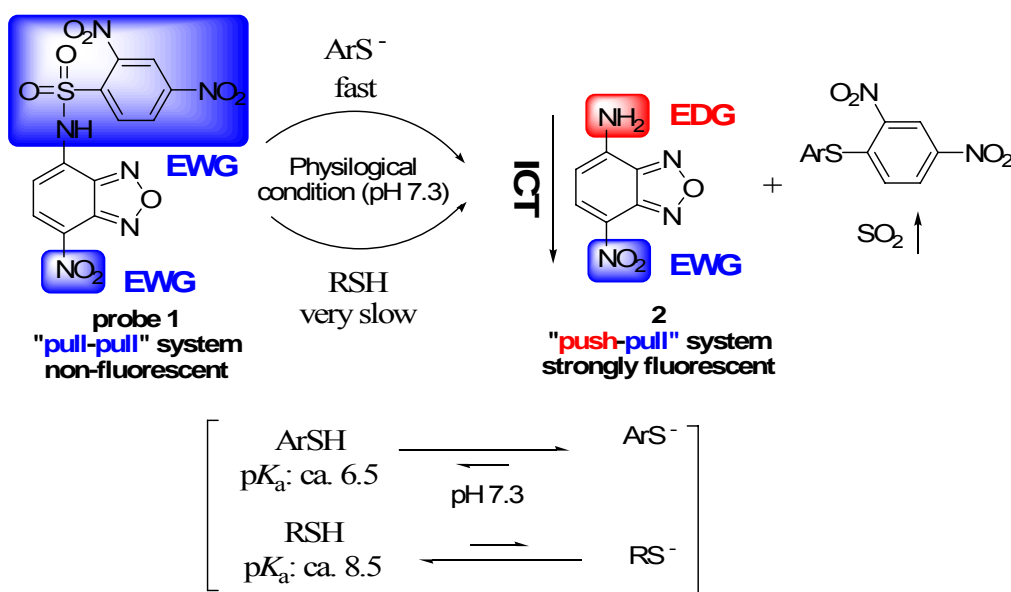
**Figure 2.5.** Change of fluorescence properties of NBD induced by 4-substituents.



Based on this observation, we hypothesized that masking the amino group by a EWG would give rise to a nonfluorescent molecule. Removal of the protecting moiety of the amino group should lead to a highly fluorescent compound. Therefore, it is possible to design a fluorescent probe for the discrimination of aliphatic thiols and thiophenols under neutral, physiological conditions. By taking advantage of the unique reactivity profile and strong EWG capacity of the 2,4-dinitrobenzenesulfonamide, we envisioned that masking the amino group in the fluorescence-active 4-amino-7-nitro-benzofurazan by the 2,4-dinitrobenzenesulfonyl moiety could generate a sensor **1** for thiophenols and aliphatic thiols. Sensor **1** is also

a pull-pull system and expected to be non-fluorescent. However, when it reacts with a thiol to yield **2**, strong fluorescence should be observed since a push-pull system is generated (Figure 2.6).

**Figure 2.6.** Proposed mechanism for sensor **1**.

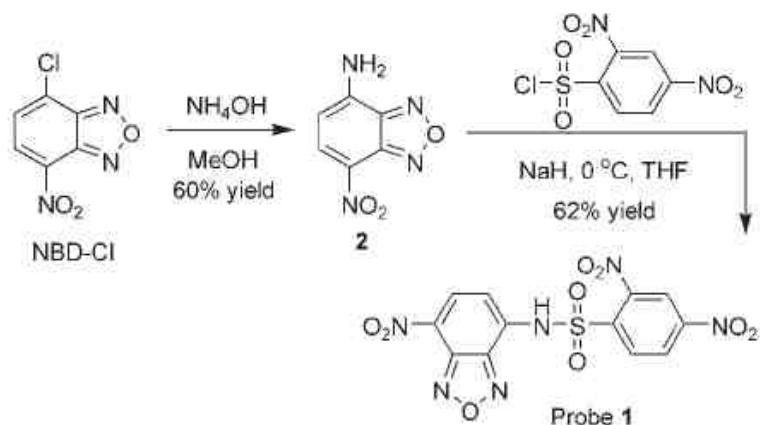


### 2.1.3. Synthesis.

To demonstrate the working hypothesis, we first synthesized the sensor **1**. Its synthesis is straightforward in two steps (Scheme 2.2). Reaction of NBD-Cl with ammonium hydroxide in methanol gave 4-amino-7-nitro-benzofurazan **2** in 60% yield. Introduction of the sulfonyl moiety into the amino group was achieved by reacting **2** with 2,4-dinitrobenzenesulfonyl chloride in the presence of NaH in THF to afford the target molecule **1** in 62% yield.



## Scheme 2.2. Synthesis of sensor 1.

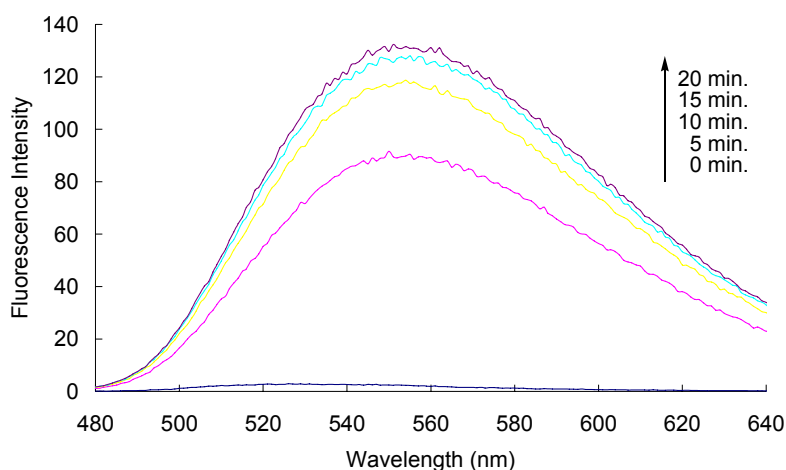


### 2.1.4. Results and discussion.

#### 2.1.4.1. The sensitivity towards thiophenol and aliphatic cysteine.

With sensor 1 in hand, we first examined its fluorescence property in the absence and presence of a thiol and established the optimal measurement conditions. Notably, compound 1 showed good solubility in water and other polar solvents like methanol. Accordingly, the experiment was performed in an aqueous phosphate buffer ( $I = 0.01\text{M}$ ,  $\text{pH } 7.3$ ) containing 1 at a concentration of  $2.0 \times 10^{-5}\text{ M}$ . As designed, this benzofurazan-based sensor 1 exhibited almost no fluorescence in the absence of a thiol with  $\lambda_{\text{ex}} = 465\text{ nm}$  since the strong electron-withdrawn DNS group blocked the ICT process. However, when thiophenol ( $4.0 \times 10^{-5}\text{ M}$ , 2.0 equiv.) was added, a significant increase of fluorescence intensity ( $>50$  times) was observed in a few minutes with a maximum at  $555\text{ nm}$  (Figure 2.7). The reaction product 2 was monitored and confirmed by a comparison study with a standard pure compound 2 through  $^1\text{H NMR}$  analysis, which proved our designed mechanism for this sensor. The

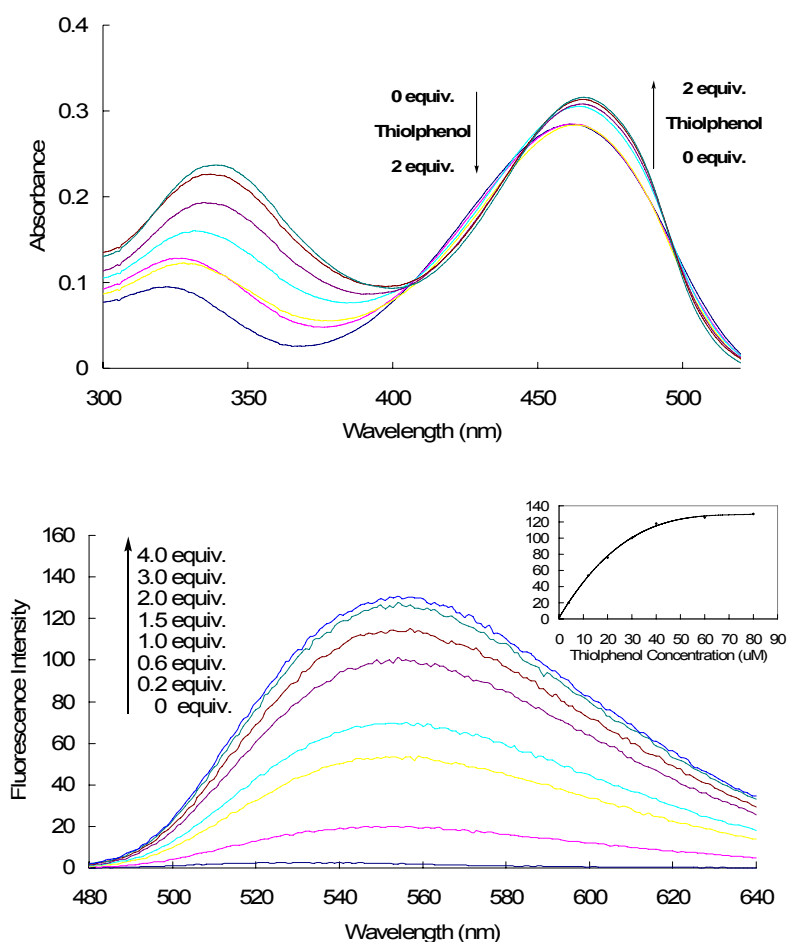
quantum yield of fluorescence for the product **2** is determined as about 0.02. Remarkably, sensor **1** showed a quick response toward thiophenol based on the study of reaction time profile. A pronounced intensity increase was obtained even after 5 min. The reaction reached completion after around 10 min. A limited change of fluorescence intensity was observed when longer reaction times were examined. Therefore, a reaction time of 10 min was selected to explore the selectivity of sensor **1** toward thiols.



**Figure 2.7.** Emission time profile of sensor **1** towards thiophenol. Sensor **1** ( $2 \times 10^{-5}$  M), prepared from a stock solution (10 mM) in EtOH, was studied in a phosphate buffer (pH 7.3, 0.01M) at room temperature in the absence and presence of thiophenol (2.0 equivalents). The reaction solution was sampled for fluorescence measurement at  $\lambda_{\text{ex}} = 465$  nm at the specified time periods.

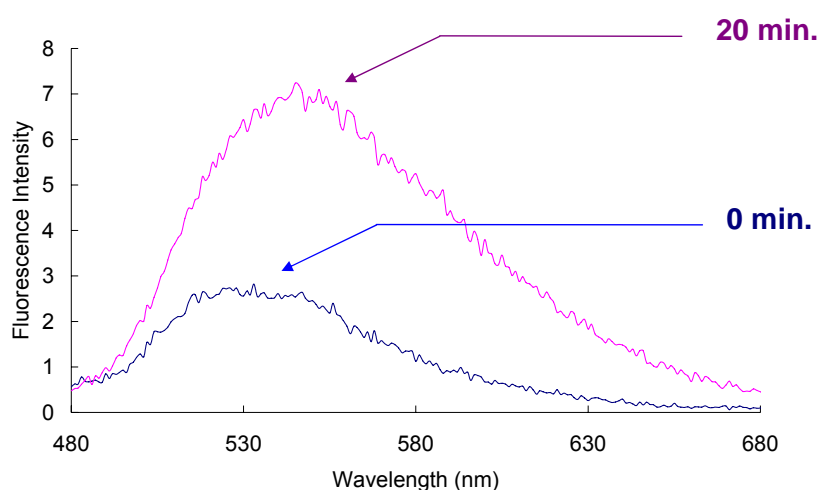
The sensitivity of this sensor **1** at  $2 \times 10^{-5}$  M was examined next by using thiophenol as an analyte with a concentration ranging from 0.2 to  $4.0 \times 10^{-5}$  M under the same reaction conditions described above (Figure 2.8). The increase in both absorption and fluorescence intensity was displayed in a concentration dependent manner. The thiol-free sensor **1** exhibited absorption bands in the visible region

centered at 460 nm ( $\epsilon = 1.4 \times 10^4 \text{ M}^{-1} \text{ cm}^{-1}$ ). Upon addition of thiophenol, the visible absorption profile shifted to a peak centered at 465 nm ( $\epsilon = 1.6 \times 10^4 \text{ M}^{-1} \text{ cm}^{-1}$ ). Correspondingly, a red shift of fluorescence spectrum was also observed from the maximum of 528 nm to 555 nm. When more than three equivalents of thiophenol were used, the enhancement of fluorescence intensity almost reached a maximum without much further alteration. Notably, a pronounced change in the fluorescence signal was observed even when the thiophenol concentration was as low as  $2 \times 10^{-6} \text{ M}$ .



**Figure 2.8.** Effect of thiophenol concentration on the absorption and fluorescence emission of sensor **1**. Sensor **1** ( $2 \times 10^{-5} \text{ M}$ ) was studied in a phosphate buffer (pH 7.3, 0.01M) at room temperature in the absence and presence of a thiol of different concentration. After 10 min, the reaction solution was sampled for absorption and emission measurement ( $\lambda_{\text{ex}} = 465 \text{ nm}$ , fluorescence intensity at  $\lambda_{\text{ex}} = 555 \text{ nm}$  is plotted vs. concentration.)

Contrary to thiophenol, sensor **1** exhibited much inert fluorescence response towards cysteine, an aliphatic thiol in the control experiments (Figure 2.9). Again the experiment was performed in the same buffer solution containing **1** at a concentration of  $2.0 \times 10^{-5}$  M and two equivalents of cysteine were added. At 20 minutes, however, only very tiny fluorescence intensity increase was achieved (the intensity is about 7 a.u.). Actually even after 1 hour's the reaction, the fluorescence intensity of sensor solution was still less than 10 a.u., which is obviously neglectable comparing to thiophenol.

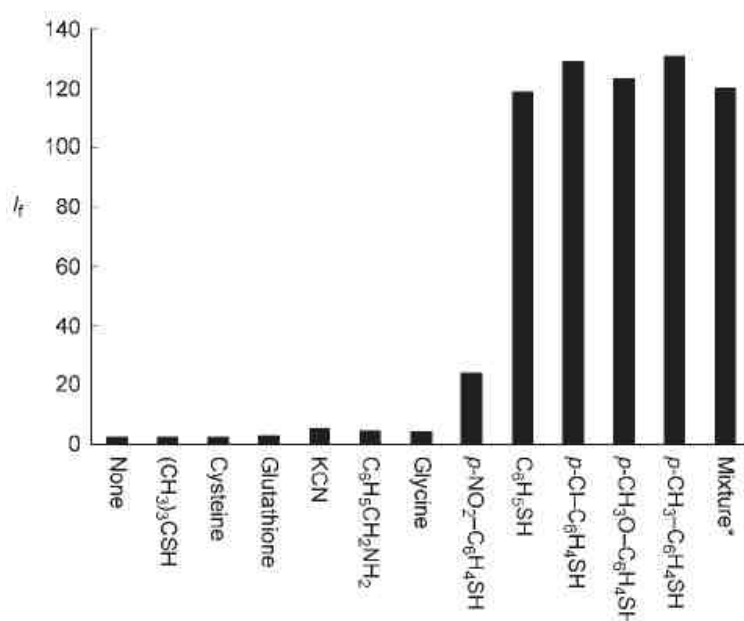


**Figure 2.9.** Emission time profile of sensor **1** towards cysteine. Sensor **1** ( $2 \times 10^{-5}$  M), prepared from a stock solution (10 mM) in EtOH, was studied in a phosphate buffer (pH 7.3, 0.01M) at room temperature in the absence and presence of cysteine (2.0 equivalents). The reaction solution was sampled for fluorescence measurement at  $\lambda_{\text{ex}} = 465$  nm before and after addition of cysteine.

#### 2.1.4.2. The specificity for thiophenols

In order to examine the specificity of our sensor, we expanded the scope of analytes. A variety of thiols, including thiophenols, thioalcohols, cysteine, and glutathione, and other nucleophiles, such as cyanide (NaCN) and benzylamine (BnNH<sub>2</sub>)

were probed to examine the selectivity of sensor **1**.



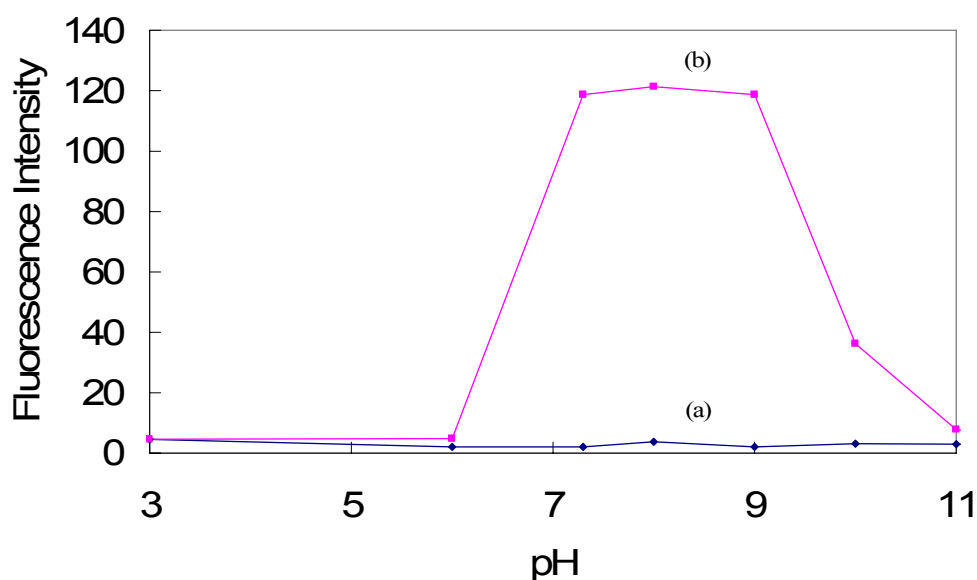
**Figure 2.10.** The selectivity of sensor **1** towards thiols and other nucleophiles. Sensor **1** ( $2 \times 10^{-5}$  M) was studied in a phosphate buffer (pH 7.3, 0.01M) at room temperature in the presence of various analytes (2.0 equivalents). After 10 min, the reaction solution was sampled for fluorescence measurement at  $\lambda_{\text{ex}} = 465$  nm. The fluorescence intensity at  $\lambda_{\text{ex}} = 555$  nm is plotted vs. analytes. \*A mixture of PhSH, cysteine, KCN, and BnNH<sub>2</sub>, each with a concentration of  $4 \times 10^{-5}$  M.

As shown in Figure 2.10, sensor **1** was highly selective to thiophenol sorts. Significant fluorescence intensity enhancement was observed for 4-chloro, 4-methoxy, and 4-methylthiophenols. An increase for 4-nitrothiophenol, which has a strong nitro EWG, was also obtained, but the magnitude was much smaller than those for the other thiophenols tested. A plausible reason is that the nitro group in 4-nitrothiophenol significantly decreases the nucleophilicity of the thiol, thus reducing its reactivity for the S<sub>N</sub>Ar reaction. Remarkably, almost no fluorescence intensity change was seen for other types of nucleophilic molecules such as NaCN, and BnNH<sub>2</sub> besides the molecules possessing aliphatic thiol moieties, such as t-butyl thioalcohol, cysteine, glutathione. More significantly, in the presence of other nucleophiles, such as cysteine,

glutathione, NaCN, and BnNH<sub>2</sub>, a similar fluorescence intensity increase was observed to that of a pure thiophenol, which indicates that sensor **1** is particularly selective toward thiophenols without interference.

#### 2.1.4.3. The effect of pH on the fluorescence intensity and reactivity.

Finally, we evaluated the effect of reaction pH on sensor **1**. As designed, no fluorescence intensity enhancement of **1** was observed for either thiophenols or aliphatic thiols at pH < 6 (Figure 2.11), as these analytes exist as less nucleophilic neutral forms. It is expected that a large increase in fluorescence intensity could be observed at pH 7 to 9 as a result of the strong ionization of thiophenols. However, we found that sensor **1** was not stable at high pH values (>10). For example, at pH 12 it decomposed to give a nonfluorescent complex mixture.



**Figure 2.11.** Effect of pH on the fluorescence response of sensor **1** ( $2 \times 10^{-5}$  M) towards thiophenol at  $\lambda_{\text{ex}} = 465$  nm and  $\lambda_{\text{em}} = 555$  nm. (a). probe only, (b). 10 minutes after addition of PhSH (2 equiv.) in the phosphate buffer (pH 7.3, 0.01M) at room temperature.

### **2.1.5. Conclusion.**

A novel sensitive and highly selective fluorescence sensor **1** for the discrimination of thiophenols from aliphatic thiols and other nucleophiles was developed. The investigation demonstrates that the manipulation of the electronic nature of the substituents of a fluorophore can affect the fluorescence emission profile through the alteration of the ICT process. Moreover, it is possible to design a highly selective fluorescent reagent based on the analyte reactivity profile and reaction conditions. Dramatic fluorescence intensity enhancement is seen with thiophenols as a result of effective cleavage of the electronwithdrawing 2,4-dinitrobenzenesulfonyl moiety from nonfluorescent sensor **1**, to generate highly fluorescent **2** in an aqueous neutral (pH 7.3) buffer with very short reaction times. However, no fluorescence is obtained with aliphatic thiols, including biologically interesting cysteine and glutathione, and other nucleophiles. Therefore, sensor **1** can be used for the specific detection and quantification of highly toxic thiophenols in environmental science.

## **2.2. Design of Fluorescent Sensor based on PET Mechanism for the Discrimination of Thiophenols and Aliphatic Thiols**

### **2.2.1. Design plan.**

In last section, we described a fluorescent sensor **1** for thiophenols based on ICT mechanism. Although sensor **1** displayed high specificity in the differentiation of thiophenols from aliphatic thiols, it has drawback that the fluorescence intensity of product **2** (4-amino-7-nitro-benzofurazan) is not strong enough in aqueous solution. We know the polarity of solvents can deeply affect the quantum yield of fluorophores

featuring charge transfer excited state. That explained why the quantum yield of fluorophore **2** in aqueous solution is only 0.02, but in organic solution like dichloromethane can be as high as 0.3. Therefore, we hoped to develop a “brighter” sensor for thiophenols to overcome this drawback and facilitate the practical application.

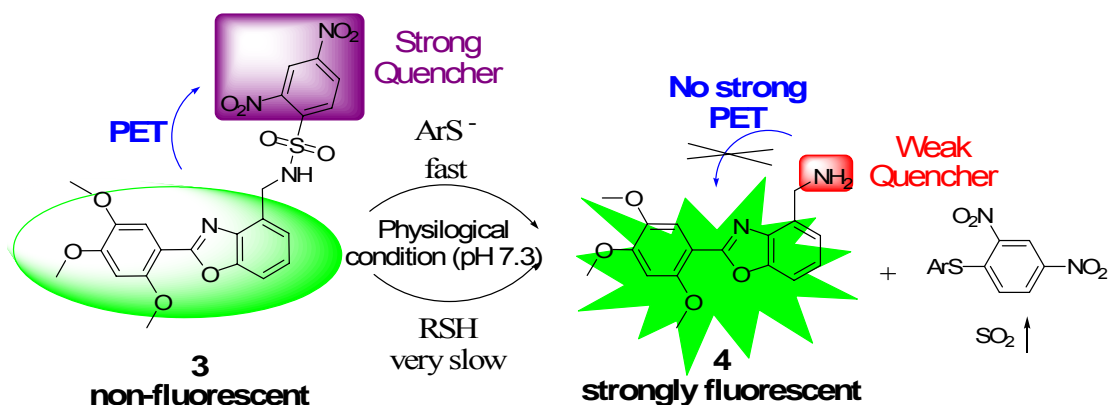
As we introduced above, 2,4-dinitrobenzenesulfonamide moiety is a eligible recognition moiety for thiophenols. Moreover, those two nitro group (strong EWG) on DNS moiety make it quite electron-deficient. As a result, it will act as oxidative quencher for a fluorophore if they are indirectly connected by a linker. This showed us a way to design a PET (photoinduced electron transfer) sensor based on a fluorophore with high quantum yield in aqueous solution.

With these studies in mind, we developed sensor **3** around the fluorescent benzoxazole core substituted with the 2,4-dinitrobenzenesulfonamide moiety. As shown in Figure 2.12, we surmised that this electron-deficient DNS group can greatly quench the fluorescence of the whole sensor molecule through an oxidative PET process. However, if a thiol was added, it could cleave the sulfonamide to release the benzoxazole-amine derivative **4** as a product. Since our preliminary have shown that **4** is strongly fluorescent in either aqueous solution or organic solution although electron-donating amino group as weak reductive quencher could slightly attenuate the fluorescence of benzoxazole conjugation, compound **3** should be able to perform as a “turn-on” fluorescent sensor for thiols. Furthermore, the differentiation between aliphatic thiols and thiophenols in the aqueous solution is still based on their disparity



in reaction activity due to their  $pK_a$  values.

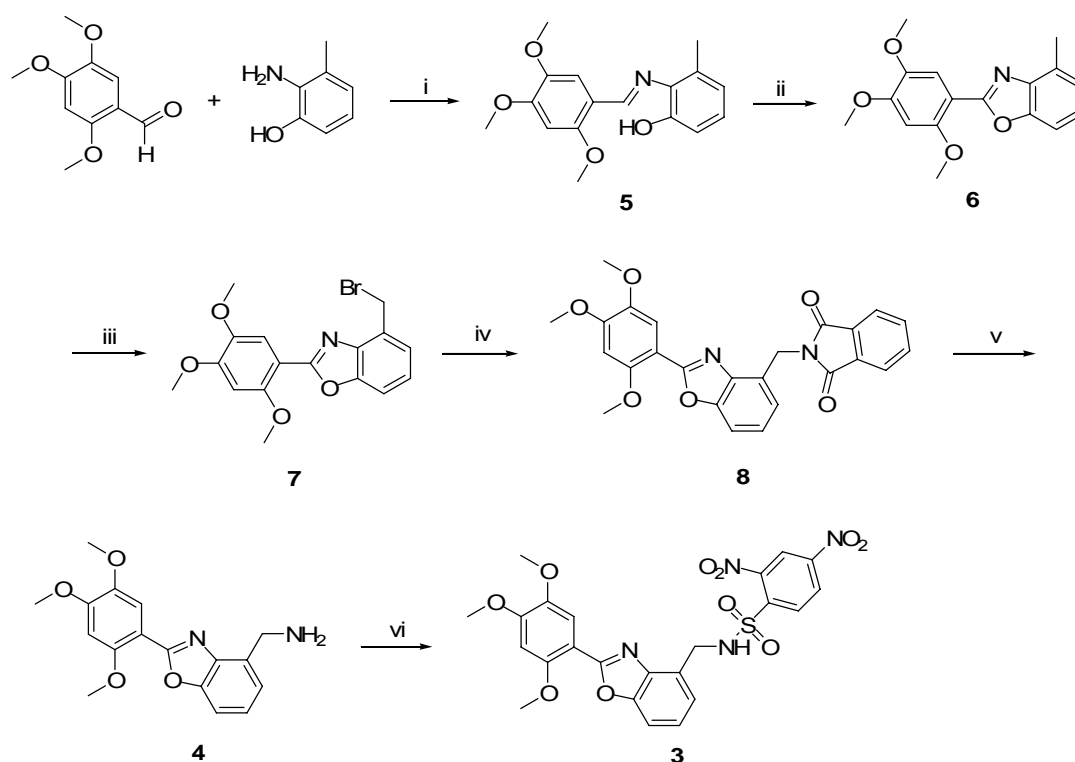
**Figure 2.12.** Proposed mechanism for sensor **3**.



### 2.2.2. Synthesis.

Sensor **3** was prepared in six steps (Scheme 2.3) starting from the condensation of commercial available 2,4,5-trimethoxy-benzaldehyde with 2-amino-3-methylphenol in hot benzene. Without further purification, the resulting compound **5** was treated with  $BaMnO_4$  in hot benzene to get benzoxazole derivative **6**. The bromination of **6** by NBS in  $CCl_4$  gave bromide **7**. Then the bromide **7** was acylated to **8** with potassium succinimide, followed by cleaving of N-succinimide with hydrazine in THF afford free amine **4** as a fluorescent compound. At last, amine **4** was sulfonylated with 2,4-dinitrobenzenesulfonyl chloride in  $CH_2Cl_2$  in the presence of pyridine provide targeting sensor molecule **3**.

### Scheme 2.3. Synthesis of Sensor 3.



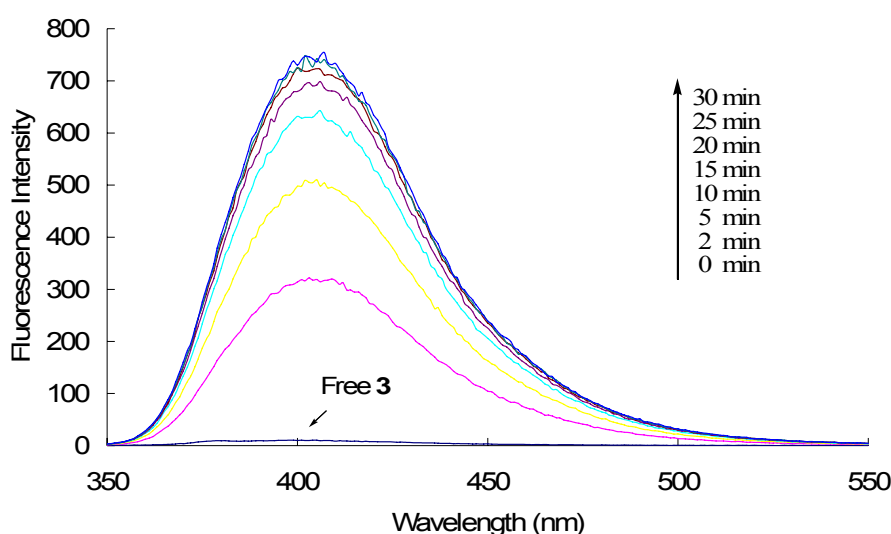
(i). Benzene, reflux, 24 h; (ii) BaMnO<sub>4</sub>, benzene, reflux, 8 h; (iii). NBS, AIBN, CCl<sub>4</sub>, reflux, 6 h; (iv). Potassium Succinimide, DMF, 50 °C, 8 h; (v). NH<sub>2</sub>NH<sub>2</sub>, THF, reflux, 2 h; (vi). 2,4-Dinitrobenzenesulfonyl chloride, pyridine, CH<sub>2</sub>Cl<sub>2</sub>, 0 °C to r.t.

### 2.2.3. Results and discussion.

#### 2.2.3.1. Dual functionality of DNS moiety.

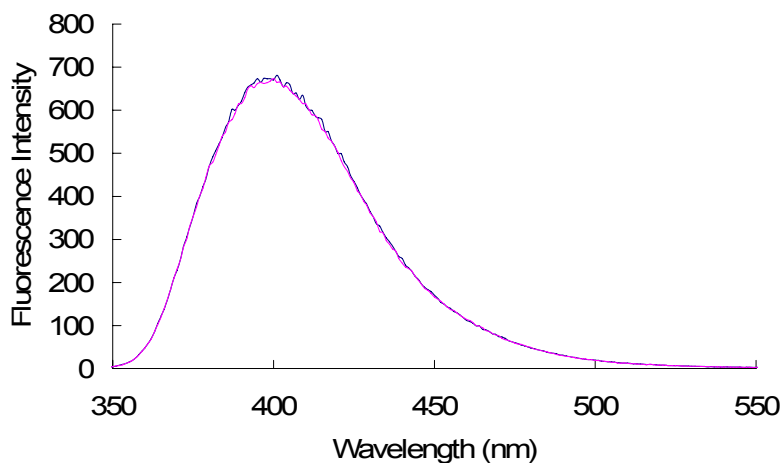
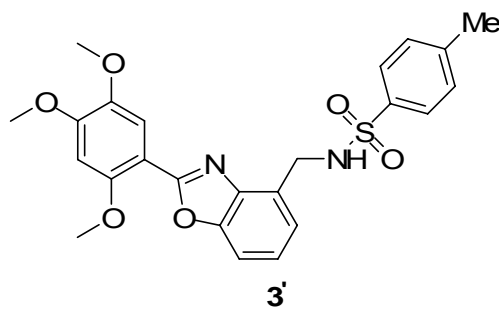
A mixture of aqueous phosphate buffer (I = 0.01M, pH = 7.3) and DMF (0.5%, v/v) was used for the titration of sensor 3 in a concentration of  $2 \times 10^{-6}$  M. The primary investigation of fluorescence property of thiol-free sensor 3 showed it is totally non-fluorescent with  $\lambda_{\text{ex}} = 335$  nm as we expected. While upon the addition of 2 equivalents ( $4.0 \times 10^{-6}$  M) thiophenols, obvious fluorescence increase was observed in a few seconds centered at 403 nm. After about 20 minutes, the fluorescence almost reached the maximum and no much change for extended time. Notably, sensor 3 exhibited much stronger fluorescence response than previous sensor 1 even if its

concentration is 10 times lower, and >100 fold fluorescence intensity increase was obtained (Figure 2.13). The reaction product was monitored and confirmed by a comparison study with a standard pure compound **4** through  $^1\text{H}$  NMR analysis, which proved our designed mechanism for this sensor. The quantum yield of fluorescence for the product **4** is determined as 0.39 ( $\epsilon = 1.2 \times 10^4 \text{ M}^{-1} \text{ cm}^{-1}$ ).



**Figure 2.13.** Emission time profile of sensor **3** towards thiophenol. Sensor **3** ( $2 \times 10^{-6} \text{ M}$ ), prepared from a stock solution (1 mM) in DMF, was studied in a phosphate buffer (pH 7.3, 0.01M) containing 0.5% of DMF at room temperature in the absence and presence of thiophenol (2.0 equivalents). The reaction solution was sampled for fluorescence measurement at  $\lambda_{\text{ex}} = 335 \text{ nm}$  at the specified time periods.

In the control study, we synthesized compound **3'** through changing DNS group of sensor **3** with *p*-methylbensensulfonyl (Ts) group. As expected, compound **3'** showed very strong fluorescence in the aqueous solution and no any response when 2 equivalents of thiophenol were added for 20 minutes (Figure 2.14). These results confirmed our hypothesis that the presence of those two nitro groups made the electron-deficient sulfonamide an oxidative quencher for the benzoxazole core and guaranteed the efficiency of the PET process.

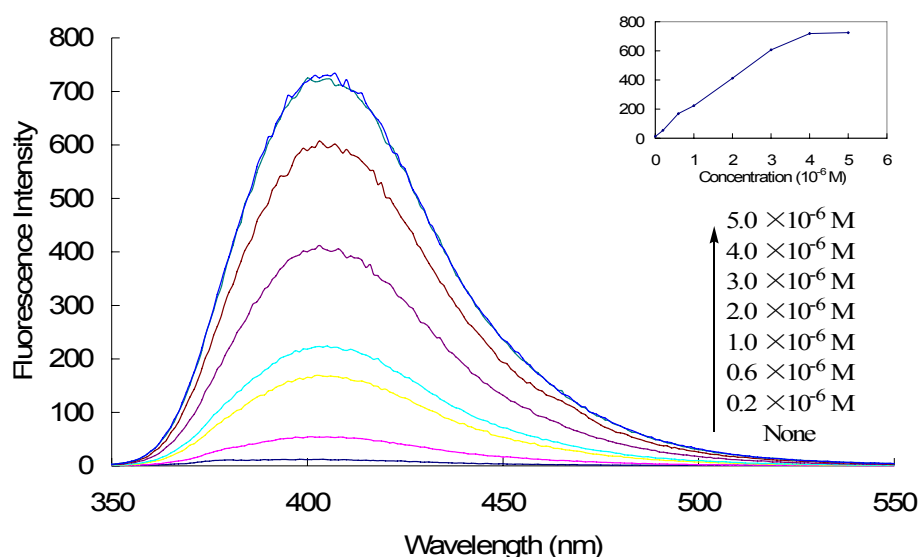


**Figure 2.14.** Structure and fluorescence response of the benzoxazole derivative **3'** towards thiophenol. Sensor **3'** ( $1 \times 10^{-6}$  M), prepared from a stock solution (1 mM) in DMF, was sampled for fluorescence measurement in a phosphate buffer (pH 7.3, 0.01 M) containing 0.5% of DMF at room temperature before and 20 minutes after the addition of thiophenol (2.0 equivalents) with  $\lambda_{\text{ex}} = 335$  nm.

### 2.2.3.2 Sensitivity and selectivity.

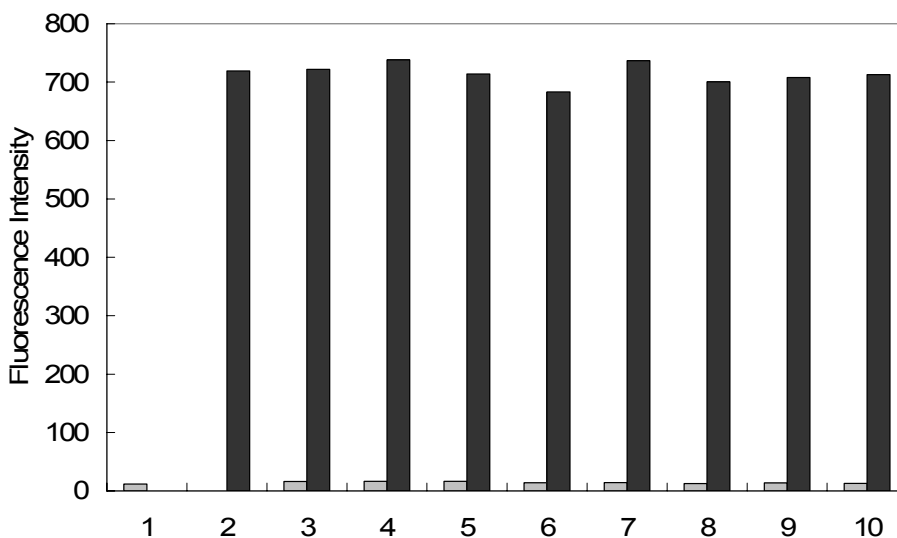
Next we examined the sensitivity of this sensor **3** at  $2 \times 10^{-6}$  M for thiophenol with a concentration ranging from  $0.2 \times 10^{-6}$  M to  $5.0 \times 10^{-6}$  M under the same reaction conditions described below (Figure 2.15). The fluorescence intensity increase displayed in a concentration dependent profile and no obvious blue or red shift of fluorescence spectrum was observed, which was in agreement with the normal PET process. When four equivalents of thiophenol were added, the enhancement of fluorescence intensity reached the maximum in 10 minutes. Addition of more

thiophenol can't make further alteration. Notably, even we lowered the concentration of thiophenol to only  $2 \times 10^{-7}$  M, a distinct fluorescence signal change still could be observed, which proved its higher sensitive than that of sensor **1**.



**Figure 2.15.** Effect of thiophenol concentration on the fluorescence emission of sensor **3**. Sensor **3** ( $2 \times 10^{-6}$  M) was studied in a phosphate buffer (pH 7.3, 0.01M) containing 0.5% of DMF at room temperature in the absence and presence of a thiol of different concentration. After 10 min, the reaction solution was sampled for emission measurement ( $\lambda_{ex} = 335$  nm, fluorescence intensity at  $\lambda_{ex} = 403$  nm is plotted vs. concentration.)

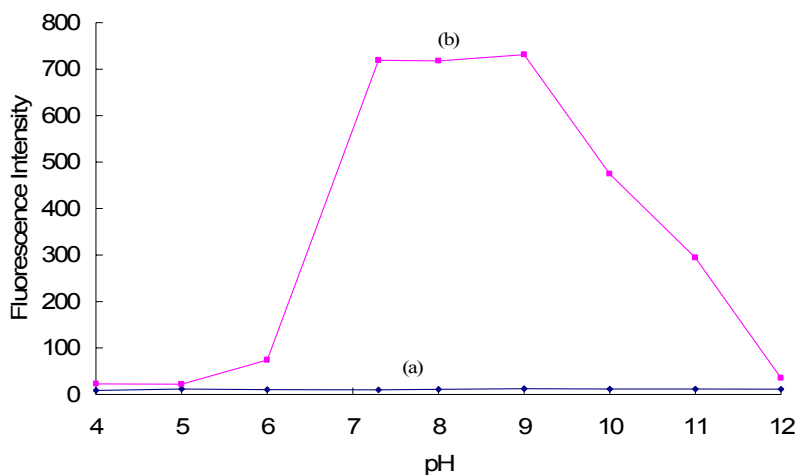
A survey of relevant aliphatic thiols and other nucleophiles showed sensor **3** also have excellent selectivity towards thiophenols (Figure 2.16). Introducing a variety of aliphatic thiols including 2-methyl-2-propanethiol, cysteine and glutathione afforded no fluorescent response to sensor **3**, let alone other nucleophiles such as  $\text{CN}^-$ ,  $\text{NH}_2$ ,  $\text{OH}$  and  $\text{I}^-$ . Moreover, the presence of these nucleophiles in the sensor solution can not cause disturbance to the detection of thiophenol and almost same fluorescence response was probed comparing to the investigation of pure thiophenol.



**Figure 2.16.** Fluorescence response of 2  $\mu\text{M}$  sensor **3** towards various nucleophilic reagents. Gray bar represent only adding nucleophilic reagents to the probe solution, black bar represent adding the mixture of nucleophilic reagents and PhSH. (1) probe only, (2) PhSH, (3) Cysteine, (4)  $(\text{CH}_3)_3\text{CSH}$ , (5) Glutathione, (6) Glycine, (7) KCN, (8) KI, (9) PhOH, (10)  $\text{PhNH}_2$ . Data shown are 4  $\mu\text{M}$  for PhSH and 10  $\mu\text{M}$  for all other substrates, and all data ( $\lambda_{\text{em}} = 403 \text{ nm}$ ) were acquired at 20 minutes after addition of each substrate in a phosphate buffer (pH 7.3, 0.01M) at room temperature with  $\lambda_{\text{ex}} = 335 \text{ nm}$ .

### 2.2.3.3. The effect of pH on the fluorescence intensity and reactivity.

At last, the effect of pH on the fluorescence intensity and reactivity of sensor **3** was evaluated (Figure 2.17). In a wide range from acidic to basic (pH from 4 to 12), **3** itself in the buffer solution was non-fluorescent. After addition of thiophenol, the fluorescence intensity of sensor **3** still hardly changed in acidic condition due to the weak nucleophilicity of thiophenol in a neutral form. However, when the pH value of buffer solution was close to 7 and continuously increased up to 9, significant enhancement of fluorescence signals were observed upon thiophenol was added as a result of the strong ionization of thiophenols. Further increasing the basicity of solution will decrease the fluorescence response of sensor **3** to thiophenol possibly due to the oxidation of thiophenol to form disulfide.



**Figure 2.17.** Effect of pH on the fluorescence response of probe **3** (2  $\mu$ M) towards thiophenol. (a). probe only, (b). 20 minutes after addition of PhSH (2 equiv.) in the phosphate buffer (pH 7.3, 0.01M) containing 0.5% DMF at room temperature with  $\lambda_{\text{ex}} = 335$  nm and  $\lambda_{\text{em}} = 403$  nm.

#### 2.2.4. Conclusion.

We developed a fluorescence sensor **3** for the detection of thiophenols in aqueous solution based on the oxidative PET mechanism. Two birds was got by one stone in the design of this sensor by using electronwithdrawing 2,4-dinitrobenzenesulfonyl moiety as both a receptor of thiols and an oxidative quencher to the signaling moiety. Sensor **3** exhibited high specificity to thiophenol as well as excellent sensitivity with a detection limit of  $10^{-7}$  M. It worked well in a wide pH range from 7 to 11. Therefore, sensor **3** should be a more sensitive supplement of sensor **1** for the detection highly toxic thiophenols in environmental science.

### 2.3. Fluorescent Sensor for Selenocysteine and Selenoproteins.

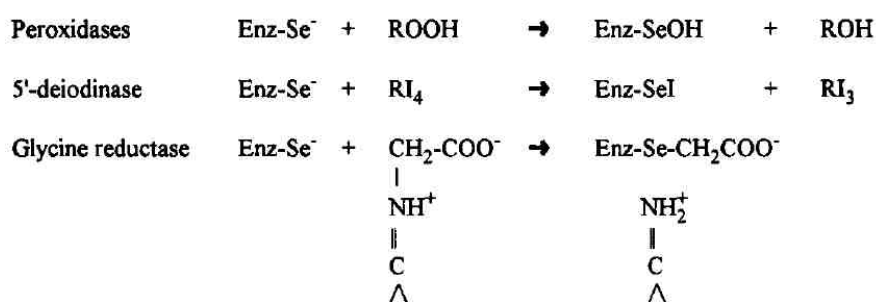
#### 2.3.1. Background and significance

Selenium is essential to human life<sup>20</sup> and occurs in selenoproteins as selenocysteins (SeCys).<sup>21</sup> A selenocysteine residue is analogous to cysteine, but a

selenium atom takes the place of sulfur. Selenocysteine is a special amino acid present in several enzymes (for example glutathione peroxidases, formate dehydrogenases and some hydrogenases), recognized as the 21<sup>st</sup> amino acid. The selenium atom endows it with unique biochemical properties including a low  $pK_a$  and a high reactivity with many electrophilic agents. Selenocysteine is cotranslationally incorporated at a predefined UGA codon that has been recoded from termination to selenocysteine insertion by species-specific mechanisms dependent on structural elements of the tRNA.<sup>22-24</sup> As a result, the function of selenoproteins are of great interest in elucidating the pathogenesis of some disorders. Moreover, new selenocysteine-containing enzymes and proteins are also reported with greater frequency (Scheme 2.4), and the specific roles of those with known catalytic functions illustrate the importance of the trace element selenium for mammalian and bacterial survival.

**Scheme 2.4.** Some reactions catalyzed by selenocysteine-containing enzymes.

**TYPE REACTIONS CATALYZED BY SELENOCYSTEINE  
CONTAINING ENZYMES**





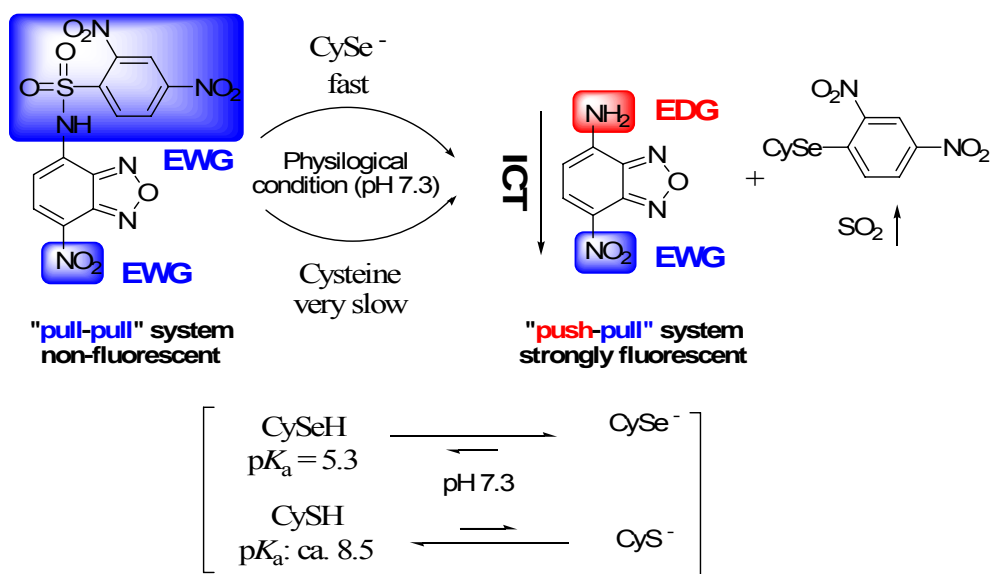
A better understanding of the roles of selenocysteine and selenoproteins in biological system requires sensitive and rapid detection techniques. However, the fact is that the development of efficient tools and measurements for the detection and tracking selenocysteine is lagging far behind the need. Especially fluorescence method, the very popular technique applied for the biological study, was restricted for the study of selenocystein and selenoproteins because of its similar structure with common cysteine which leads to the difficulty of recognizing selenocystein from cysteine. Currenly chromatographic methods coupled with fluorometric or mass spectrometric detection are mostly used for the determination of selenocysteine.<sup>25</sup> To our knowledge, only one relavant fluorescent sensor for selenocysteine was reported by Maeda's group,<sup>26</sup> but that sensor could only work in acidic solution and failed to defferentiate selenocysteine from cysteine in physiological condition (pH 7.3). Therefore, we would like to come out a fluorescent sensor specifically detecting selenocysteine in physiological condition to facilitate the its biological study.

### **2.3.2. Design plan.**

In above section, we introduced a fluorescent sensor **1** for facile detection of thiophenols and discrimination thiophenols from aliphatic thiols in aqueous solution. The fluorogenic reaction of sensor **1** occurred through the deprotection of DNS-protected NBD-NH<sub>2</sub> by the aromatic nucleophilic substitution of thiolate anions. During the design of this sensor, we realized the degree of thiol dissociation is crucial for the functionality of sensor **1** towards the differentiation of thiophenols and

aliphatic thiols. In the physiological condition, the high degree of dissociation of thiophenols results in the predominant generation of the corresponding thiolate, which can effectively react with 2,4-dinitrobenzenesulfonamide. However, under the same reaction conditions, the aliphatic thiols remain as a less reactive neutral form and thus the cleavage of the sulfonamide is much slower. We also noticed a fact that the  $pK_a$  values of selenols are even lower than thiophenols (for example the  $pK_a$  of selenocysteine is 5.2), which make them easier to dissociate in the physiological condition. Moreover, the unique characters of selenium would make selenols to behave as stronger nucleophiles than thiols, which indicates its reaction with 2,4-dinitrobenzenesulfonamide will be much more effective comparing to aliphatic thiols like cysteine. As a result, the detection of selenocysteine and discrimination of it with regular cysteine in the physiological condition could be performed by sensor **1** based on the same concept as for thiophenols. As we described above, sensor **1** is a pull-pull system and exhibits non-fluorescent. We envisioned if it reacts with a selenocysteine, however, fluorophore **2** should be yielded and strong fluorescence would be observed since a push-pull system is generated (Figure 2.18). Meanwhile, because the target of this design focuses on the study of selenocysteine and selenoproteins in the biological system, the inference of non-natural thiophenols can be neglected.

**Figure 2.18.** Proposed mechanism of sensor **1** for the detection of selenocysteine.

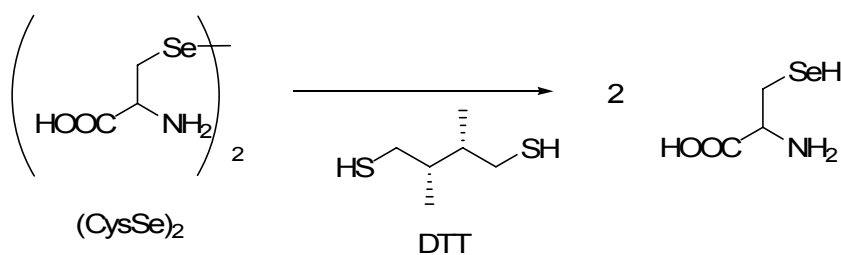


### 2.3.3. Results and discussion.

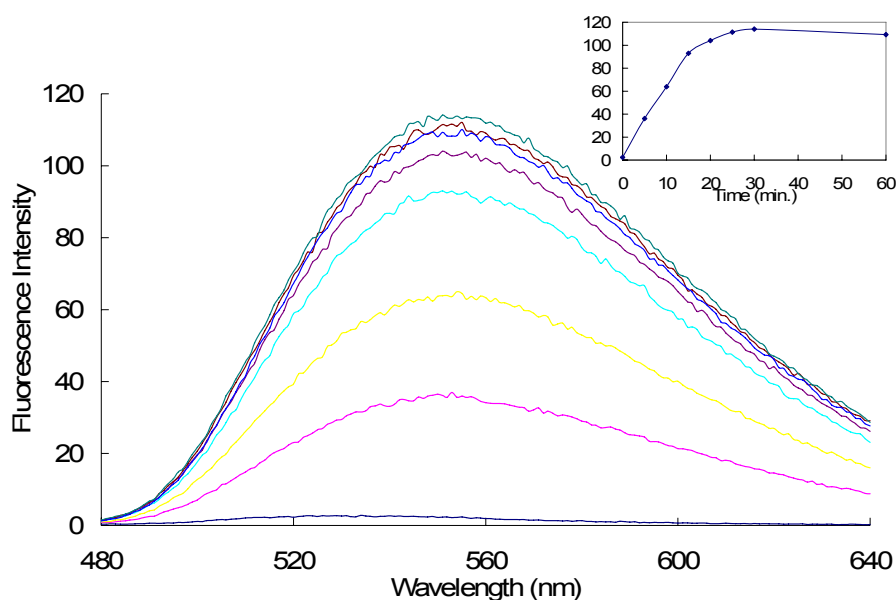
#### 2.3.3.1. The sensitivity towards selenocysteine.

The experiment was performed in an aqueous phosphate buffer ( $I = 0.01\text{M}$ , pH 7.3) containing **1** at a concentration of  $2.0 \times 10^{-5}\text{M}$ . Selenocysteine was generated from the reduction of  $(\text{CysSe})_2$  by excess amounts (10 equivalents) of dithiothreitol (DTT) to make sure the reaction was performed under reductive circumstance (Scheme 2.5).

#### Scheme 2.5. Generation of selenocysteine from $(\text{CysSe})_2$

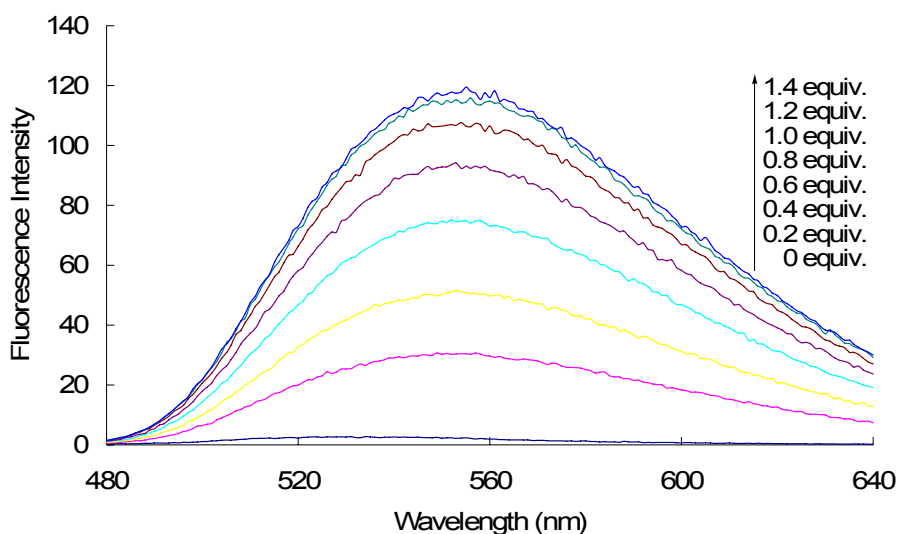


Originally, free sensor **1** is non-fluorescent in the solution as we have shown before. However, when  $4.0 \times 10^{-5}$  M selenocysteine (generated from  $2.0 \times 10^{-5}$  M of  $(\text{CysSe})_2$  and  $2.0 \times 10^{-4}$  M of DTT) was added, a significant increase of fluorescence intensity ( $>40$  times) centered at 555 nm was observed in a few minutes. The reaction product was monitored and confirmed to be compound **2** as we expected by a comparison study with a standard pure **2** through  $^1\text{H}$  NMR analysis. Notably sensor **1** showed a very sensitive response toward selenocysteine, pronounced signals was obtained even after only 5 minutes. The reaction reached completion after around 30 minutes and a limited change of fluorescence intensity was observed when longer reaction times were examined (Figure 2.19). Therefore, a reaction time of 30 min was selected to explore the sepecificity of probe **1** toward selenocysteine.



**Figure 2.19.** Emission time profile of sensor **1** towards selenocysteine. Sensor **1** ( $2 \times 10^{-5}$  M), prepared from a stock solution (10 mM) in EtOH, was studied in a phosphate buffer (pH 7.3, 0.01M) at room temperature in the absence and presence of selenocysteine generated by  $(\text{CysSe})_2$  (1.0 equivalent) and DTT (equivalents). The reaction solution was sampled for fluorescence measurement at  $\lambda_{\text{ex}} = 465$  nm at the specified time periods and emission intensity was acquired at 555 nm.

Next the sensitivity of this sensor **1** at  $2 \times 10^{-5}$  M was examined with a concentration of  $(\text{CySe})_2$  ranging from 0.2 to  $1.4 \times 10^{-5}$  M (0.2 equiv. to 1.4 equiv.) under the same reaction conditions described above (Figure 2.20). The increase of fluorescence intensity was displayed in a concentration dependent manner. When more than 1.2 equivalents of  $(\text{CySe})_2$  were used, the enhancement of fluorescence intensity almost reached a maximum without much further alteration. Correspondingly, a red shift of fluorescence spectrum was also observed from the maximum of 528 nm to 555 nm like previous experiments for thiophenols. Notably, a pronounced change in the fluorescence signal was observed even when the concentration of  $(\text{CySe})_2$  was as low as  $2 \times 10^{-6}$  M.

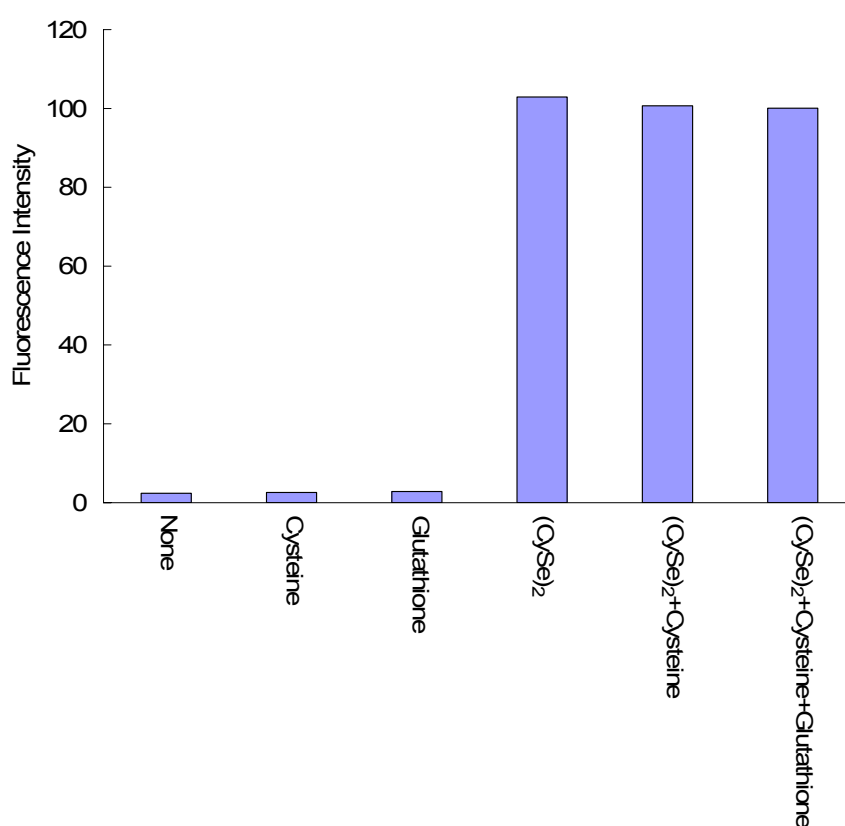


**Figure 2.20.** Fluorescence response of the sensor **1** ( $2 \times 10^{-5}$  M) toward selenocysteine generated from  $(\text{CysSe})_2$  and dithiothreitol (DTT). These data were measured at 20 minutes after addition of different amounts of  $(\text{CysSe})_2$  with DTT (10 equiv.) in a pH 7.3 phosphate buffer at room temperature with  $\lambda_{\text{ex}} = 465$  nm.

### 2.3.3.2. The specificity towards selenocysteine.

In order to examine the specificity of sensor towards selenocysteine, some

common biological thiols including cysteine and glutathione were probed in the same condition. As shown in Figure 2.21, sensor **1** was highly selective to selenocysteine and almost no fluorescence intensity change was seen for cysteine, glutathione. More significantly, in the presence of these biological thiols, a similar fluorescence intensity increase was observed to that of a pure selenocysteine, which indicates that probe **1** is particularly selective toward selenocysteine without interference.



**Figure 2.21.** The selectivity of sensor **1** toward SeCys and bio-thiols. Sensor **1** ( $2 \times 10^{-5}$  M) was studied in a phosphate buffer (pH 7.3, 0.01M) at room temperature in the presence of various analytes (2.0 equivalents each). After 30 min, the reaction solution was sampled for fluorescence measurement at  $\lambda_{\text{ex}} = 465$  nm. The fluorescence intensity at  $\lambda_{\text{em}} = 555$  nm is plotted vs. analytes.

### 2.3.4. Conclusion

We successfully employed sensor **1** as the first fluorescent probe for the detection of selenocysteine and differentiate it from bio-thiols such as cysteine and glutathione

in the physiological condition. Dramatic fluorescence intensity enhancement was seen towards selenocysteine as a result of effective cleavage of the electronwithdrawing 2,4-dinitrobenzenesulfonyl moiety from nonfluorescent sensor **1**, to generate highly fluorescent **2** in an aqueous solution with very short reaction times. Moreover, sensor **1** has a fluorescence emission wavelength more than 500 nm, which make it suitable for the in vivo study. Therefore, probe **1** potentially can be used as a tool not only for the detection of either known or unknown selenoproteins, but also study of their functionality and mechanism in the biological system.

## **2.4. Experimental Section**

### **General information.**

Commercial reagents were used as received, unless otherwise stated. Merck 60 silica gel was used for chromatography, and Whatman silica gel plates with fluorescence F254 were used for thin-layer chromatography (TLC) analysis.  $^1\text{H}$  and  $^{13}\text{C}$  NMR spectra were recorded on Bruker Avance 500, and tetramethylsilane (TMS) was used as a reference. Data for  $^1\text{H}$  are reported as follows: chemical shift (ppm), and multiplicity (s = singlet, d = doublet, t = triplet, q = quartet, m = multiplet). Data for  $^{13}\text{C}$  NMR are reported as ppm. Mass Spectra were obtained from University of New Mexico mass spectral facility.

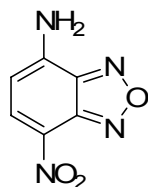
### **Spectroscopic materials and methods.**

Millipore water was used to prepare all aqueous solutions. The pH was recorded by a Beckman  $\Phi\text{TM}$  240 pH meter. UV absorption spectra were recorded on a Shimadzu UV-2410PC UV-Vis spectrophotometer. Fluorescence emission spectra were obtained on a Varian Eclipse fluorescence spectrophotometer.



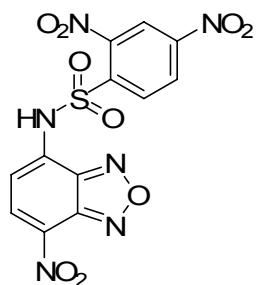
## Synthesis of Sensor 1

Sensor 1 was synthesized following the procedures in Scheme 2.3.



### 4-Amino-7-nitrobenzofurazane (2).

To a solution of 4-Chloro-7-nitro-benzofurazan (NBD-Cl, 204 mg, 1 mmol) in MeOH (20 mL) was added ammonium hydroxide (4 mL, 30% in water) at room temperature. The reaction solution was stirred at room temperature for 24h under a nitrogen atmosphere. The solvent was evaporated *in vacuo*, then the crude product was purified by silica gel chromatography with 50% ethyl acetate in hexane to afford desired product as a dark green solid (108 mg, 0.6 mmol, yield 60%). <sup>1</sup>H NMR (500 MHz, d<sub>4</sub>-MeOH): δ 8.47 (d, 1H, *J* = 9.0 Hz), 6.39 (d, 1H, *J* = 9.0 Hz); <sup>13</sup>C NMR (125 MHz, d<sub>4</sub>-MeOH): δ 148.7, 145.8, 145.7, 138.6, 123.4, 103.3.

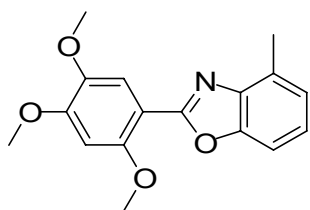


### 2,4-dinitro-N-(7-nitrobenzo[c][1,2,5]oxadiazol-4-yl)benzenesulfonamide (1).

To a solution of **2** (17 mg, 0.094 mmol) in anhydrous THF (2 mL) was added NaH (3.4 mg, 0.141 mmol) at 0 °C. After stirring for 15 minutes, 2,4-dinitrobenzenesulfonyl chloride (38 mg, 0.141 mmol) in 1ml anhydrous THF was added dropwise to the reaction mixture. Warmed the reaction mixture to room temperature and stirred for another 1h. Then the reaction mixture was quenched with sat. NaHCO<sub>3</sub> and extracted with 20 mL ethyl acetate 2 times. The combined organic layers were washed with brine, dried with magnesium sulfate and then filtered and evaporated *in vacuo*. The crude product was purified by silica gel chromatography with 30% hexane in acetyl acetate and afforded desired product as an orange solid (24 mg, 0.053 mmol, yield 62%). <sup>1</sup>H NMR (500 MHz, d<sub>4</sub>-MeOH): δ 8.58 (d, 1H, *J* = 2.0 Hz), 8.50 (dd, 1H, *J*<sub>1</sub> = 8.5 Hz, *J*<sub>2</sub> = 2.0 Hz), 8.40 (t, 2H, *J* = 9.0 Hz); <sup>13</sup>C NMR (125 MHz, d<sub>4</sub>-MeOH): δ 150.8, 150.6, 150.3, 149.6, 145.6, 142.0, 137.4, 132.9, 127.5, 125.2, 120.7, 110.3.

### Synthesis of sensor **3**

Sensor **3** was synthesized following the procedures in Scheme 2.4.

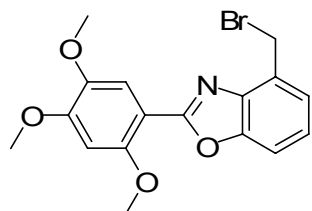


### 4-methyl-2-(2,4,5-trimethoxyphenyl)benzo[d]oxazole (**6**).

A mixture of 2,4,5-trimethoxybenzaldehyde (1.96 g, 10 mmol) and

2-amino-*m*-cresol (1.23 g, 10 mmol) in 100 mL benzene was refluxed for 24 h under a nitrogen atmosphere with an Dean-stark apparatus to remove water. The reaction mixture was cooled down to room temperature and the solvent was removed in *vacuo* to afford the Schiff base compound **5** as a dark orange solid, which was used for the next reaction without further purification.

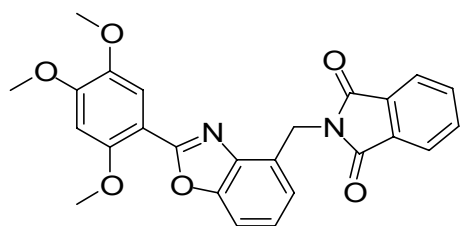
To a solution of unpurified **5** in 100 mL dry benzene was added BaMnO<sub>4</sub> (10.3 g, 40 mmol) and the solution was refluxed for 6 hours under a nitrogen atmosphere. After the reaction mixture was cooled down to room temperature, BaMnO<sub>4</sub> was removed through Celite and the filtrate was concentrated in *vacuo*. The black residue was purified by silica gel chromatography using ethyl acetate/hexane (1:2) as elute to afford **6** as a pale yellow solid in 66 % yield. <sup>1</sup>H NMR (500 MHz, CDCl<sub>3</sub>): δ 7.67 (s, 1H), 7.39 (d, 1H, J = 8.0 Hz), 7.20 (t, 1H, J = 8.0 Hz), 7.11 (d, 1H, J = 7.0 Hz), 6.63 (s, 1H), 3.98 (s, 3H), 3.96 (s, 6H), 2.69 (s, 3H); <sup>13</sup>C NMR (125 MHz, CDCl<sub>3</sub>): δ 161.3, 154.0, 152.6, 150.3, 143.4, 141.4, 130.2, 124.9, 124.3, 113.5, 108.1, 107.8, 98.1, 57.3, 56.6, 56.2, 16.8.



#### **4-(bromomethyl)-2-(2,4,5-trimethoxyphenyl)benzo[d]oxazole (7).**

A mixture of **6** (345 mg, 1.15 mmol), *N*-bromosuccinimide (218 mg, 1.21 mmol), and AIBN (20 mg, 0.12 mmol) in 30 mL anhydrous CCl<sub>4</sub> was refluxed for 10 h under

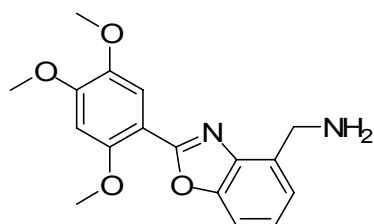
a nitrogen atmosphere. The reaction mixture was cooled to 0 °C and the precipitate was removed by filtration while maintaining the temperature at 0 °C. After the solvent was evaporated, the residue was directly purified by silica gel chromatography using ethyl acetate/hexane (1:2) as elute to afford **7** in 83% yield. <sup>1</sup>H NMR (500 MHz, CDCl<sub>3</sub>): δ 7.69 (s, 1H), 7.51 (d, 1H, J = 7.5 Hz), 7.39 (d, 1H, J = 7.5 Hz), 7.28 (q, 1H, J = 8.0 Hz), 6.63 (s, 1H), 4.97 (s, 2H), 4.00 (s, 3H), 3.99 (s, 6H); <sup>13</sup>C NMR (125 MHz, CDCl<sub>3</sub>): δ 162.5, 154.3, 153.1, 150.7, 143.6, 140.9, 129.3, 125.4, 124.7, 113.6, 110.6, 107.8, 98.3, 57.5, 56.7, 56.3, 28.3.



**2-((2-(2,4,5-trimethoxyphenyl)benzo[d]oxazol-4-yl)methyl)isoindoline-1,3-dione (8).**

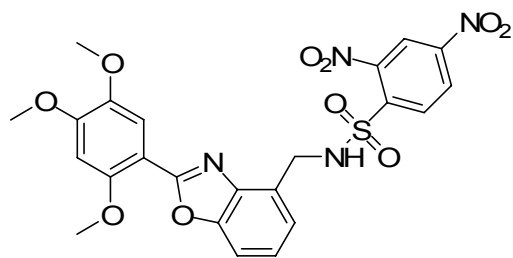
A mixture of **7** (320 mg, 0.85 mmol) and potassium phthalimide (176 mg, 0.93 mmol) in 30 mL DMF was heated at 50 °C for 8 h under a nitrogen atmosphere. The reaction mixture was cooled to room temperature and the solvent was removed in *vacuo*. The residue was dissolved in water and extracted with dichloromethane (3×20 mL). The combined organic layer was washed by brine, dried with magnesium sulfate, filtered and evaporated in *vacuo*. The residue was purified by silica gel chromatography using ethyl acetate/hexane (2:3) as elute to afford **8** in 90% yield. <sup>1</sup>H NMR (500 MHz, CDCl<sub>3</sub>): δ 7.88 (s, 2H), 7.71(s, 2H), 7.58 (s, 1H), 7.47 (s, 1H),

7.27-7.19 (m, 2H), 6.61 (s, 1H), 3.96 (s, 6H), 3.90 (s, 3H);  $^{13}\text{C}$  NMR (125 MHz,  $\text{CDCl}_3$ ):  $\delta$  168.3, 162.1, 154.3, 152.9, 150.8, 143.5, 140.4, 134.1, 132.6, 127.7, 124.5, 123.5, 122.5, 113.7, 109.8, 108.1, 98.4, 57.4, 56.7, 56.3, 37.9.



**(2-(2,4,5-trimethoxyphenyl)benzo[d]oxazol-4-yl)methanamine (4).**

A mixture of **8** (280 mg, 0.63 mmol) and hydrazine (0.8 mL, 25 mmol) in 20 mL THF was refluxed for 2 h under a nitrogen atmosphere, during which a large amount of white solid appeared. The reaction mixture was cooled to room temperature and the solvent was removed in *vacuo*. The residue was dissolved in 10 mL ethyl acetate, 10 mL HCl (1N) was added and the mixture solution for 30 minutes. Aqueous layer was separated and the organic layer was exacted with 1N HCl (2×10 mL). Combined the aqueous layers and concentrated to 10 mL. Sodium hydroxide was added to just the pH of solution to 13, which was then extracted with dichloromethane (3×20 mL). The combined organic layer was washed by brine, dried with magnesium sulfate, filtered and evaporated in *vacuo* to afford **4** in 75% yield.  $^1\text{H}$  NMR (500 MHz,  $\text{CDCl}_3$ ):  $\delta$  7.66 (s, 1H), 7.454 (d, 2H,  $J = 7.5$  Hz), 7.25-7.21 (m, 2H), 6.62 (s, 1H), 4.27 (s, broad, 2H), 3.98 (s, 3H), 3.95 (s, 6H);  $^{13}\text{C}$  NMR (125 MHz,  $\text{CDCl}_3$ ):  $\delta$  161.5, 154.0, 152.7, 150.5, 143.3, 140.3, 135.1, 124.4, 122.4, 113.4, 108.9, 107.8, 98.1, 57.2, 56.5, 56.1, 42.9.

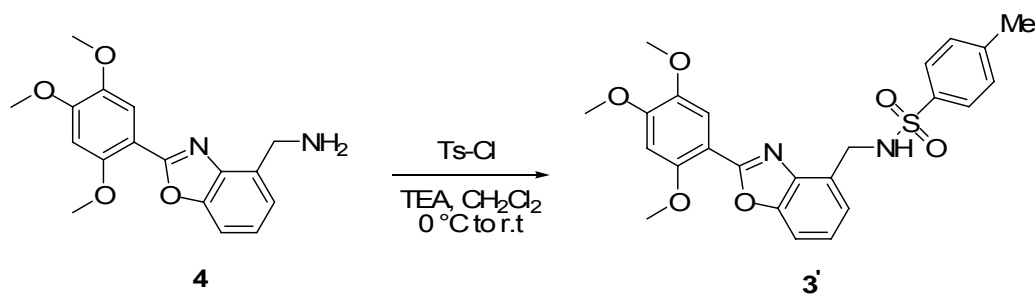


**2,4-dinitro-N-((2-(2,4,5-trimethoxyphenyl)benzo[d]oxazol-4-yl)methyl)benzenesulfonamide (3).**

To a solution of **4** (150 mg, 0.478 mmol) and pyridine (116  $\mu$ L, 1.433 mmol) in 30 mL dichloromethane was added 2,4-dinitrobenzenesulfonyl chloride (158 mg, 0.573 mmol) in 2 mL dichloromethane dropwise at 0  $^{\circ}$ C. The reaction solution was stirred overnight under a nitrogen atmosphere and let it warm up to room temperature gradually, during which yellow solid appeared. The solvents were evaporated *in vacuo*. The residue was dissolved in 50 mL chloroform and washed with 1N HCl and brine, dried with magnesium sulfate, filtered and evaporated *in vacuo*. The residue was recrystallized in dichloromethane to give **3** as bright yellow solid in 50% yield.  $^1\text{H}$  NMR (500 MHz, DMSO- $d_6$ ):  $\delta$  9.06 (s, 1H), 8.72 (s, 1H), 8.36 (d, 1H,  $J = 8.0$  Hz), 8.04 (d, 1H,  $J = 8.5$  Hz), 7.59 (d, 1H,  $J = 4.0$  Hz), 7.51 (s, 1H), 7.29 (s, 2H), 6.87 (s, 1H), 4.61 (d, 2H,  $J = 5.0$  Hz), 3.92 (s, 6H), 3.82 (s, 3H);  $^{13}\text{C}$  NMR (125 MHz, DMSO- $d_6$ ):  $\delta$  161.6, 153.8, 153.2, 149.6, 149.2, 147.4, 142.7, 139.5, 138.1, 131.2, 127.7, 126.6, 124.5, 123.5, 119.7, 113.4, 109.7, 105.8, 98.6, 56.7, 56.2, 55.9, 41.9.

**Synthesis of sensor 3'.**

Sensor **3'** was synthesized following the procedure in the scheme below:



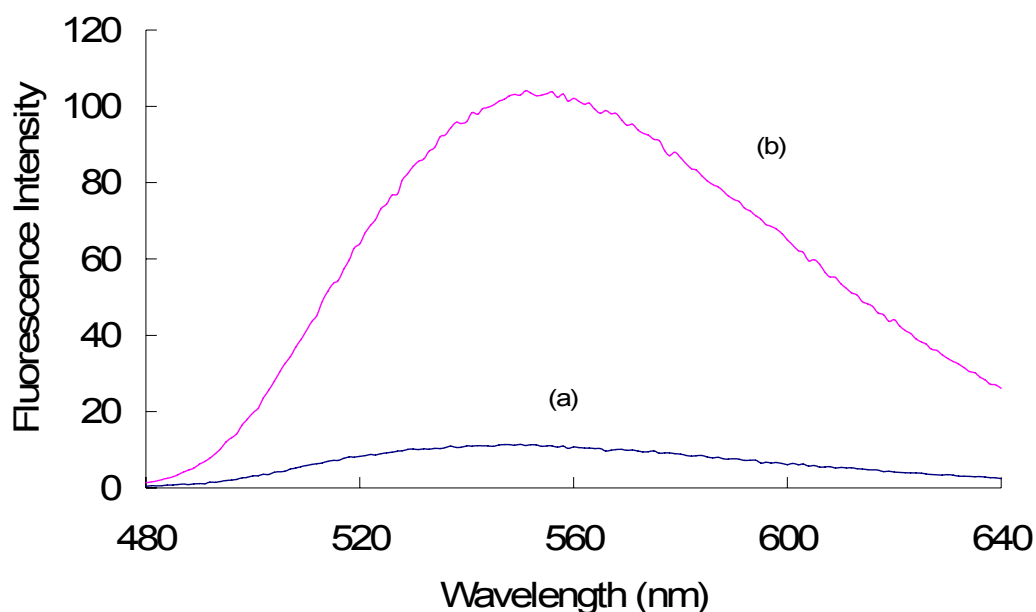
**4-methyl-N-((2-(2,4,5-trimethoxyphenyl)benzo[d]oxazol-4-yl)methyl)benzenesulfonamide (3').**

To a solution of **4** (32 mg, 0.10 mmol) and triethylamine (40  $\mu$ L, 0.3 mmol) in 3 mL dichloromethane was added p-toluenesulfonyl chloride (29 mg, 0.15 mmol) at 0  $^{\circ}$ C. The reaction solution was stirred 3 h under a nitrogen atmosphere and let the solution warmed up to room temperature gradually. The residue was washed with water, and the aqueous layer was extracted with dichloromethane (2 $\times$ 10 mL). The combined organic layer was washed by brine, dried with magnesium sulfate, filtered and evaporated in *vacuo*. The residue was purified by silica gel chromatography to afford **3'** in 92% yield.  $^1\text{H}$  NMR (500 MHz, DMSO- $d_6$ ):  $\delta$  7.64 (d, 2H,  $J$  = 8.0 Hz), 7.61 (s, 1H), 7.38 (d, 1H,  $J$  = 8 Hz), 7.15 (t, 1H,  $J$  = 8.0 Hz), 7.05 (d, 3H,  $J$  = 7.5 Hz), 6.66 (s, 1H), 6.50 (t, 1H,  $J$  = 5.5 Hz), 4.57 (d, 2H,  $J$  = 5.5 Hz), 4.04 (s, 3H), 4.00 (s, 3H), 3.98 (s, 3H), 2.30 (s, 3H);  $^{13}\text{C}$  NMR (125 MHz,  $\text{CDCl}_3$ ):  $\delta$  161.5, 154.6, 153.3, 150.2, 143.5, 140.2, 137.1, 129.3, 127.4, 127.2, 124.5, 123.3, 113.2, 109.6, 107.1, 98.0, 57.2, 56.8, 56.3, 45.0, 21.6.

### Preparation of selenocysteine by (CysSe)<sub>2</sub> and DTT.

To 10 mL degassed phosphate buffer (pH 7.3, I = 0.01 M) was added 0.1 mmol (CysSe)<sub>2</sub> followed with 1 mmol DTT and stirred the solution for 30 minutes under a nitrogen atmosphere, during which (CysSe)<sub>2</sub> solid was gradually dissolved. Then this solution was used immediately for the fluorescence experiments of sensor **1**.

**Examine the effect of DTT on the fluorescence response of sensor 1 towards selenocysteine.**



**Figure 2.22.** Effect of DTT on the fluorescent response of sensor **1** towards selenocysteine. (a) Emission spectra of the probe ( $2 \times 10^{-5} \text{M}$ ) towards dithiothreitol (DTT) ( $2 \times 10^{-4} \text{M}$ ); (b) Emission spectra of the probe ( $2 \times 10^{-5} \text{M}$ ) towards (CysSe)<sub>2</sub> ( $2 \times 10^{-5} \text{M}$ ) and dithiothreitol (DTT) ( $2 \times 10^{-4} \text{M}$ ). These data were measured at 30 minutes after addition of DTT without/with (CysSe)<sub>2</sub> in a pH 7.3 phosphate buffer at room temperature with the excitation of 465nm.

The reaction of dithiothreitol (DTT) as an aliphatic thiol was much slower than selenols. For  $2 \times 10^{-5} \text{M}$  of sensor **1**, after only addition of  $2 \times 10^{-4} \text{M}$  of DTT (20 equiv.



of “SH”) 30 minutes, very little fluorescence intensity increase was obtained (about 10 a.u.). However, if we added  $2 \times 10^{-5}$  M of (CySe)<sub>2</sub> as well as  $2 \times 10^{-4}$  M of DTT, significant fluorescence signals was observed after 30 minutes. This result indicates that major fluorescence intensity increase was caused by the reaction of sensor **1** with selenocysteine, and biological thiols have very limited effects on sensor **1**.

## 2.5. Reference

1. (a) Fersht, A. *Enzyme Structure and Mechanism, 2nd ed., Freeman, New York, 1984*, pp. 2 – 4. (b) Shahrokhian, S. *Anal. Chem.* **2001**, *73*, 5972.
2. An irregular level of homocysteine is associated with a variety of diseases, such as cardiovascular-related and AlzheimerBs diseases. For a review, see: (a) Refsum, H.; Ueland, P. M.; NygErd, O. and Vollset, S. E. *Annu. Rev. Med.* **1989**, *40*, 31. (b) Seshadri, S.; Beiser, A.; Selhub, J.; Jacques, P. F.; Rosenberg, I. H.; D'Agostino, R. B. and Wilson, P.W. F. *N. Engl. J. Med.* **2002**, *346*, 476.
3. Rahman, I. and MacNee, W. *Free Radical Biol. Med.* **2000**, *28*, 1405.
4. Thiols are useful chemicals in organic synthesis, analytical chemistry, and materials science. For applications, see: “Thiols and Organic Sulfides”, (a) Roy K. M. in *Ullmann-s Encyclopedia of Industrial Chemistry, 7th ed., Wiley, NewY ork, 2007*. (b) Shimada, K. and Mitamura, K. *J. Chromatogr. B.* **1994**, *659*, 227. (c) Love, J. C.; Estroff, L. A.; Kriebel, J. K.; Nuzzo, R. G. and Whitesides, G. M. *Chem. Rev.* **2005**, *105*, 1103. (d) EychmKller, A. and Rogach, A. L. *Pure Appl. Chem.* **2000**, *72*, 179.
5. Heil, T. P. and Lindsay, R. C. *J. Environ. Sci. Health Part B.* **1989**, *24*, 349.
6. (a) Amrolia, P.; Sullivan, S. G.; Stern, A. And Munday, R. *J. Appl. Toxicol.* **1989**, *9*, 113. (b) Munday, R. *J. Appl. Toxicol.* **1985**, *5*, 402. (c) Juneja, T. R.; Gupta, R. L. and Samanta, S. *Toxicol. Lett.* **1984**, *21*, 185. (d) Fairchild II, E. J. and Stokinger, H. E. *Am. Ind. Hyg. Assoc. J.* **1958**, *19*, 171.
7. (a) Material safety data sheet of thiophenol from Sigma–Aldrich:

- [http://www.castleviewuk.com/Frameless/Safe/msds/ex/MSDS\\_thiophenol.htm](http://www.castleviewuk.com/Frameless/Safe/msds/ex/MSDS_thiophenol.htm). (b) Health Council of the Netherlands: Committee on Updating of Occupational Exposure Limits. Benzenethiol: Health-Based Reassessment of Administrative Occupational Exposure Limits, 2000/15OSH/095, Health Council of the Netherlands, The Hague, **2004**. (c) Anon, USA, *Dangerous Properties of Industrial Materials Report*, **1994**, 14, 92.
8. (a) Ekinci, E.; Yardim, F.; Razvigorova, M.; Minkova, V.; Goranova, M.; Petrov, N. and Budinova, T. *Fuel Process. Technol.* **2002**, 77–78, 309. (b) Zhao, H. and Xia, D. H. *Prepr. Am. Chem. Soc. Div. Pet. Chem.* **2002**, 47, 323. (c) Xia, D. H.; Zhu, G. Q.; Yin, C. L.; Xiang, Y. Z.; Su, Y. X. and Qian, J. *Petrol. Sci. Technol.* **2002**, 20, 17. (d) Fan, Z. M.; Ke, M. and Liu, X. F.; *Shiyou Daxue Xuebao Ziran Kexueban.* **1998**, 22, 86. (e) Shmakov, V. S.; Ulendeeva, A. D.; Lyapina, N. K. and Furlei, I. I. *Neftekhimiya.* **1989**, 29, 14. (f) Lyapina, N. K.; Shmakov, V. S.; Parfenova, M. A. and Zinchenko, L. I. *Neftekhimiya.* **1989**, 29, 165.
9. Shirokov, Y. G. *Kauch. Rezina.* **1959**, 18, 43.
10. Schwarzbauer, J.; Heim, S.; Brinker, S. and Littke, R. *Water Res.* **2002**, 36, 2275.
11. For a review of methods using HPLC or capillary electrophoresis, see: (a) Nekrassova, O.; Lawrence, N. S. and Compton, R. G. *Talanta.* 2003, **60**, 1085. (b) Refsum, H.; Smith, A. D.; Ueland, P. M.; Nexø, E.; Clarke, R.; McPartlin, J.; Johnston, C.; Engbaek, F.; Schneede, J.; McPartlin, C. and Scott, J. M. *Clin. Chem.* **2004**, 50, 3.
12. Haugland, R. P. *Handbook of Fluorescent Probes and Research Products*, 9th ed.,

*Molecular Probes, Eugene. 2002, 79.*

13. Ellman method: (a) Ellman, G. L. *Arch. Biochem. Biophys.* **1959**, 82, 70. (b) Ellman, G. L.; Courtney, K. D.; Andres, Jr., V. and Featherstone, R. M. *Biochem. Pharmacol.* **1961**, 7, 88.
14. For recent examples of fluorescent probes for the detection of thiols, see: (a) Chow, C.; Chiu, B. K. W.; Lam, M. H.W. and Wong, W. *J. Am. Chem. Soc.* **2003**, 125, 7802. (b) Kim, D. H. and Han, M. S. *Bioorg. Med. Chem. Lett.* **2003**, 13, 2543. (c) Rusin, O.; Luce, N. N. St.; Agbaria, R. A.; Escobedo, J. O.; Jiang, S.; Warner, I. M. and Strongin, R. M. *J. Am. Chem. Soc.* **2004**, 126, 438. (d) Wang, W. H.; Escobedo, J. O.; Lawrence, C. M. and Strongin, R. M. *J. Am. Chem. Soc.* **2004**, 126, 3400. (e) Tanaka, F.; Mase, N. and Barbas III, C. F. *Chem. Commun.* **2004**, 1762. (f) Chen, S. J. and Chang, H. T. *Anal. Chem.* **2004**, 76, 3727. (g) Ros-Lis, J. V.; Garcia, B.; Jimenez, D.; Martinez-Manez, R.; Sanceron, F.; Soto, J.; Gonzalvo, F. and Valdecabres, M. C. *J. Am. Chem. Soc.* **2004**, 126, 4064. (h) Wang, W. H.; Rusin, O.; Xu, X. Y.; Kim, K. K.; Escobedo, J. O.; Fakayode, S. O.; Fletcher, K. A.; Lowry, M.; Schowalter, C. M.; Lawrence, C. M.; Fronczek, F. R.; Warner, I. M. and Strongin, R. M. *J. Am. Chem. Soc.* **2005**, 127, 15949. (i) Li, S. H.; Yu, C. W. and Xu, J. G. *Chem. Commun.* **2005**, 450. (j) Maeda, H.; Matsuno, H.; Ushida, M.; Katayama, K.; Saeki, K. and Itoh, N. *Angew. Chem.* **2005**, 117, 2982; *Angew. Chem. Int. Ed.* **2005**, 44, 2922. (k) Fu, Y. Y.; Li, H. X.; Hu, W. P. and Zhu, D. B. *Chem. Commun.* **2005**, 3189. (l) Fu, N. N.; Wang, H.; Li, M. L.; Zheng, G. J.; Zhang, H. S. and Liang, S. C. *Anal. Lett.* **2005**, 38, 791. (m) Maeda,

- H.; Katayama, K.; Matsuno, H. and Uno, T. *Angew. Chem.* **2006**, *118*, 1842;  
*Angew. Chem. Int. Ed.* **2006**, *45*, 1810. (n) Pullela, P. K.; Chiku, T.; Carvan III, M.  
J. and Sem, D. S. *Anal. Biochem.* **2006**, *352*, 265.
15. (a) Adamczyk, M. and Grote, J. *Bioorg. Med. Chem. Lett.* **2003**, *13*, 2327. (b)  
Mandala, M.; Serck-Hanssen, G.; Martino, G. and Helle, K.B. *Anal. Biochem.*  
**1999**, *274*, 1. (c) Haugland R.P. *Handbook of fluorescent probes and research  
chemicals, sixth ed., Molecular Probes, Eugene OR, 1996.* (d) Adamczyk, M. and  
Grote, J. *Bioorg. Med. Chem. Lett.* **2000**, *10*, 1539.
16. (a) Müller, P. and Phuong, N. T. M. *Helv. Chim. Acta.* **1979**, *62*, 494. (b)  
Fukuyama, T.; Cheung, M.; Jow, C. K.; Hidai, Y. and Kan, T. *Tetrahedron Lett.*  
**1997**, *38*, 5831.
17. Ghosh, P. B. and Whitehouse, M.W. *Biochem. J.* **1968**, *108*, 155.
18. For reviews on the design of fluorescent sensors, see: (a) Rettig, W. *Angew. Chem.*  
**1986**, *98*, 969; *Angew. Chem. Int. Ed. Engl.* **1986**, *25*, 971. (b) Scheller, F.W.;  
Schubert, F. and Fedrowitz, J. *Frontiers in Biosensorics I: Fundamental Aspects,*  
*BirkhRuser, Berlin, 1997.* (c) Scheller, F.W. and Schubert, F. *J. Fedrowitz,*  
*Frontiers in Biosensorics II: Practical Applications, BirkhRuser, Berlin, 1997.* (d)  
de Silva, A. P.; Gunaratne, H. Q. N.; Gunnlaugsson, T.; Uhxley, A. J.; McCoy,  
M. C. P.; Rademacher, J. T. and Rice, T. E. *Chem. Rev.* **1997**, *97*, 1515. (e) Pu, L.  
*Chem. Rev.* **2004**, *104*, 1687.
19. (a) Uchiyama, S; Santa, T. and Imai, K. *J. Chem. Soc., Perkin Trans. 2.* **1999**,  
2525. (b) Uchiyama, S.; Santa, T.; Fukushima, T.; Homma, H. and Imai, K. *J.*

- Chem. Soc., Perkin Trans. 2*, **1998**, 2165. (c) Uchiyama, S.; Santa T. and Imai, K. *J. Chem. Soc., Perkin Trans. 2*. **1999**, 569. (c) Heberer H. and Matschiner, H. *J. Prakt. Chem.* **1986**, 328, 261. (d) Lin S. and Struve, W. S. *Photochem. Photobiol.* **1991**, 54, 361. (e) Forgues, S. F.; Fayet J. P. and Lopez, A. *J. Photochem. Photobiol. A: Chem.* **1993**, 70, 229.
20. For reviews on the selenium biochemistry, see: (a) Stadtman, T. C. *Annu. Rev. Biochem.* **1990**, 59, 111. (b) Stadtman, T. C. *J. Biol. Chem.* **1991**, 266, 16257. (c) Stadtman, T. C. *Adv. in Inorg. Biochem.* **1994**, 10, 157. (d) Stadtman, T. C. *Annu. Rev. Biochem.* **1996**, 65, 83. (e) Böck, A; Forchhammer, K.; Heider, J.; Bardon, C. *Trends Biochem. Sci.* **1991**, 16, 463. (f) Böck, A; Forchhammer, K.; Heider, J.; Leinfelder, W.; Sawers, G.; Veprek, B. and Zinoni, F. *Mol. Microbiol.* **1995**, 5, 515.
21. (a) Rayman, M. P. *Lancet.* **2000**, 356, 233. (b) Schomburg, L.; Schweizer, U. and Kfhrle, J. *Cell. Mol. Life Sci.* **2004**, 61, 1988. (c) Driscoll, D. M. and Copeland, P. R. *Annu. Rev. Nutr.* **2003**, 23, 17. (d) Arthur, J. R. *Cell. Mol. Life Sci.* **2000**, 57, 1825. (e) Mustacich, D. and Powis, G. *Biochem. J.* **2000**, 346, 1.
22. Zinoni, F.; Birkmann, A.; Stadtman, T. C. and Büick, A. *Proc. Natl. Acad. Sci. USA.* **1986**, 83, 4650.
23. Chambers, I.; Frampton, J.; Goldfarb, P.; Affara, N.; McBain, W. and Harrison, P. P. *EMBO J.* **1986**, 5, 1221.
24. Leinfelder, W.; Zehelin, E.; Mandrand-Berthelot, M. A. and Bock, A. *Nature.* **1988**, 331, 723.

25. Hawkes, W. C. and Kutnink, M. A. *J. Chromatogr.* **1992**, 576, 263.
26. Zheng, J.; Shibata, Y. and Furuta, N. *Talanta.* **2003**, 59, 27.
27. Encinar, J. R.; Schaumöffel, D.; Ogra, Y. and Lobinski, R. *Anal. Chem.* **2004**, 76, 6635.
28. Iscioglu, B. and Henden, E. *Anal. Chim. Acta.* **2004**, 505, 101.
29. Gómez-Ariza, J. L.; Caro de la Torre, M. A.; Giráldez, I. and Morales, E. *Anal. Chim. Acta.* **2004**, 524, 305.
30. Maeda, H.; Katayama, K.; Matsuno, H. and Uno, T. *Angew. Chem. Int.Ed.* **2006**, 45, 1810.

## Chapter 3

### Development of Sensors for the Detection of Explosive Peroxy Acids

#### 3.1. Introduction

The development of highly sensitive and selective sensing technologies for the detection of highly explosive peroxides is of considerable healthy, scientific and economic importance. Although very popular in labs and industry, explosive peroxides are among the greatest hazards that lab researchers and workers can come across since they are shock-sensitive and spark-sensitive.<sup>1</sup> More seriously, an increasing number of incidents that involved the use of these explosive chemicals by terrorism groups have created a significant threat to the security, stability and economy of our society.<sup>2</sup> For example, terrorists used peroxides as explosives for the Madrid, Spain train bombings of March, 2004, which killed hundreds of innocent people and for the July 7<sup>th</sup>, 2005 bombings in London, UK, which killed at least 54 people and injured hundreds.<sup>2c</sup>

**Figure 3.1.** Photographs of Spain bombings in 2004 (left) and London bombings in 2005 (right).





One reason why peroxides have become one of the major chemicals for bomb production by terrorist groups is that these substances are readily accessed since they are commercially available<sup>3</sup> or easily made in a straightforward manner from readily available precursor chemicals.<sup>4</sup> The second reason is that these odorless chemicals can be easily concealed for entry into airplanes, trains and other public transportation means because they cannot be detected by sniffer dogs. Furthermore, peroxides cannot be detected by conventional explosive detection devices, which like those used at airports rely typically on the presence of nitro compounds or metals for detection.<sup>5</sup> Accordingly the detection of odorless peroxides represents a formidable challenge.

The currently available methods used for the detection of peroxides are limited to infrared and Raman spectroscopy,<sup>6</sup> HPLC,<sup>7</sup> enzyme-based assays,<sup>8</sup> electrochemistry,<sup>9</sup> and mass spectrometry.<sup>10</sup> While peroxides can be measured by using these techniques, the methods either have limited detection sensitivity and/or slow responsive times, complicated and highly technical procedures for their use, or the need for large expensive instrumentation. These drawbacks have thus far limited their practical applications. Therefore, an urgent need exists for the development of simple methods for the direct detection of peroxides without the requirements of sample pre-treatment, and with high sensitivity, selectivity and operational simplicity. A great number of efforts have focused on the development of detection methods for TATP.<sup>7f,10</sup> However, highly sensitive sensors for probing other explosive peroxides such as readily accessible peroxy acids and benzoyl peroxide, have been much less explored despite the fact that they are also strong explosives and could be used in arson and explosion

incidents.<sup>11</sup> Therefore, we wish to develop highly sensitive and selective fluorescence sensor for the direct and rapid detection of explosive epoxides that do not require the use of complicated procedures and expensive facilities.

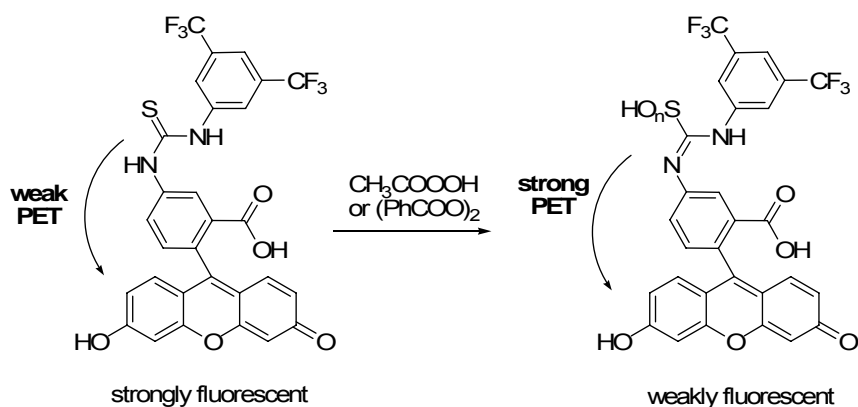
Fluorescence methods are known to provide high sensitivity, easy detection and experimental convenience. As a consequence of these features and their high sensitivity and operational simplicity, fluorescence-based assays have been widely used in biological studies.<sup>12</sup> Several fluorescent sensors have been developed for the detection of reactive oxygen species (ROS) in biological systems.<sup>13</sup> For example, 2',7'-dichlorodihydrofluorescein (DCFH), dihydrorrodamine 123, and hydroethidine, which are non-fluorescent molecules, react with hydrogen peroxide (H<sub>2</sub>O<sub>2</sub>) to produce fluorescent compounds.<sup>13a,b</sup> However, the practical application of these molecules suffers from a significant drawback since each readily undergoes autooxidation in the air (O<sub>2</sub>), resulting in a spontaneous increase in fluorescence and creating significant fluorescent background. Moreover, many of these sensors seemed to be devoid of specificity towards various peroxides species. Therefore, these fluorescent sensors cannot be used for the detection of strong oxidant peroxides. As a result, a strong need exists to develop stable and highly sensitive fluorescent sensors which could specifically respond to certain explosive peroxides with significant fluorescent signal changes.

### **3.2. Design plan**

It was known that thiourea is a simple and reactive sulfur compound that can be readily oxidized by strong oxidative reagents such as peroxides.<sup>14</sup> As a result, the

“C=S” double bond was converted to sulphur-containing acid. This made thiourea a potential recognition moiety for peroxides. Accordingly in the previous work, our group had developed a “turn-off” fluorescent sensor for the detection of benzoyl peroxide (BPO) and peracetic acid (PAA) based on thiourea (act as a recognition moiety) and fluorescein (act as a signalling moiety) (Figure 3.2). During the mechanism study of this sensor, we noticed that an imine “C=N” was also formed in the detection process of this sensor, which enlighten us to design a “turn-on” fluorescent sensor based on “ring-open” mechanism.

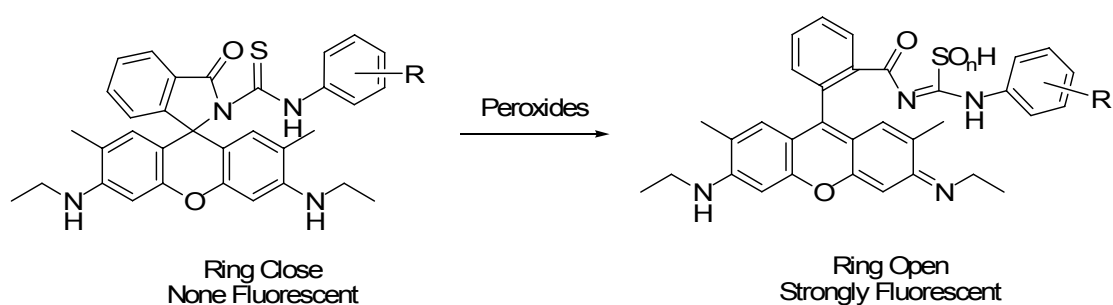
**Figure 3.2.** Sensor for the detection of BPO and PAA



Rhodamine-based fluorescent probes have received increasing interest in recent years by virtue of their high quantum yields and long-wavelength emission. Moreover, many rhodamine derivatives can undergo transformation between spiro-cyclic lactam (non-fluorescent) and ring-open form (strongly fluorescent) in dependant on the amide “N” that participate in the detection process, which made it an ideal model for the design of “on-off” switchable sensors. Therefore, in our design, we combined the

thiourea moiety into the rhodamine scaffold to construct the sensor for the detection of explosive peroxides. We hypothesized the sensor **1a** is non-fluorescent due to its ring-close lactam configuration. However, the reaction with peroxides will oxidize the thiourea as well as generate an imine-based benzamide, which could result in a strongly fluorescent rhodamine derivative (Figure 3.3).

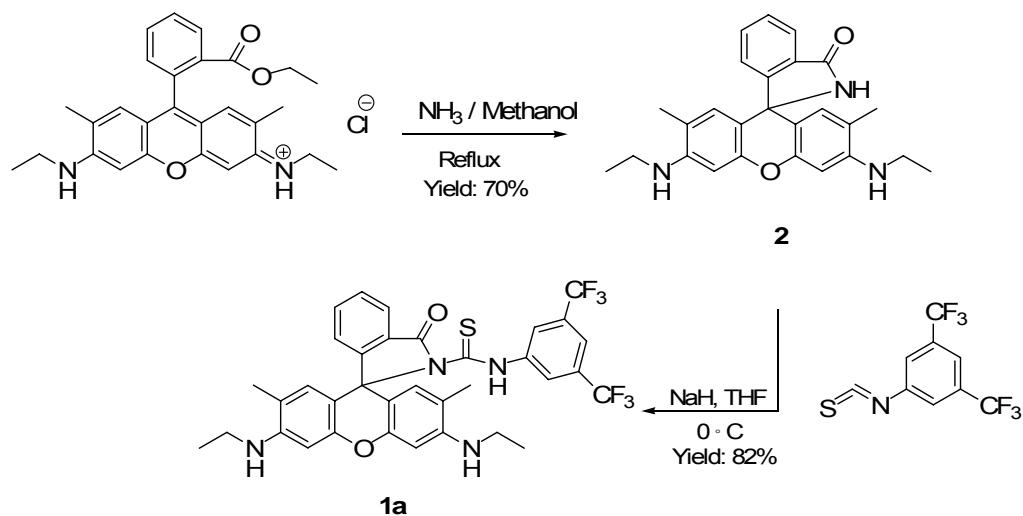
**Figure 3.3.** Proposed mechanism for sensor **1a**.



### 3.3 Results and Discussion

#### 3.3.1. Synthesis and confirmation of the configuration.

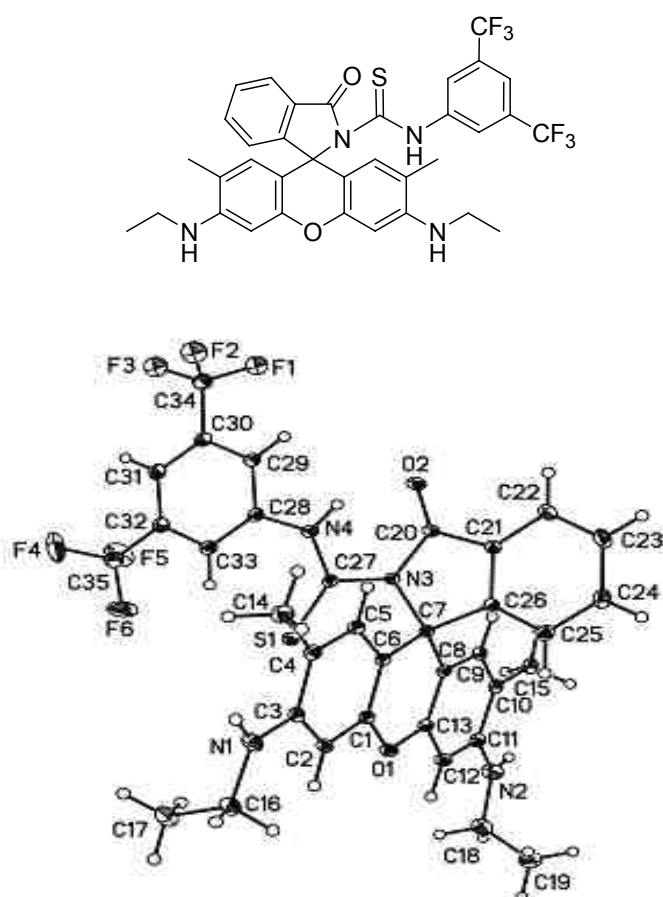
**Scheme 3.1.** Synthesis of sensor **1a**.



Sensor **1a** was prepared straightforward in two steps (Scheme 3.1). Briefly, commercially available rhodamine 6G was heated with ammonium in methanol at 100 °C in a sealed tube to give a pink solid as its amide derivative **2**, which was treated with 3,5-bis(trifluoromethyl) phenyl isothiocyanate in anhydrous THF in the presence of NaH to afford **1a** in good yields.

Configuration of sensor **1a** was confirmed by X-Ray structural analysis, which exhibited a typical spiro-lactam configuration as we expected (Figure 3.4).

**Figure 3.4.** X-ray crystal structure of compound **1a**.

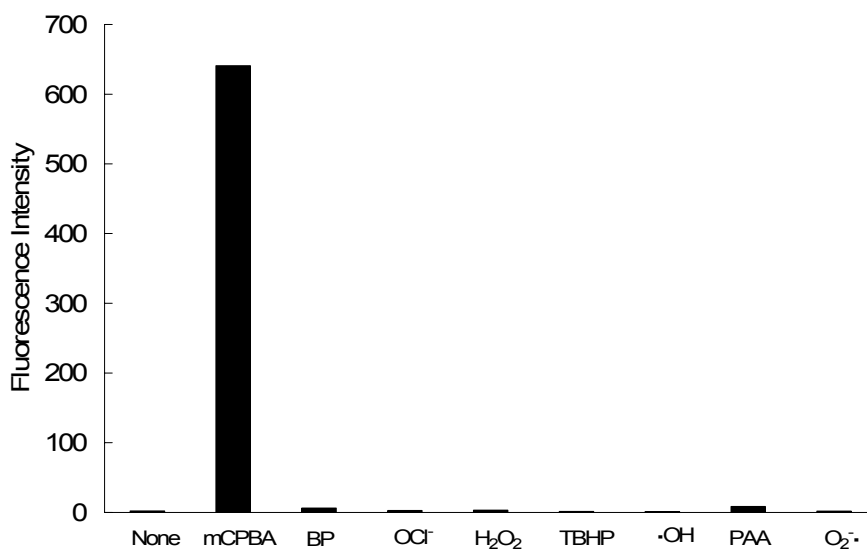


### 3.3.2 Fluorescence response towards peroxides and ROS.

With the designed sensor in hand, we first examined its fluorescence properties. The experiment was performed in a phosphate buffer (PH 7.3, I = 0.01 M) containing **1a** at a concentration of  $1.0 \times 10^{-6}$  M, which showed **1a** was completely non-fluorescent as we designed.

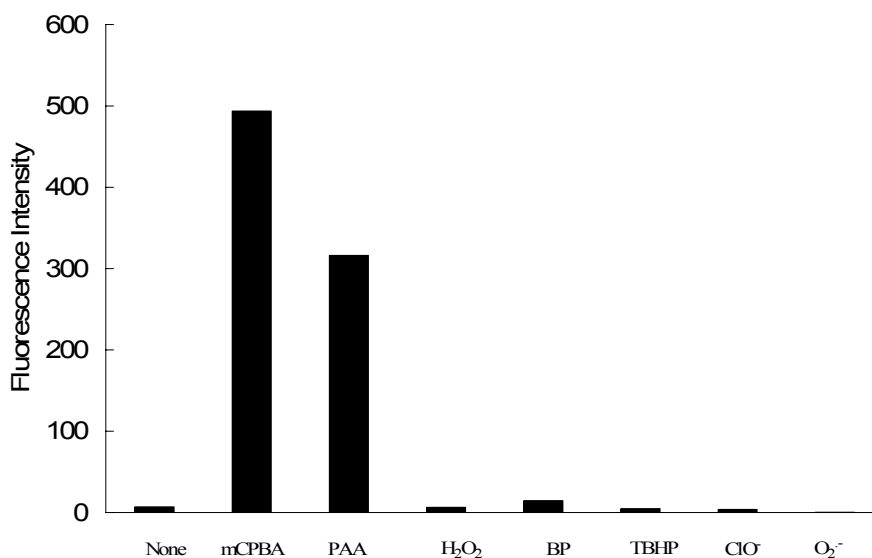
Then we evaluated the specificity of sensor **1a** towards peroxides. A variety of peroxides and ROS including *m*CPBA, H<sub>2</sub>O<sub>2</sub>, *t*-BuOOH, O<sub>2</sub><sup>-</sup>, ·OH, peracetic acid, benzoyl peroxide and HClO were probed to determine the specificity of sensor **1a** (Figure 3.5). After stirring 20 minutes, the reaction solution was taken for fluorescence measurement. Sensor **1a** showed almost no fluorescence response towards most of peroxides and ROS. However, when 10 μM of *m*CPBA was added, strong fluorescence intensity signals were observed in a few seconds, and the colorless solution gradually turned into pink. Remarkably, after 20 minutes of the reaction, more than 200 folds of fluorescence intensity increase were obtained. Meanwhile, addition of more than 100 μM peracetic acid (PAA) also caused moderate enhancement of fluorescence intensity. But if the concentration of PAA was decreased to 10 μM (the same concentration as *m*CPBA), the fluorescence enhancement was quite limited. As we know, *m*CPBA and peracetic acid are both peroxy acids, but they have obvious distinction in hydrophilicity: *m*CPBA is relatively lipophilic while peracetic acid is quite hydrophilic. Therefore, we hypothesize the reason why *m*CPBA gave rise to a much faster response to sensor **1a** than peracetic

acid was that its better lipophilicity led to its formation of highly concentrated micro-capsule in aqueous solution which greatly accelerated its reaction with **1a**.



**Figure 3.5.** Selectivity of probe **1a** towards various peroxides in H<sub>2</sub>O. The figure showed the fluorescence intensity change of **1a** (final 1  $\mu$ M in pH 7.3 phosphate buffer, 0.1% methanol as a cosolvent), measured at 553 nm with excitation at 530 nm, in the presence of various ROS. Data shown are for 10  $\mu$ M for *m*CPBA (*meta*-Chloroperoxybenzoic acid) and PAA (peroxyacetic acid), 1 mM for O<sup>2-</sup>, and 100  $\mu$ M for BP (benzoyl peroxide), OCl<sup>-</sup>, H<sub>2</sub>O<sub>2</sub>, TBHP (*tert*-Butyl hydroperoxide) and ·OH.

To prove our assumption, we re-evaluated the reactivity of sensor **1a** towards *m*CPBA and peracetic acid in methanol, a good organic solvent for both of these two peroxy acids. As shown in Figure 3.6, with the same concentration (10  $\mu$ M each), *m*CPBA and peracetic acid eventually caused similar strong fluorescence intensity enhancements after the same reaction time. In addition, sensor **1a** also showed almost no fluorescence response towards other peroxides in methanol like in aqueous solution (only has very weak response towards benzoyl peroxide), which indicated that sensor **1a** is particularly selective towards peroxy acids.



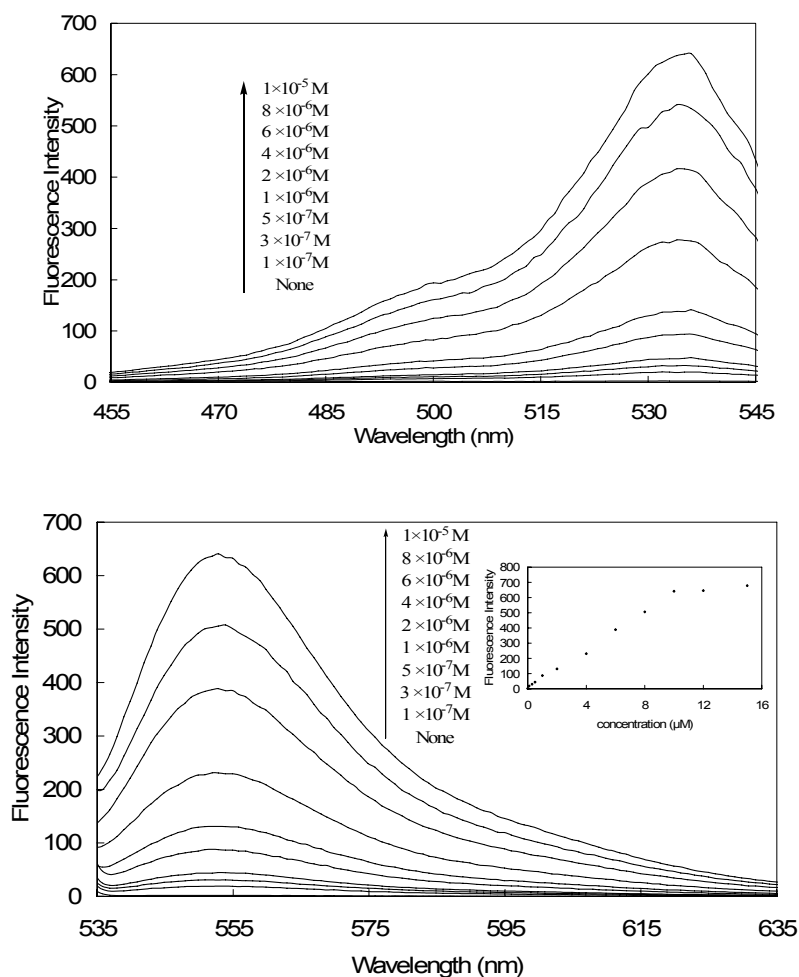
**Figure 3.6.** Selectivity of probe **1a** toward various peroxides in methanol. The figure showed the change of fluorescence intensity (final 1  $\mu$ M), measured at 553 nm with excitation at 530 nm, in the presence of various peroxides. Data shown are for 10  $\mu$ M for *m*CPBA (*meta*-Chloroperoxybenzoic acid) and PAA (peroxyacetic acid), 1 mM for O<sup>2-</sup>, and 100  $\mu$ M for H<sub>2</sub>O<sub>2</sub>, BP (benzoyl peroxide), TBHP (*tert*-Butyl hydroperoxide), and ClO<sup>-</sup>.

### 3.3.3. Examination of sensitivity and reactivity.

We next probed the detection limit of sensor **1a** for peroxy acids (Figure 3.7). Again, the same reaction protocols were employed using  $1 \times 10^{-6}$  M of **1a** in a phosphate buffer (pH 7.3, 0.01 M) at room temperature and in the presence of *m*CPBA as the representative of peroxy acids. The increase of both fluorescence excitation and emission intensity was displayed in a concentration dependent manner with a range of 0.1 to 10 equivalents of *m*CPBA. At 20 minutes, when more than 10 equivalents of *m*CPBA were used, the enhancement of fluorescence intensity almost reached a maximum without much further alteration. Remarkably, sensor **1a** exhibited extremely high sensitivity for *m*CPBA. A pronounced change in the fluorescence signal was observed even when the *m*CPBA concentration was as low as  $1.0 \times 10^{-7}$  M. The major product of the oxidation reaction was determined to be compound **3** by

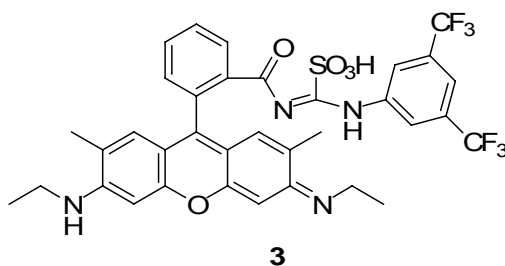


high resolution mass spectroscopy (HRMS) when either insufficient or excess amount of *m*CPBA was used (Figure 3.8).



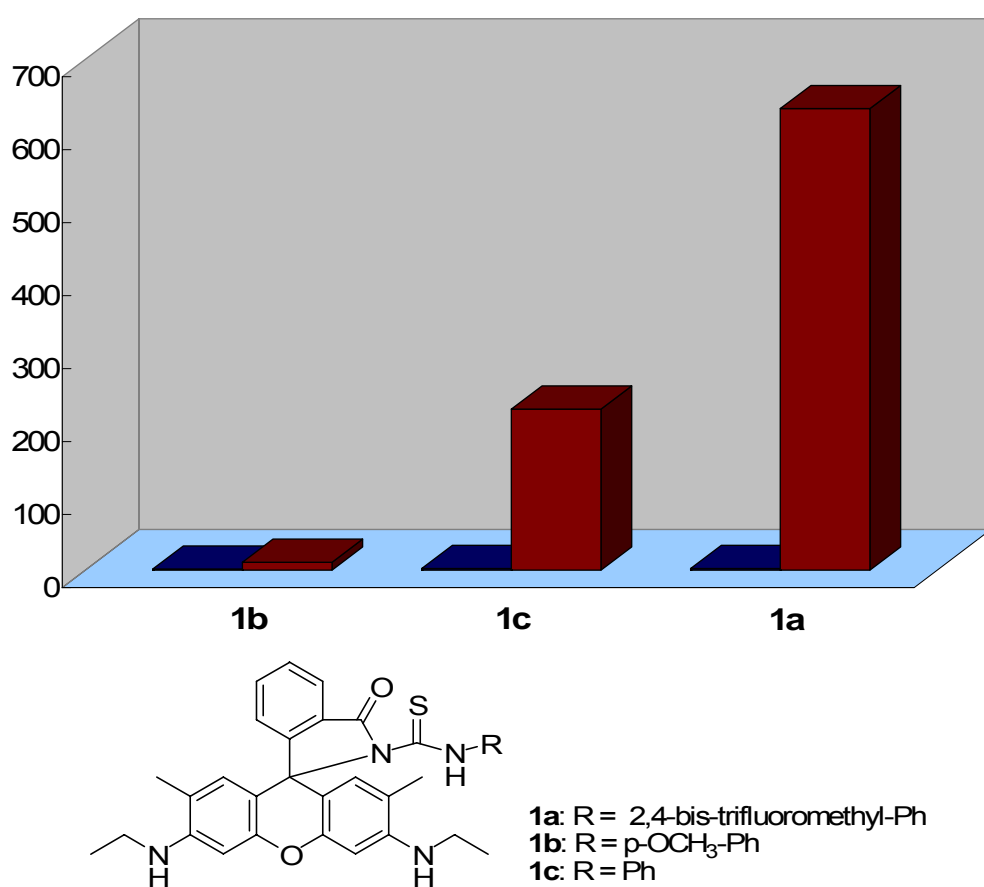
**Figure 3.7.** Fluorescence excitation ( $\lambda_{em} = 550$  nm) and emission ( $\lambda_{ex} = 530$  nm) response of 1  $\mu$ M sensor **1a** toward various concentration of *m*CPBA. Figure shown were achieved before and 20 minutes after *m*CPBA was added in pH 7.3 phosphate buffer (I = 0.01 M).

**Figure 3.8.** Proposed structure of final product **3**.



### 3.3.4. The effect of thiourea substituent group on the fluorescence intensity and reactivity.

In the control study, we noticed that the electronic character of the substituent group connecting with thiourea receptor also has influence on sensor's reactivity. We synthesized sensor **1b** and **1c** with different isothiocyanate and performed the control experiments in the same condition as sensor **1a** (Figure 3.9).

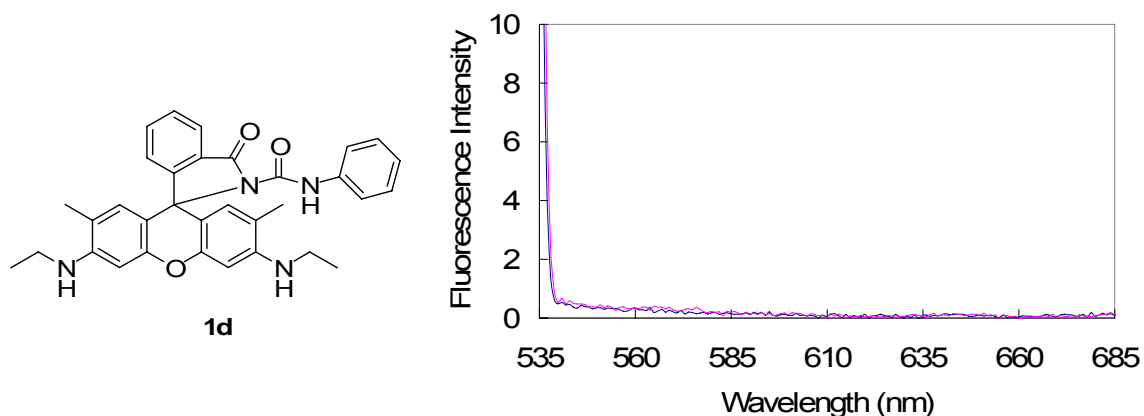


**Figure 3.9.** Reactivity of probe **1a**, **1b**, **1c** (final 1  $\mu$ M) towards for *m*CPBA. The figure showed the change of fluorescence intensity, measured at 553 nm with excitation at 530 nm before (left bar) and 20 minutes after (right bar) the addition of 10  $\mu$ M *m*CPBA in pH 7.3 phosphate buffer, 0.1% methanol as a cosolvent.

For sensor **1b** with an electron-donating *p*-CH<sub>3</sub>O-Phenyl group (EDG) connecting with thiourea receptor, surprisingly only very weak fluorescence signals was obtained

in 20 minutes upon adding 10 equivalents of *m*CPBA. For sensor **1c** with only phenyl group connecting to thiourea moiety, its fluorescence response to *m*CPBA was much higher than **1b**, although the reactivity was still lower than that of sensor **1a**. This result suggested the strong electron-withdrawing group (EWG) adjacent to thiourea (for example 3,5-bis(trifluoromethyl) phenyl group) could make the ring-open oxidation process more quickly proceed so as to increase the reactivity.

We also synthesized compound **1d** by replacing the thiourea group of sensor **28** with a urea group to evaluate the importance of the reductive “C=S” bond. As we expected, compound **29** kept totally non-fluorescent before and after excess amounts of *m*CPBA was added (Figure 3.10), which again proved the functionality of thiourea is essentially necessary for the recognition process.

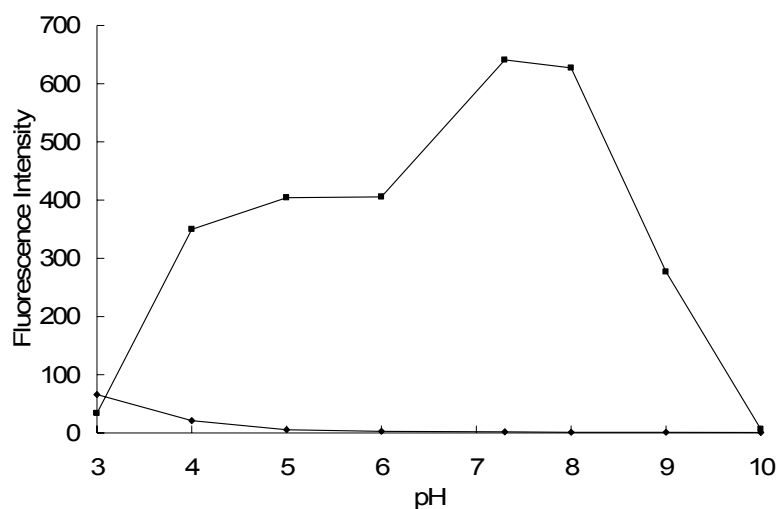


**Figure 3.10.** Reactivity of probe **1d** (final 1  $\mu$ M) towards *m*CPBA. The figure showed the change of fluorescence intensity, measured at 553 nm with excitation at 530 nm before and 20 minutes after the addition of 10  $\mu$ M *m*CPBA in pH 7.3 phosphate buffer, 0.1% methanol as a cosolvent.

### 3.3.5. The effect of pH on the fluorescence intensity and reactivity.

At last we evaluated the effect of solution pH on the reactivity of sensor **1a** (Figure 3.11). In a large pH ranger from acidic to basic (pH 5 to 9), compound **1a**

always showed non-fluorescent and addition of *m*CPBA could give rise to significant fluorescence signals. When we further increase or decrease the pH of solution, **1a** still exhibited weak or no fluorescence. However, its reactivity was dramatically weakened. Therefore, **1a** could act as a highly sensitive sensor for the detection of peroxy acids from pH 5 to pH 9.



**Figure 3.11.** Effect of pH on the fluorescence response of probe **1a** ( $1 \mu\text{M}$ ) towards *m*CPBA. In these experiments,  $1.0 \times 10^{-6}$  M of probe **1a** at room temperature in the presence of  $1.0 \times 10^{-5}$  M of *m*CPBA were performed from pH = 3 to pH = 10. After 20 minutes, the reaction solution was taken for fluorescence measurement at  $\lambda_{\text{ex}} = 465$  nm and  $\lambda_{\text{em}} = 555$  nm.

### 3.4. Summary

We successfully developed a novel turn-on fluorescent probe **1a** for highly sensitive and selective detection of peroxy acids, a kind of explosive peroxide. Sensor **1a** could directly detect peroxy acids in a trace amount based on oxidized ring-open mechanism and showed excellent fluorescence signal increase. Moreover, different peroxy acids (such as *m*CPBA and peracetic acid) is readily to be differentiated by performing the experiments in either aqueous solution or organic solution. Therefore, this sensor is expected to be a useful tool with the applicable usage for the detection of peroxy acids. More significantly, the new promising technology and strategy we have established in this sensor can serve as a foundation for building new fluorescence sensing systems for various explosive peroxides.

### **3.5. Experimental section**

#### **General information.**

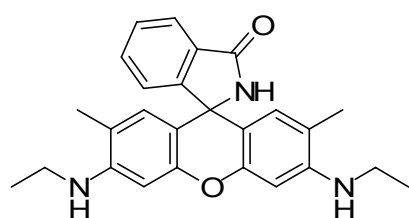
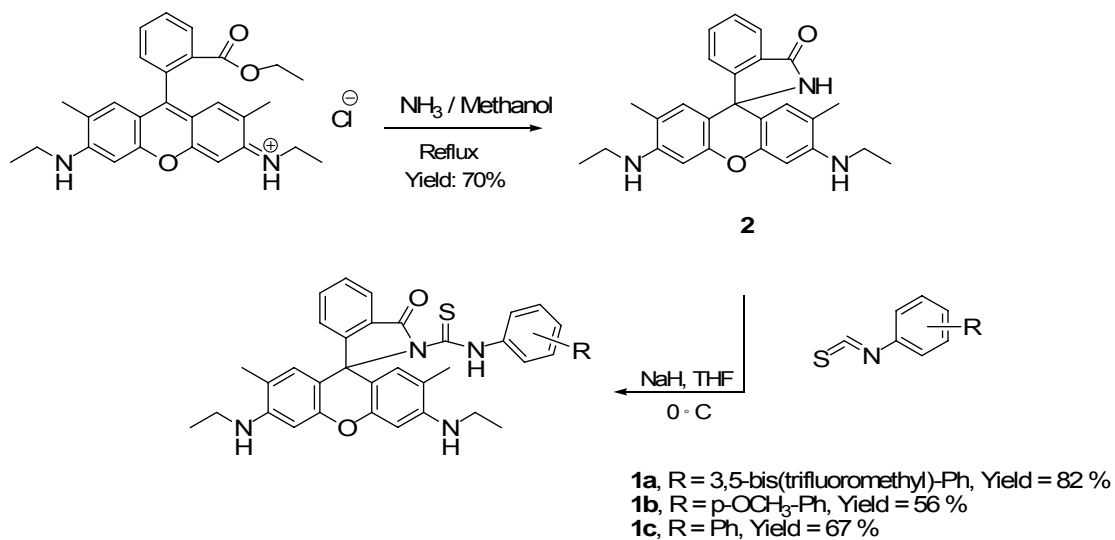
Commercial reagents were used as received, unless otherwise stated. Merck 60 silica gel was used for chromatography, and Whatman silica gel plates with fluorescence F254 were used for thin-layer chromatography (TLC) analysis.  $^1\text{H}$  and  $^{13}\text{C}$  NMR spectra were recorded on Bruker Avance 500, and tetramethylsilane (TMS) was used as a reference. Data for  $^1\text{H}$  are reported as follows: chemical shift (ppm), and multiplicity (s = singlet, d = doublet, t = triplet, q = quartet, m = multiplet). Data for  $^{13}\text{C}$  NMR are reported as ppm. Mass Spectra were obtained from University of New Mexico mass spectral facility.

#### **Spectroscopic materials and methods.**

Millipore water was used to prepare all aqueous solutions. The pH was recorded by a Beckman  $\Phi\text{TM}$  240 pH meter. UV absorption spectra were recorded on a Shimadzu UV-2410PC UV-Vis spectrophotometer. Fluorescence emission spectra were obtained on a Varian Eclipse fluorescence spectrophotometer.

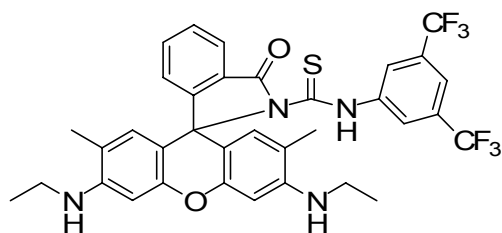
## Synthesis of compound 1a-1d:

Compound **1a**, **1b** and **1c** was synthesized following the procedures in Figure.



### *N*-(Rhodamine-6G)lactam (**2**).

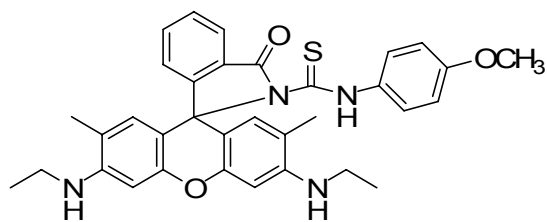
A solution of rhodamine 6G (959 mg, 2 mmol) in 7N ammonium/methanol (5 mL) was heated at 100 °C in a sealed tube. Orange precipitate was observed during the reaction. After stirring 48 h, the reaction was cooled down to 0 °C. The reaction mixture was filtered and washed with methanol to get pink solid as product (580 mg, 70 % yield) which was used for the next step without further purification.



**N-(Rhodamine-6G)lactam-N'-[3,5-bis(trifluoromethyl)phenyl]-thiourea (1a).**

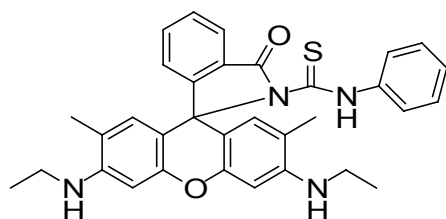
To a solution of **2** (414 mg, 1 mmol) in 40 mL anhydrous THF was added NaH (100 mg, 2.5 mmol) at 0 °C under a nitrogen atmosphere. After stirring 30 minutes, 3,5-bis(trifluoromethyl)phenyl isothiocyanate (224  $\mu$ L, 1.2 mmol) was added dropwise at 0 °C. The reaction was warmed up to room temperature gradually and stirred overnight. Evaporated solvents *in vacuo*, redissolved the reaction residue in aqueous NaHCO<sub>3</sub> and extracted with dichloromethane (3  $\times$  20 mL). The combined organic layers were washed with brine, dried with magnesium sulfate and then filtered and evaporated *in vacuo*. The crude product was purified by silica gel chromatography using ethyl acetate/hexane (1:4) as elute to afford CSP1 as orange solid (294 mg, 82 % yield). <sup>1</sup>H NMR (500 MHz, CDCl<sub>3</sub>):  $\delta$  8.24 (s, 2H),  $\delta$  8.03 (d, 1H, J = 7.5 Hz),  $\delta$  7.59-7.51 (m, 3H),  $\delta$  7.05 (d, 1H, J = 7.5 Hz),  $\delta$  6.35 (s, 2H),  $\delta$  6.19 (s, 2H),  $\delta$  3.45 (s, 2H),  $\delta$  3.20 (q, 4H, J = 7 Hz),  $\delta$  1.90 (s, 6H),  $\delta$  (t, 6H, J = 7 Hz); <sup>13</sup>C NMR (125 MHz, CDCl<sub>3</sub>):  $\delta$  176.9, 171.5, 155.1, 151.9, 147.7, 140.1, 136.0, 131.9, 131.6, 129.0, 127.0, 126.9, 125.1, 124.4, 123.9, 118.9, 117.4, 107.1, 96.6, 70.6, 38.5, 29.9, 17.1, 15.0.





**N-(Rhodamine-6G)lactam-N'-(4-methoxyphenyl)-thiourea (1b).**

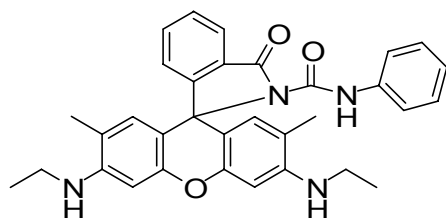
The titled compound was prepared in 56% yield according to a procedure similar to that mentioned in the preparation of CSP1.  $^1\text{H}$  NMR (500 MHz,  $\text{CDCl}_3$ ):  $\delta$  8.00 (d, 1H,  $J = 7.5$  Hz),  $\delta$  7.53-7.44 (m, 4 Hz),  $\delta$  7.02 (d, 1H,  $J = 7.5$  Hz),  $\delta$  6.79 (d, 2H,  $J = 9$  Hz),  $\delta$  6.33 (s, 2H),  $\delta$  6.21 (s, 2H),  $\delta$  3.75 (s, 3H),  $\delta$  3.41 (s, 2H),  $\delta$  3.18 (q, 4H,  $J = 7$  Hz),  $\delta$  1.89 (s, 6H),  $\delta$  1.28 (t, 6H,  $J = 7$  Hz);  $^{13}\text{C}$  NMR (125 MHz,  $\text{CDCl}_3$ ):  $\delta$  177.5, 171.3, 157.6, 155.2, 151.7, 147.4, 135.4, 131.7, 128.7, 127.3, 127.1, 126.4, 125.0, 124.1, 117.2, 113.8, 108.0, 96.8, 55.6, 38.5, 17.1, 15.0.



**N-(Rhodamine-6G)lactam-N'-phenyl-thiourea (1c).**

The titled compound was prepared in 67% yield according to a procedure similar to that mentioned in the preparation of CSP1.  $^1\text{H}$  NMR (500 MHz,  $\text{CDCl}_3$ ):  $\delta$  8.01 (d, 1H,  $J = 7.5$  Hz),  $\delta$  7.61 (d, 2H,  $J = 8$  Hz),  $\delta$  7.54 (t, 1H,  $J = 7.5$  Hz),  $\delta$  7.48 (t, 1H,  $J = 7.5$  Hz),  $\delta$  7.28-7.24 (m, 2H),  $\delta$  7.11 (t, 1H,  $J = 7.5$  Hz),  $\delta$  7.03 (d, 1H,  $J = 7.5$  Hz),  $\delta$  3.18 (q, 4H,  $J = 7$  Hz),  $\delta$  1.87 (s, 6H),  $\delta$  1.29 (t, 6H,  $J = 7$  Hz);  $^{13}\text{C}$  NMR (125 MHz,

CDCl<sub>3</sub>):  $\delta$  177.1, 171.3, 155.2, 151.7, 147.5, 138.7, 135.5, 128.7, 128.6, 127.3, 127.0, 125.9, 125.0, 124.6, 124.2, 117.2, 107.9, 96.8, 70.2, 38.6, 29.9, 17.1, 15.0.



**N-(Rhodamine-6G)lactam-N'-phenyl-urea (1d).**

The titled compound was prepared by **2** and phenyl isocyanate in 42% yield according to a procedure similar to that mentioned in the preparation **1a**. <sup>1</sup>H NMR (500 MHz, CDCl<sub>3</sub>):  $\delta$  10.84 (s, 1H),  $\delta$  8.01 (d, 1H, J = 7.5 Hz),  $\delta$  7.59-7.53 (m, 2H),  $\delta$  7.43 (d, 2H, J = 7.5 Hz),  $\delta$  7.18 (t, 2H, J = 7.5 Hz),  $\delta$  7.12 (d, 1H, J = 7.5 Hz),  $\delta$  6.96 (t, 1H, J = 7.5 Hz),  $\delta$  6.42 (s, 2H),  $\delta$  6.21 (s, 2H),  $\delta$  3.45 (s, 2H),  $\delta$  3.20 (q, 4H, J = 7 Hz),  $\delta$  1.88 (s, 6H),  $\delta$  1.30 (t, 6H, J = 7 Hz); <sup>13</sup>C NMR (125 MHz, CDCl<sub>3</sub>):  $\delta$  170.3, 154.1, 151.9, 148.8, 147.5, 138.0, 135.3, 128.9, 128.8, 127.5, 124.9, 124.0, 123.6, 120.2, 117.3, 107.5, 97.2, 66.4, 38.6, 17.0, 15.1.

### 3.6. References.

1. (a) Wu, S.H.; Wang, Y. W.; Wu, T. C.; Hu, W. N. and Shu, C.M. *J Therm Anal Calorim.* **2008**, *93*, 189. (b) Chen, J. R.; Wu, S. H.; Lin, S. Y.; Hou, H. Y. and Shu, C. M. *J Therm Anal Calorim.* **2008**, *93*, 127.
2. (a) Evans, H. K.; Tulleners, F. A. J.; Sanchez, B. L. and Rasmussen, C. A. J. *J. Forensic. Sci.* **1986**, *31*, 1119. (b) Cooper, R. T. *Los Angeles Times* **2001**, December 29, p A12. (c) Ember, L. S. *Chem. Eng. News.* **2005**, *83*, 11. (d) Ember, L. S. *Chem. Eng. News* **2006**, *84*, 10.
3. Peracetic acid and benzoyl peroxide can be purchased from chemical distributors such as Aldrich.
4. J. C. Oxley, J. L. Smith, H. Chen, *Propellants, Explos., Pyrotech.* **2002**, *27*, 209.
5. (a) Zitrin, S.; Kraus, S. And Glattstein, B. *Fed. Bur. Invest. Washington, DC, Quantico, VA*, **1983**, 137. (b) Thomas, S. W.; Amara, J. P.; Bjork, R. E. And Swager, T. M. *Chem. Commun.* **2005**, 4572.
6. Janotta, M.; Vogt, F.; Voraberger, H. S.; Waldhauser, W.; Lackner, J. M.; Stotter, C.; Beutl, M. and Mizaikoff, B. *Anal. Chem.* **2004**, *76*, 384.
7. (a) Pinkernell, U.; Karst, U. and Cammann, K. *Anal. Chem.* **1994**, *66*, 2599. (b) Pinkernell, U.; Luke, H. J. and Karst, U. *Analyst* **1997**, *122*, 567. (c) Baj, S.; Chrobok, A.; Cieslik, M. and Krawczyk, T. *Anal. Bioanal. Chem.* **2003**, *375*, 327. (d) Wada, M.; Inoue, K.; Ihara, A.; Kishikawa, N.; Nakashima, K. and Kuroda, N. *J. Chromatogr. A* **2003**, *987*, 189. (e) Schulte-Ladbeck, R.; Kolla, P. and Karst, U. *Anal. Chem.* **2003**, *75*, 731. (f) Henneken, H.; Assink, L.; de Wit, J.; Vogel, M.

- and Karst, U. *Anal. Chem.* **2006**, *78*, 6547.
8. Keinan, E. and Itzhaky, H. *Israel, Patent WO9943846*. **1999**.
9. (a) Qi, X. and Baldwin, R. P. *Electroanalysis* **1993**, *5*, 547. (b) Ruttinger, H. H. and Radschuweit, A. *J. Chromatogr. A* **2002**, *868*, 127. (c) Wang, J.; Escarpa, A.; Pumera, M. and Feldman, J. *J. Chromatogr. A* **2002**, *952*, 249. (d) Toniolo, R.; Pizzariello, A.; Susmel, S.; Dossi, N. and Bontempelli, G. *Electroanalysis* **2006**, *18*, 2079. (e) Lu, D.; Cagan, A.; Munoz, R. A. A.; Tangkuaram, T. and Wang, J. *Analyst* **2006**, *131*, 1279.
10. (a) Widmer, L.; Watson, S.; Schlatter, K. and Crowson, A. *Analyst* **2002**, *127*, 1627. (b) Cotte-Rodríguez, I.; Chen, H. and Cooks, R. G. *Chem. Commun.* **2006**, 953. (c) Schulte-Ladbeck, R.; Kolla, P. and Karst, U. *Analys.* **2002**, *127*, 1152. (d) Itzhaky, H. and Keinan, E. *United States Patent*. **2004**, US 6,767,717 B1. (e) Todd, M.W.; Provencal, R. A.; Owano, T. G.; Paldus, B. A.; Kachanov, A.; Vodopyanov, K. L.; Hunter, M.; Coy, S. L.; Steinfeld, J. I. and Arnold, J. T. *Appl Phys, B*. **2002**, *75*, 367. (f) Buttigieg, G.A.; Knight, A.K.; Denson, S.; Pommier, C. and Bonner-Denton, M. *Forensic Sci Int.* **2003**, *135*, 53.
11. (a) Widmer, L.; Watson, S.; Schlatter, K. and Crowson, A. *Analyst* **2002**, *127*, 1627. (b) Cotte-Rodríguez, I.; Chen, H. and Cooks, R. G. *Chem. Commun.* **2006**, 953. (c) Tzou, T. L.; Edwards, D. W. and Chung, P. W. H. *Institution of Chemical Engineers Symposium Series*. **2003**, *149*, 591. (d) Wu, K. W.; Chou, Y. P.; Yun, R. L. and Shu, C. M. in *Proceedings of the NATAS Annual Conference on Thermal Analysis and Applications*, Douliu, Yunlin, Taiwan, **2006**.

12. Selected reviews of fluorescence sensors, see: (a) Scheller, F. W.; Schubert, F. and Fedrowitz, J. *Frontiers in Biosensorics I. Fundamental Aspects*, Birkhauser Verlag, Berlin, **1997**. (b) Scheller, F. W.; Schubert, F. and Fedrowitz, J. *Frontiers in Biosensorics II. Practical Applications*, Birkhauser Verlag, Berlin, **1997**. (c) de Silva, A. P.; Gunaratne, H. Q. N.; Gunnlaugsson, T.; Uxley, A. J. M.; McCoy, C. P.; Rademacher, J. T. and Rice, T. E. *Chem. Rev.* **1997**, *97*, 1515. (d) McQuade, D. T.; Pullen, A. E. and Swager, T. M. *Chem. Rev.* **2000**, *100*, 2537. (e) Haugland, R. P. *Handbook of Fluorescent Probes and Research Products, Ninth ed., Molecular Probes, Inc., Eugene, OR, USA*, **2002**. (f) Pu, L. *Chem. Rev.* **2004**, *104*, 1687. (g) James, T. D.; Phillips, M. D. and Shinkai, S. *Boronic Acids in Saccharide Recognition*, Royal Society of Chemistry, Cambridge, UK, **2006**. (h) Anslyn, E. V. *J. Org. Chem.* **2007**, *72*, 687. For selected examples of fluorescence sensors, see: (i) James, T. D.; Sandanayake, K. R. A. S. and Shinkai, S. *Nature* **1995**, *374*, 345. (j) de Silva, A. P.; Gunaratne, H. Q. N. and McCoy, C. P. *J. Am. Chem. Soc.* **1997**, *119*, 7891. (k) Rusin, O.; Luce, N. N. St.; Agbaria, R. A.; Escobedo, J. O.; Jiang, S.; Warner, I. M.; Dawan, F. B.; Lian, K. and Strongin, R. M. *J. Am. Chem. Soc.* **2004**, *126*, 438. (l) Zhao, J.; Davidson, M. G.; Mahon, M. F.; Gabriele, K. K. and James, T. D. *J. Am. Chem. Soc.* **2004**, *126*, 16179. (m) Tanaka, F.; Mase, N. and Barbas, C.F. *Chem. Commun.* **2004**, 1762. (n) Li, Z. B.; Lin, J. and Pu, L. *Angew. Chem.* **2005**, *117*, 1718; Li, Z. B.; Lin, J. and Pu, L. *Angew. Chem. Int. Ed.* **2005**, *44*, 1690. (o) Boduroglu, S.; El Khoury, J. M.; Reddy, D. V.; Rinaldi, P. L. And Hu, J. *Bioorg. Med. Chem. Lett.* **2005**, *15*, 3974.

- (p) Zhang, Y.; Gao, X.; Hardcastle, K. and Wang, B. *Chem. Eur. J.* **2006**, *12*, 1377.
13. (a) Hempel, S. L.; Buettner, G. R.; O'Malley, Y. Q.; Wessels, D. A. and Flaherty, D. M. *Free Radic. Biol. Med.* **1999**, *27*, 146. (b) Peterson, S. L.; Morrow, D.; Liu, S. and Liu, K. J. *Epilepsy Res.* **2002**, *49*, 226. (c) Maeda, H.; Matsu-Ura, S.; Nishida, M.; Yamauchi, Y. And Ohmori, H. *Chem. Pharm. Bull.* **2002**, *50*, 169. (d) Setsukinai, K.; Urano, Y.; Kakinuma, K.; Majima, H. J. and Nagano, T. *J. Bio. Chem.* **2003**, *278*, 3170. (e) Yang, D.; Wang, H. L.; Sun, Z. N.; Chung, N. W. and Shen, J. G. *J. Am. Chem. Soc.* **2006**, *128*, 6004.
14. Simoyi, R. H. *J. Phys. Chem.* **1994**, *98*, 551.

## Chapter 4

### Development of Fluorescent Sensors for Bio-interesting Metal Ions

#### 4.1. Background and Significance

Detecting biologically important metal ions is of great interest to many scientists, including chemists, biologists, clinical biochemists and environmentalists. It is well known that most bio-active metals are essential in biological systems. For example, sodium, potassium, magnesium and calcium are involved in a number of biological functions such as transmission of nerve impulses, muscle contraction, regulation of cell activity, etc. Zinc and iron are most abundant transition metal in organisms and play important roles in “metalloenzymes” as well as copper. In contrast, some heavy transition metals like mercury, lead and cadmium are toxic for organisms and human beings, and early detection in the environment is desirable.

Traditionally a number of analytical methods have been developed for the detection of metal ions such as flame photometry, atomic absorption spectrometry, ion sensitive electrodes, electron microprobe analysis, neutron activation analysis, etc.,. However most of them have drawbacks that they are high-costed, often require samples of large size and do not allow continuous monitoring. In contrast, fluorescent sensors can offer distinct advantages in terms of sensitivity, selectivity, response time and local observation. As a result, considerable efforts are being made to develop selective fluorescent sensors for the detection of metal ions.

In this section, we described two highly sensitive and selective fluorescent sensors for bio-interesting metal ions. First we developed a sensor for the detection of

bio-active  $Zn^{2+}$  based on PET mechanism. Then a chemodosimeter for toxic  $Hg^{2+}$  was developed through a novel  $Hg^{2+}$ -facilitated desulfurization–lactonization cascade reaction by transforming a weakly fluorescent precursor to a highly fluorescent coumarin derivative.

## **4.2. Development of Fluorescent Sensor for Zinc Ion**

### **4.2.1. Introduction.**

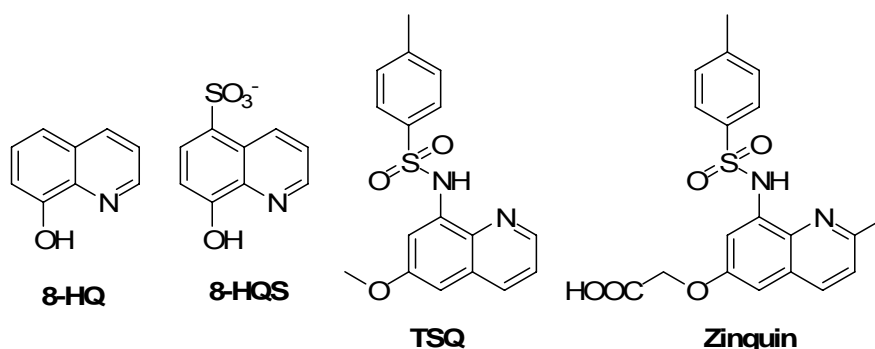
Zinc ion ( $Zn^{2+}$ ), the second most abundant transition metal in the human body, plays myriad roles in numerous cellular functions such as the regulation of gene expression, apoptosis, co-factors in metalloenzyme catalysis, and neurotransmission in biological systems.<sup>1</sup> Deregulation of  $Zn^{2+}$  is implicated in several diseases including Alzheimer's disease,<sup>2</sup> prostate cancer,<sup>3</sup> and diabetes.<sup>4</sup> Accordingly, the development of  $Zn^{2+}$ -specific molecular probes has been of considerable interest in the areas of chemical and biological sciences.

Fluorescent probes for sensing  $Zn^{2+}$  based on various fluorophores such as quinoline,<sup>5</sup> bipyridyl,<sup>6</sup> dansyl,<sup>7</sup> ferrocene,<sup>8</sup> fluorescein,<sup>9</sup> anthracene,<sup>10</sup> benzofuran and benzoxazole,<sup>11</sup> naphthalimide<sup>12</sup> and cyanine<sup>13</sup> have been reported. While each of these agents has unique advantages, there also remain different issues. Traditionally, quinoline and its derivatives have been used as fluorescent indicators for metal ions for long time (Figure 4.1). The first of them for  $Zn^{2+}$  is 8-hydroxyquinoline (8-HQ), often called oxine, and its derivatives, mainly 8-hydroxyquinoline-5-sulfonic acid (8-HQS).<sup>14</sup> The most widely used fluorescent probes for  $Zn^{2+}$  are TSQ



(6-methoxy-8-(*p*-toluenesulfonamide)quinoline) and its derivatives. This stain was the only useful Zn<sup>2+</sup>-specific fluorophore that worked in the presence of physiological concentrations of Ca<sup>2+</sup> and Mg<sup>2+</sup>. The complex of TSQ with free Zn<sup>2+</sup> apparently has a stoichiometry of 2:1 TSQ/Zn<sup>2+</sup>, but a 1:1 complex may equilibrate with protein-bound Zn<sup>2+</sup>. These TSQ-Zn<sup>2+</sup> complexes were not fully identified nor fully characterized because of their complex structures and their stability constants were not determined. The fluorescence intensity (*i.e.*, quantum yield) of the complex ( $\epsilon$ ) varies with the media. Whilst the TSQ-Zn<sup>2+</sup> complexes were still chemically to be characterized, a modified TSQ, Zinquin,<sup>15</sup> can detect intracellular Zn<sup>2+</sup> in living cells.<sup>16</sup> Although quinoline-based probes are useful, they are not ideal because the excitation wavelength is in the ultraviolet range, which may cause cell damage and is subject to interference by autofluorescence from biological molecules such as pyridine nucleotides.

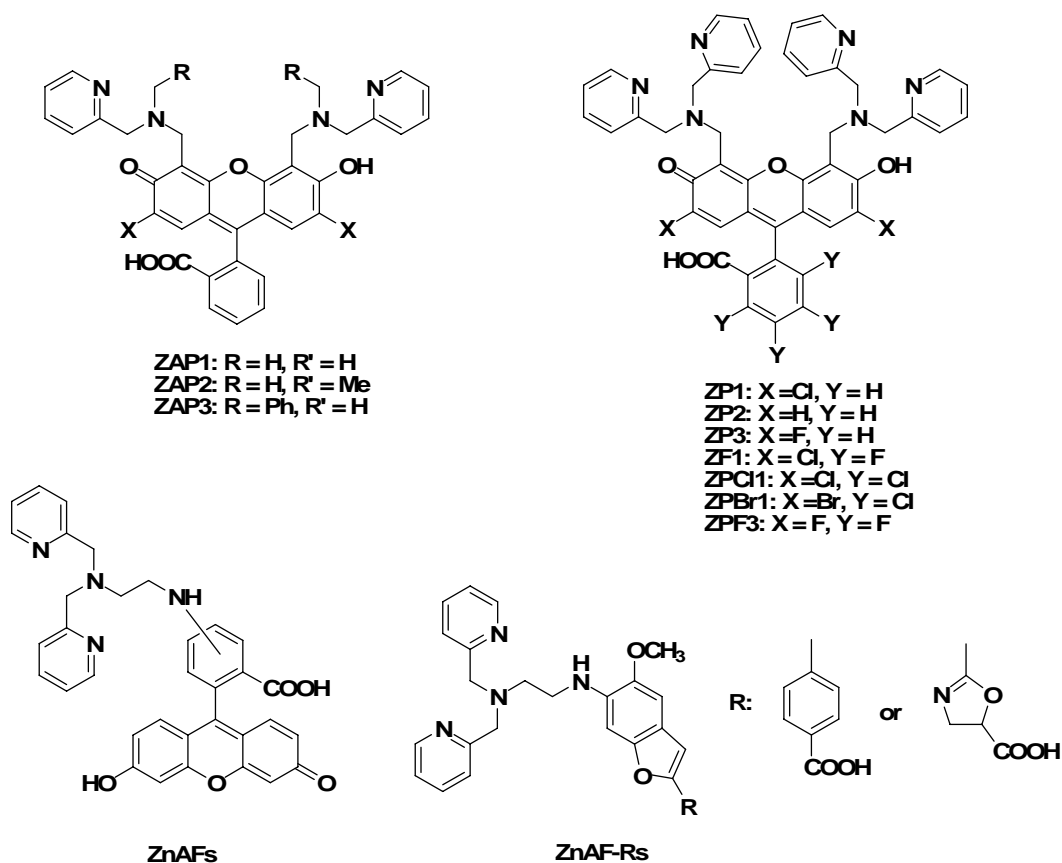
**Figure 4.1.** Schematic drawing of quinoline-based sensors.



TPEN (N,N,N',N'-tetrakis(2-pyridylmethyl)ethylenediamine) and DPA (bis(2-pyridylmethyl)amine) as membrane-permeable chelators,<sup>17</sup> provide good

binding site specific for zinc ions by those nitrogen atoms as well as electron donors, give a variety of design choice of fluorescent sensor for  $Zn^{2+}$ . In recent years, a bunch of sensor based on TPEN or DPA chelators were reported for zinc detection. A representative example is that Lippard's group developed a series of sensor using fluorescein as fluorophore and modified TPEN/DPA as receptors for the study on biological functions of  $Zn^{2+}$  (Figure 4.2).<sup>18</sup>

**Figure 4.2.** Schematic drawing of fluorescein-based sensors developed by Lippard's group.



An ideal  $Zn^{2+}$  chemical probe with potential for biological applications should possess: (1) good water solubility, (2) the capability to determine  $Zn^{2+}$  concentration

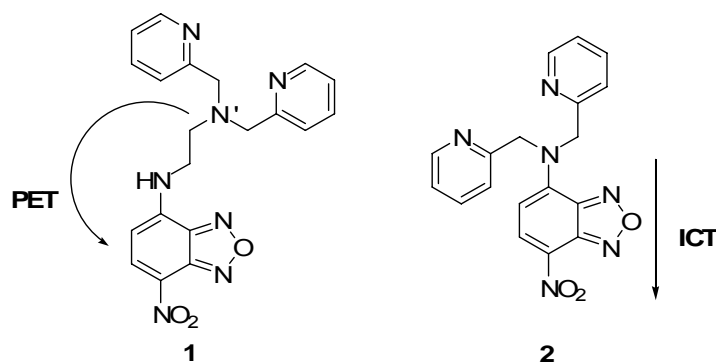
quantitatively, (3) long excitation wavelength to avoid cell damage, (4) high stability, (5) high selectivity and sensitivity toward  $Zn^{2+}$  and (6) easy preparation. The development of fluorescent chemosensors for probing  $Zn^{2+}$  has been an active topic as a result of operational simplicity and high sensitivity. However, the search for readily accessible fluorescent  $Zn^{2+}$  probes with good water solubility and high specificity is still a challenging task. It is a particular challenge to develop a chemosensor which makes it possible to determine the concentration of  $Zn^{2+}$  and to discriminate  $Zn^{2+}$  from  $Cd^{2+}$  owing to their closely related properties. The bipyridyl,<sup>6</sup> dansyl,<sup>7</sup> ferrocene,<sup>8</sup> anthracene<sup>10</sup> and naphthalimide<sup>12</sup> based probes have poor water solubility. Generally a mixture of organic solvent and water is used, thus limiting their biological applications. The widely used quinoline and fluorescein derived chemosensors provide good water solubility, but their selectivity for  $Zn^{2+}$  and  $Cd^{2+}$  is not clear. Moreover, their syntheses are not trivial. However, to the best of our knowledge, 7-nitrobenz-benzofurazan (NBD) derived fluorescent  $Zn^{2+}$  chemical probe has not been described, despite the fact that it has excellent water solubility and has been widely used in molecular imaging in biological systems.<sup>19</sup> Therefore, we want to develop a sensor for  $Zn^{2+}$  based on NBD fluorophore that have most potential for practical application.

#### **4.2.2. Design plan.**

In the design of fluorescent sensors for  $Zn^{2+}$ , the critical issue is that  $Zn^{2+}$  binding to the sensor should generate a detectable signal so that the binding event can be

monitored conveniently. Therefore, TPEN and DPA must be the chelators of choice since they display high specificity for binding to  $Zn^{2+}$  over other metal cations, and favorable kinetic and thermodynamic properties which result in quick formation of a stable  $Zn^{2+}$  complex. Then by placing the active amines of TPEN or DPA moiety at the 4-position of NBD fluorophore, we constructed two potential sensors **1** and **2** for  $Zn^{2+}$  mannering in reverse fluorescent characteristics (Figure 4.3).

**Figure 4.3.** Design of  $Zn^{2+}$  sensor **1** and **2**.



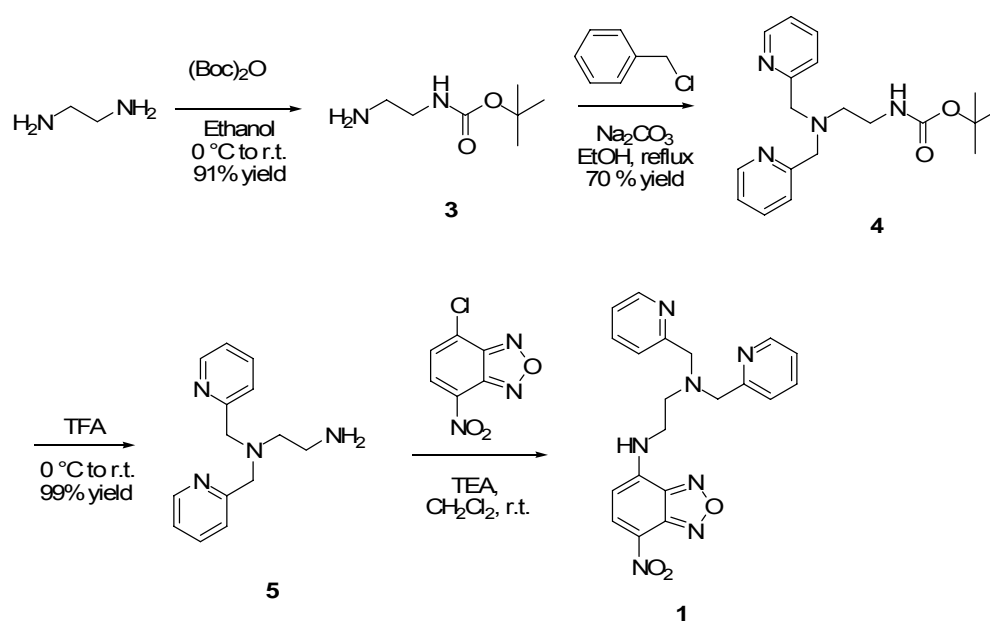
We envisioned that compound **1** should be a turn-on fluorescent sensor for  $Zn^{2+}$  proceeding PET mechanism.<sup>20</sup> Hopefully in zinc-free status, an electron transfer mainly from N' atom as an electron donor could quench the fluorescence of the molecule. While chelation of  $Zn^{2+}$  with compounds **1** would cause the fluorescence intensity to increase as a result of blocking PET of the nitrogen atoms. On the contrary, we thought compound **2** might be a turn-off sensor proceeding ICT mechanism. Without presence of a strong quencher, zinc-free sensor **2** would be strong fluorescent featuring charge-transfer excited state after excitation. However, chelation of  $Zn^{2+}$  would attenuate the electron-donating ability of the nitrogen atom at

4-position of NBD fluorophore so as to decrease the fluorescence intensity.

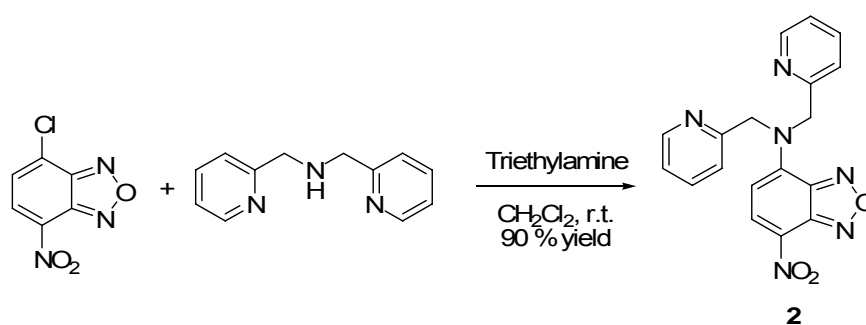
### 4.2.3. Synthesis

Compounds **1** and **2** were prepared in a straightforward manner. First TEPN was synthesized in three steps according to reported paper in an overall 63% yield. Then direct aromatic nucleophilic substitution of TEPN or commercial available DPA with NBD-Cl in dichloromethane in the presence of triethylamine affords **1** or **2** in 73% and 90% yields separately (Scheme 4.1).

**Scheme 4.1.** Synthesis of (a) sensor **1**, and (b) sensor **2**



(a) Synthesis of sensor **1**



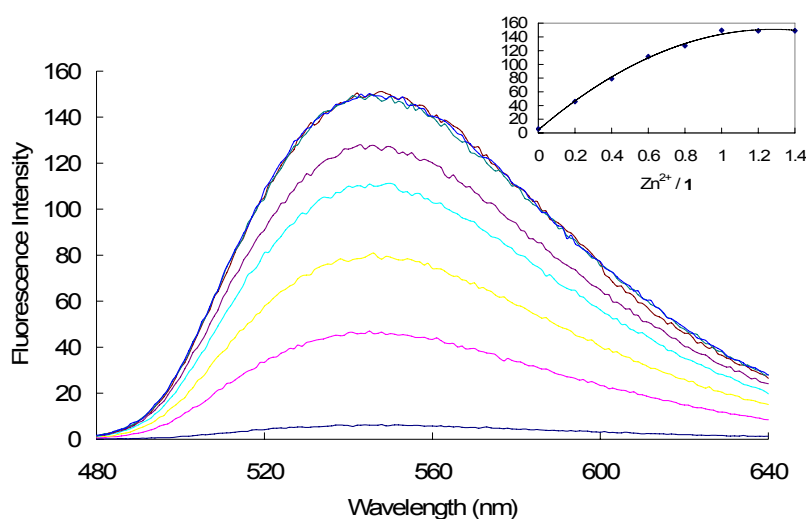
(b) Synthesis of sensor **2**

## 4.2.4. Results and Discussion

### 4.2.4.1. Fluorescent properties and response towards $Zn^{2+}$ .

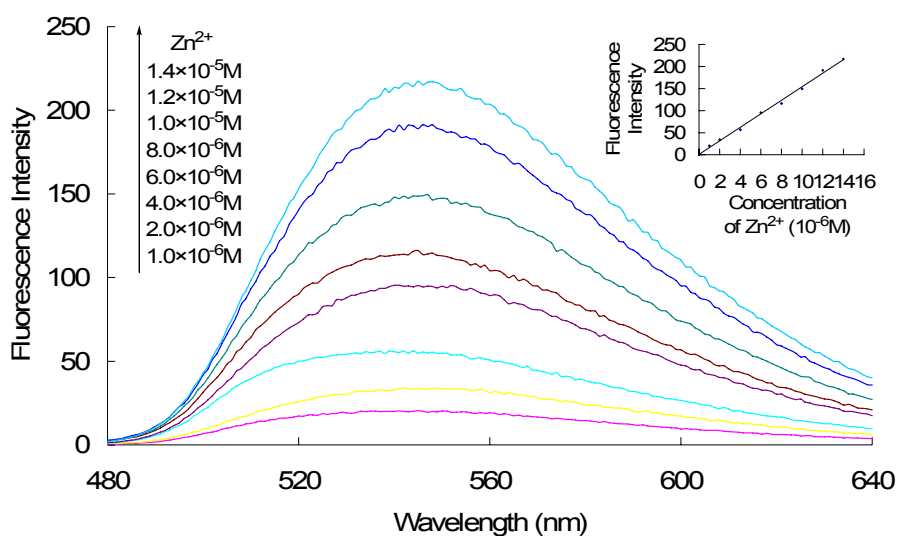
In spectroscopic experiments, we first investigate the fluorescent properties of **1** and **2**. The experiment was performed in an aqueous phosphate buffer ( $I = 0.01M$ , pH 7.3) containing **1** or **2** at a concentration of  $1.0 \times 10^{-5} M$ . As we designed, compound **1** showed very low background fluorescence under physiological conditions attributed to the quenching of PET process, while **2** displayed strong fluorescence signals.

Upon addition of  $Zn^{2+}$ , the fluorescence intensity of sensor **1** is enhanced significantly in a concentration dependent manner. When 1.0 equivalent of  $Zn^{2+}$  is added, the fluorescence intensity reached the maximum by more than 25-folds and almost no more increase was observed for further addition of  $Zn^{2+}$  (tested up to 1.4 equivalents) (Figure 4.4). Notably The sensor **1** is highly sensitive to  $Zn^{2+}$ . Even we lowered the concentration of thiophenol to only  $1.0 \times 10^{-6} M$ , an obvious fluorescence signal increase still could be observed.

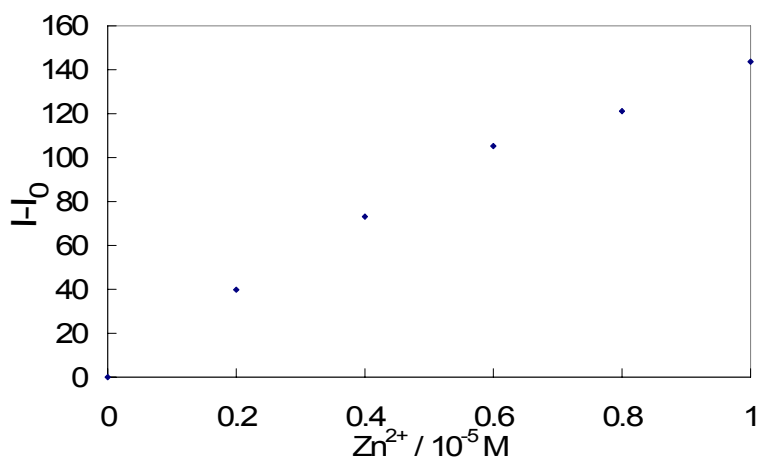


**Figure 4.4.** Effect of  $Zn^{2+}$  concentration on the fluorescence of sensor **1**. Sensor **1** ( $10^{-5} M$ ) was studied in a phosphate buffer (pH 7.3, 0.01M) at room temperature in the absence and presence of a range amount of  $Zn^{2+}$  ( $0 - 1.4 \times 10^{-5} M$ ) with  $\lambda_{ex} = 470$  nm.

The stoichiometric titration of **1** with 1:1 ratio of concentration versus  $\text{Zn}^{2+}$  also showed **1** had a sensitive response towards  $\text{Zn}^{2+}$  as low as  $1.0 \times 10^{-6}$  M (Figure 4.5). More significantly, a nearly linear relationship between the fluorescence intensity increase of sensor **1** and the concentration of  $\text{Zn}^{2+}$  is observed (Fig 4.6), so the sensor could be used for the quantitative determination of the concentration of  $\text{Zn}^{2+}$ .

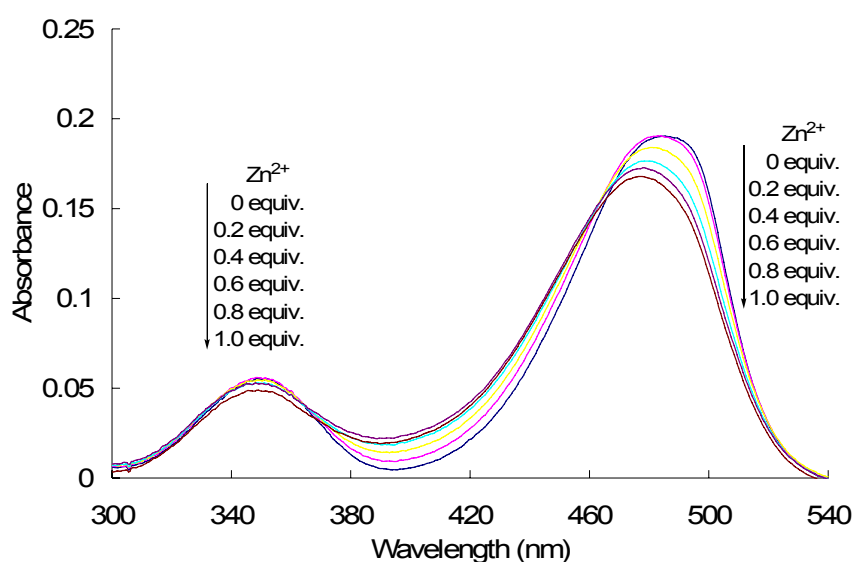


**Figure 4.5.** Emission spectra ( $\lambda_{\text{ex}} = 470$  nm) of sensor **1** in a range concentration of  $0 - 1.4 \times 10^{-5}$  M after addition of the same amounts of  $\text{Zn}^{2+}$  at room temperature in phosphate buffer (pH 7.3).



**Figure 4.6.** Plot of the concentration of  $\text{Zn}^{2+}$  vs.  $\Delta I$ , where  $\Delta I = I - I_0$ ,  $I$ : the fluorescence intensity of probe **1** ( $10^{-5}$  M) with addition of  $\text{Zn}^{2+}$  and  $I_0$ : the fluorescence intensity of sensor **1** without  $\text{Zn}^{2+}$  at  $\lambda_{\text{ex}} = 550$  nm.

A slight change of absorption spectra also occurred during the titration experiments (Figure 4.7). Originally the  $\text{Zn}^{2+}$ -free **1** exhibited absorption bands in the visible region centered at 485 nm ( $\epsilon = 1.9 \times 10^4 \text{ M}^{-1} \text{ cm}^{-1}$ ). Upon addition of  $0-1.0 \times 10^{-5} \text{ M}$  of  $\text{Zn}^{2+}$ , the visible absorption profile blue-shifted to a peak center at 476 nm, and the intensity maximum of  $\mathbf{1} \cdot \text{Zn}^{2+}$  complex decreased a little bit ( $\epsilon = 1.68 \times 10^4 \text{ M}^{-1} \text{ cm}^{-1}$ ).

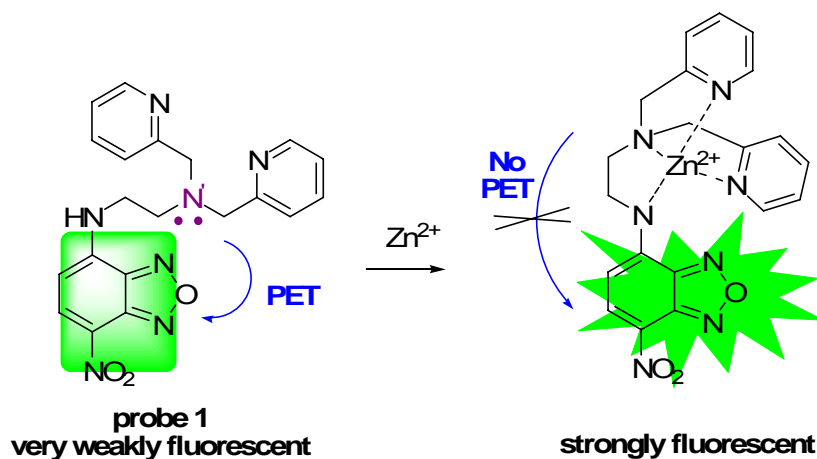


**Figure 4.7.** Effect of  $\text{Zn}^{2+}$  concentration on the absorption of sensor **1**. Data were acquired after addition of a range amount of  $\text{Zn}^{2+}$  ( $0 - 1.0 \times 10^{-5} \text{ M}$ ) to  $10^{-5} \text{ M}$  sensor **1** in a phosphate buffer (pH 7.3) at room temperature.

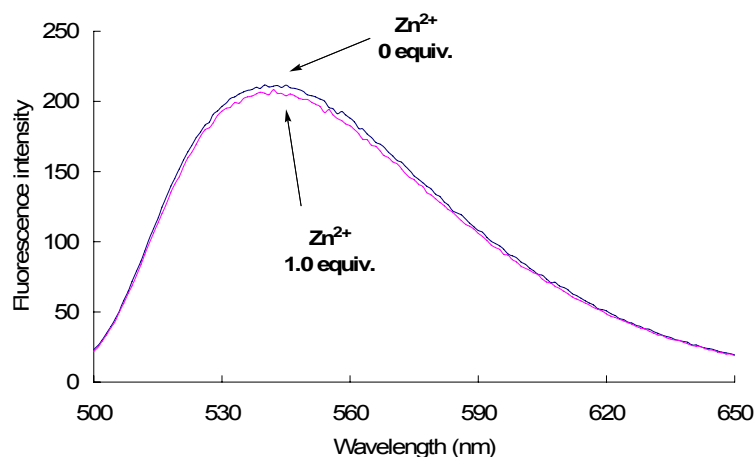
These phenomena suggested the nitrogen at the 4-position of benzofurazan fluorophore maybe involve in the binding of  $\text{Zn}^{2+}$  so as to cause the blue-shift of the absorption wavelength as well as the decrease of absorption intensity maximum (Figure 4.8).



**Figure 4.8.** Proposed binding model of **1** with  $\text{Zn}^{2+}$



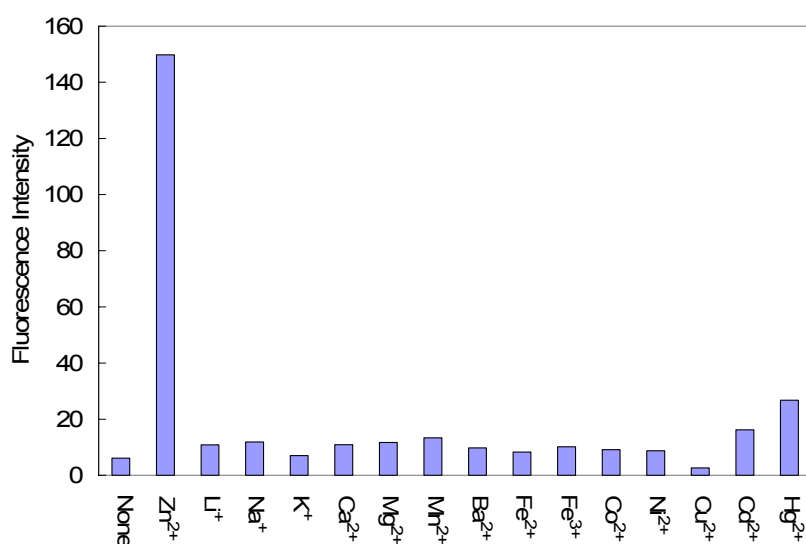
In contrast to **1**, almost no fluorescence alternation for sensor **2** was observed before and after addition of  $\text{Zn}^{2+}$  (Figure 4.9). We think the reason is that the whole conjugated system largely attenuated the binding affinity of the long-pair electron of the nitrogen at 4-position of benzofurazan. As a result, these three nitrogens of DPA ligand failed to provide strong chelation to  $\text{Zn}^{2+}$ . This also indicates that the “N” in probe **11** is critical in the PET process as well as binding profile.



**Figure 4.9.** Fluorescence response of sensor **2** towards  $\text{Zn}^{2+}$ . The spectra was acquired before and after addition of  $1.0 \times 10^{-5}$  M  $\text{Zn}^{2+}$  to  $10^{-5}$  M sensor **2** in PBS buffer (pH 7.3) at room temperature with  $\lambda_{\text{ex}} = 470$  nm.

#### 4.2.4.2. Examination of Selectivity.

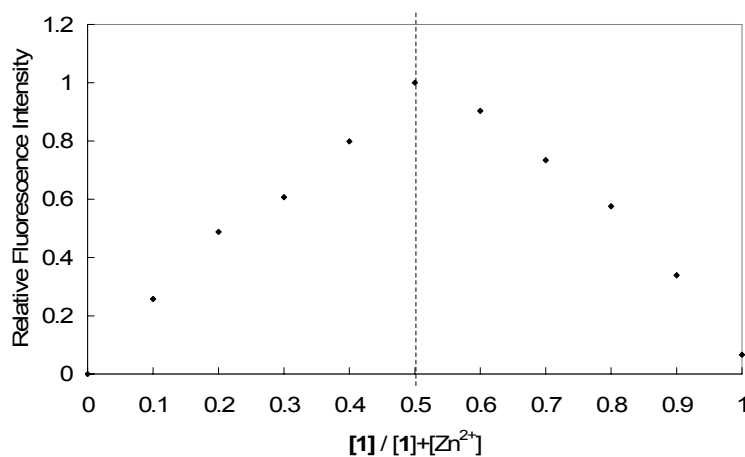
The above studies prompted us to select chemical sensor **1** for further evaluation aimed at determining its selectivity. The fluorescence titration of **1** with various metal ions exhibited high selectivity to  $\text{Zn}^{2+}$  (Fig 4.10). Metal ions which possess a broad spectrum of biological activities and functions in living cells, such as  $\text{Na}^+$ ,  $\text{K}^+$ ,  $\text{Mg}^{2+}$ ,  $\text{Ca}^{2+}$ ,  $\text{Mn}^{2+}$ ,  $\text{Fe}^{2+}$ , and  $\text{Fe}^{3+}$ , did not give rise to any responses under the same conditions. Actually even we enhanced their concentration to micromolar level, still no obvious fluorescence changes were observed. Most heavy transition metal ions, including  $\text{Cd}^{2+}$ ,  $\text{Ni}^{2+}$ , and  $\text{Co}^{2+}$ , also showed no interference.  $\text{Hg}^{2+}$  induces very limited fluorescence enhancement, while  $\text{Cu}^{2+}$  quenches fluorescence. Like TPEN, sensor **1** probably form complexes with some transition metal ions, but the fluorescence is weakend because of the electron or energy transfer between metal ion and fluorophore, which is known as the fluorescence quenching mechanism.



**Figure 4.10.** The selectivity of sensor **1** towards various metal ions. In these experiments, the fluorescence measurement was taken at  $\lambda_{\text{ex}} = 470$  nm from  $10^{-5}$  M of probe **11** in a PBS buffer ( $I = 0.01$  M, pH 7.3) at room temperature and in the absence and presence of 1.0 equiv. of a metal ion. The fluorescence intensity at  $\lambda_{\text{em}} = 550$  nm is used for plotting versus an analyte.

#### 4.2.4.3. Kinetic analysis of the complex formation with Zn<sup>2+</sup>.

As we mentioned, upon addition of various concentrations of Zn<sup>2+</sup>, the fluorescence intensity of probe **1** (10<sup>-5</sup> M) almost linearly increased up to a 1 equivalent of Zn<sup>2+</sup>, and didn't change towards further addition. Moreover, a Job's plot analysis exhibited a point of inflection value at 0.5, which meant maximum fluorescence was obtained at a 1:1 ratio (Fig 4.11). These data revealed that probe **1** should form a 1:1 complex with Zn<sup>2+</sup>.



**Figure 4.11.** Job's plot of **1** and Zn<sup>2+</sup>. The total concentration of probe **1** and Zn<sup>2+</sup> were kept at a constant 10  $\mu$ M. Excitation was provided at 470 nm and emission intensity was measured at 550 nm. Spectra were acquired in pH 7.3 phosphate buffer.

Therefore, the binding constants,  $K_d$ , was determined from the fluorescence intensity in the 0.01 M phosphate buffer at pH 7.3 with 0-10<sup>-5</sup> M Zn<sup>2+</sup> at room temperature. The fluorescence intensity data were fitted to equation below, and  $K_d$  was calculated,

$$F = (F_{\max} [Zn^{2+}] + F_{\min} K_d) / (K_d + [Zn^{2+}])$$

where F is the observed fluorescence,  $F_{\max}$  is the fluorescence for the Probe\*Zn<sup>2+</sup> (1 : 1) complex, and  $F_{\min}$  is the fluorescence in the absence of Zn<sup>2+</sup>. The observed  $K_d$  value

was determined as 4.6  $\mu\text{M}$ , which is sufficiently sensitive for the application in some biological studies in mammalian cells.

#### **4.2.5. Conclusion.**

A novel NBD-derived water-soluble fluorescent sensor **1** has been designed and synthesized, and it displayed high selectivity and sensitivity for  $\text{Zn}^{2+}$  in a neutral buffer aqueous solution. In the presence of  $\text{Zn}^{2+}$ , significant fluorescence enhancement was achieved. Since the concentration of  $\text{Zn}^{2+}$  in a biological system, for example, in synaptic vesicles, is reported to be in the micromolar to millimolar range, the sensor **1**, which displays a good sensitivity in the micro-range, can be used for the imaging of  $\text{Zn}^{2+}$ . Moreover, the magnitude of the fluorescence intensity increase corresponds nearly linearly to the concentration of  $\text{Zn}^{2+}$ , indicating that the sensor could be used for the quantitative measurement of  $\text{Zn}^{2+}$  concentrations.

### **4.3. Development of Fluorescent Sensor for Mercury Ion**

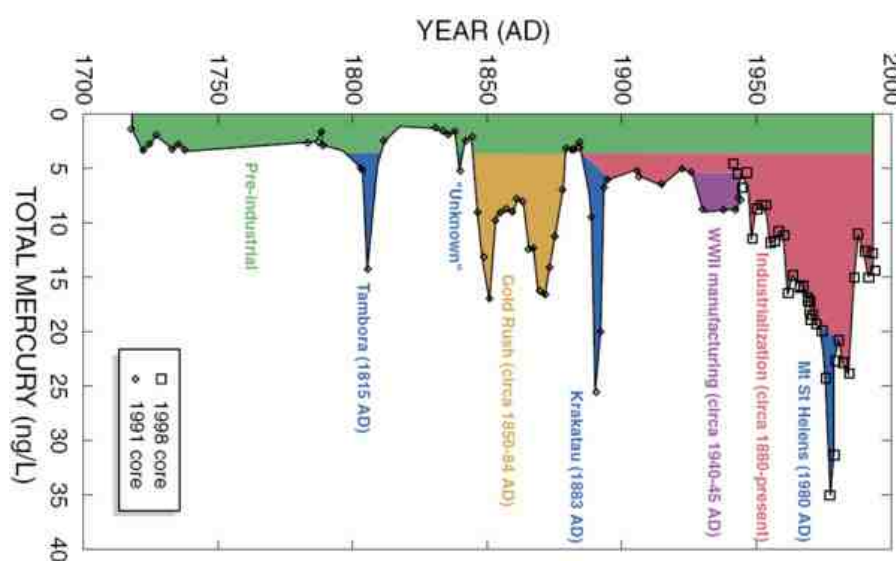
#### **4.3.1. Introduction.**

The development of fluorescent sensors for the detection of  $\text{Hg}^{2+}$  is fuelled by its high toxicity and widespread distribution in the environment.<sup>21</sup> The resulting contamination has created a significant threat to human health and our living systems. The mercury induced toxicity can cause a number of severe health problems such as brain damage, kidney failure, and various cognitive and motion disorders.<sup>22</sup>

#### 4.3.1.1. Sources of Mercury Contamination and Bioaccumulation.

The biogeochemical cycling of mercury is complex and influenced by many factors that include climate fluctuations, geology, natural disasters and more and more, human activities (Figure 4.12).

**Figure 4.12.** Amount of atmospheric mercury deposited at Wyoming's Upper Fremont Glacier over the last 270 years.



Inorganic mercury ( $\text{Hg}^0$  and  $\text{Hg}^{2+}$ ) is released into the environment through a variety of anthropogenic and natural sources. Natural sources such as volcanic, oceanic emissions and forest fires are responsible for approximately half of atmospheric mercury emissions. Moreover, industrial sources include coal and gold mining, solid waste incineration, wood pulping, fossil fuel combustion, and chemical manufacturing release constituting the other half of inorganic mercury.

Emitted elementary mercury vapors are easily transported in the atmosphere, often across continents and oceans, and are eventually oxidized to  $\text{Hg}^{2+}$ . Atmospheric

deposition of  $\text{Hg}^{2+}$  results in its accumulation on plants, in topsoil, and in waters. Irrespective of the source and initial site of deposition,  $\text{Hg}^{2+}$  ultimately enters freshwater and marine ecosystems. A fraction of this  $\text{Hg}^{2+}$  is reduced to  $\text{Hg}^0$  by microorganisms, including algae and cyanobacteria, and is subsequently released back to the atmosphere.<sup>23</sup> Another portion of the  $\text{Hg}^{2+}$  accumulates in underwater sediments. Some prokaryotes that live in these sediments convert this inorganic mercury to methylmercury, which we define as any  $\text{CH}_3\text{HgX}$  species, as do bacteria that reside in fish gills and gut. In addition to this acknowledged source, some ecological studies point to the occurrence of abiotic mercury methylation under certain environmental conditions, but more work is needed to evaluate this hypothesis.<sup>24</sup> Because methylmercury is lipophilic, readily absorbed, and poorly excreted, it enters the food chain and biomagnifies in higher organisms, especially in the muscles of large predatory fish, and is subsequently ingested by humans.<sup>25-27</sup>

Although often overlooked, at least in the chemical literature, mercury bioaccumulation also occurs in plants, which provides additional routes of entry into the food web.<sup>28</sup> Mosses take up  $\text{Hg}^{2+}$  from atmospheric deposition and tree leaves are another  $\text{Hg}^{2+}$  repository. Mercury reduces photosynthesis and transpiration in plants, the former of which may impact the global carbon cycle. The bioaccumulated mercury reenters soils and natural waters following plant decay or is consumed by birds and mammals, and thereby further enters the food chain. Additional sources of human exposure to mercury include the household and workplace, religious practices, dental amalgams, and vaccines.<sup>29</sup>

#### **4.3.1.2. Consequences Mercury Toxicity for Human Health.**

The biological targets and toxicity profile of mercury depend on its chemical composition.<sup>30</sup> Methylmercurials, the species of greatest concern, are readily absorbed by the human GI tract, cross the blood-brain barrier, and target the central nervous system. In the absence of accidental poisoning, the only known source of human exposure to methylmercury is through seafood consumption. Neurological problems associated with methylmercury intoxication are manifold and include prenatal brain damage, cognitive and motion disorders, vision and hearing loss, and death. The ramifications of long-term and low-level exposure to methylmercury are less clear and warrant thorough toxicological investigations. This mode of exposure is currently of particular concern for human embryos, the developing fetus, and children.<sup>31</sup> At the molecular and cellular levels, methylmercury causes oxidative stress<sup>32a</sup> and lipid peroxidation,<sup>32b</sup> and it inhibits the division and migration of neurons. It accumulates in astrocytes, preventing glutamate uptake, and thereby causes excitotoxic injury to neurons.<sup>30c,32c</sup> Inorganic mercury targets the renal epithelial cells of the kidney, causing tubular necrosis and proteinuria.<sup>12d,e</sup> It is also a neurotoxin and causes immune system dysfunction.<sup>29b</sup>

#### **4.3.1.3. Fluorescent detection of mercury.**

Traditional quantitative approaches to  $\text{Hg}^{2+}$  analysis in water samples employ a number of analytical techniques that include atomic absorption spectroscopy, cold vapor atomic fluorescence spectrometry, and gas chromatography. Many of these

methods require complicated, multi-step sample preparation and/or sophisticated instrumentation. As a result, obtaining new mercury detection methods that are cost-effective, rapid, facile and applicable to the environmental and biological milieus become an important goal. This objective has recently emerged as a focal point in the chemistry and, more broadly, sensing communities. Because of its operational simplicity, low cost, real time monitoring and high sensitivity, fluorescence detection is becoming the dominant strategy used for Hg<sup>2+</sup> sensing.<sup>33-37</sup> However, the search for readily accessible fluorescent Hg<sup>2+</sup> probes with good water solubility and high specificity and sensitivity is still a challenging task.

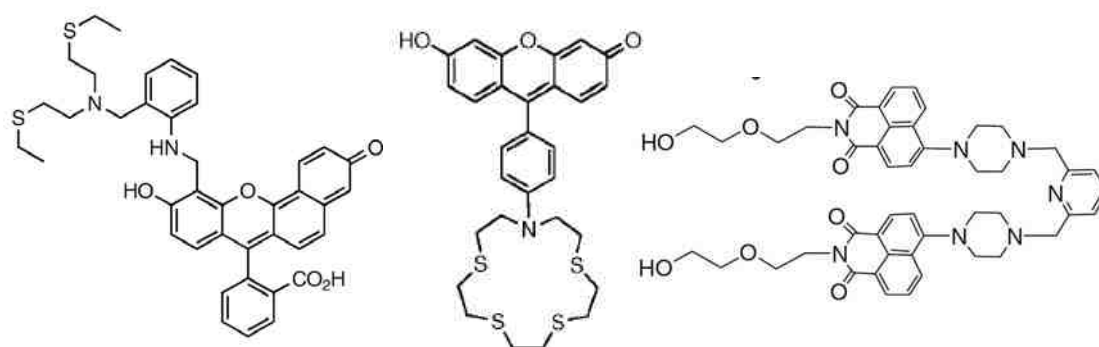
Most of the small molecule-derived fluorescence sensors for Hg<sup>2+</sup> reported so far compose of two components: a recognition moiety containing nitrogen/sulfur atoms and a fluorophore that signals the fluorescence change upon exposure to Hg<sup>2+</sup> (Figure 4.13).<sup>33-35</sup> In many cases interference from other metal ions can affect the selectivity or sensitivity.

Alternative approaches in the design of selective fluorescence chemosensors for Hg<sup>2+</sup> take advantage of the unique high binding affinity of Hg<sup>2+</sup> to sulfur species (Figure 4.14). A variety of strategies including coordination,<sup>34</sup> and chemodosimeters such as hydrolysis,<sup>35a,g,h</sup> cyclization,<sup>35d,l</sup> ring opening of rhodamine spiro systems,<sup>35b,f,m-r,38</sup> and elimination reactions have been applied to the design of Hg<sup>2+</sup> specific fluorescence sensors. Notably, Mánez and Rurack and co-workers explored the Hg<sup>2+</sup> catalyzed desulfurization to generate a fluorescent conjugate system.<sup>32e</sup> However, among all these probes, to our knowledge, only a handful of fluorescent

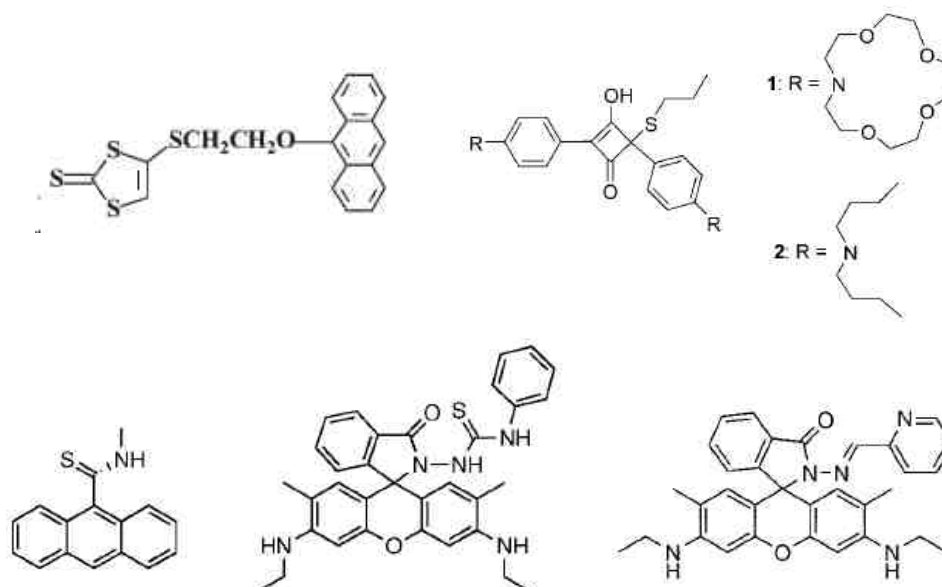


probes displayed good water solubility, which mainly relied on coordination strategy. So far no chemodosimeters for  $\text{Hg}^{2+}$  in pure aqueous solution have been disclosed. Therefore, we wish to disclose a novel highly sensitive and selective fluorescence probe for  $\text{Hg}^{2+}$  in aqueous solution without the requirement for additional organic solvent.

**Figure 4.13.** Examples of fluorescent sensors for  $\text{Hg}^{2+}$  based on ligand binding.



**Figure 4.14.** Examples of fluorescent sensors for  $\text{Hg}^{2+}$  based on other principles.

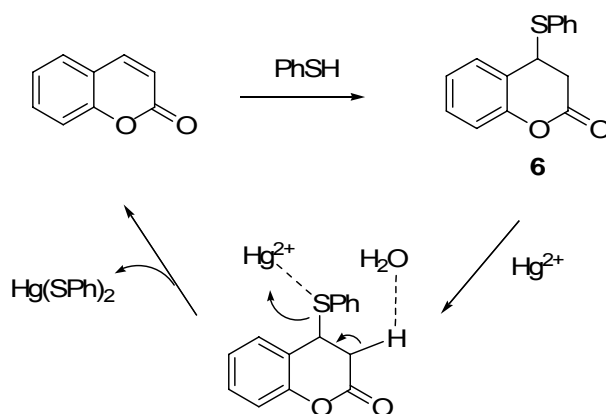


## 4.3.2. Research Design

### 4.3.2.1. Design of first model

In the beginning, our design of  $\text{Hg}^{2+}$  sensor was constructed on coumarin scaffold since coumarin and its derivatives are widely used fluorophores with favorable physical and optical properties and stability. Enlightened by the previous sensors based on the desulfurization mechanism, we aimed to prepare compound **6** as our first sensory sample. We hoped this Michael adduct **6** of thiophenol to coumarin is non-fluorescent as a non-conjugated cyclic system; whereas when  $\text{Hg}^{2+}$  was added, the  $\text{Hg}^{2+}$ -assisted retro-michael desulfurization could re-produce coumarin fluorophore and thus recover the fluorescence (Figure 4.15).

**Figure 4.15.** Design principle of fluorescence sensor **6** for  $\text{Hg}^{2+}$ .



### 4.3.2.2. Problems and solutions.

Compound **6** was synthesized by heating coumarin in thiophenol at 100 °C catalyzed by piperidine without other solvents according to the reported literature.<sup>39</sup>

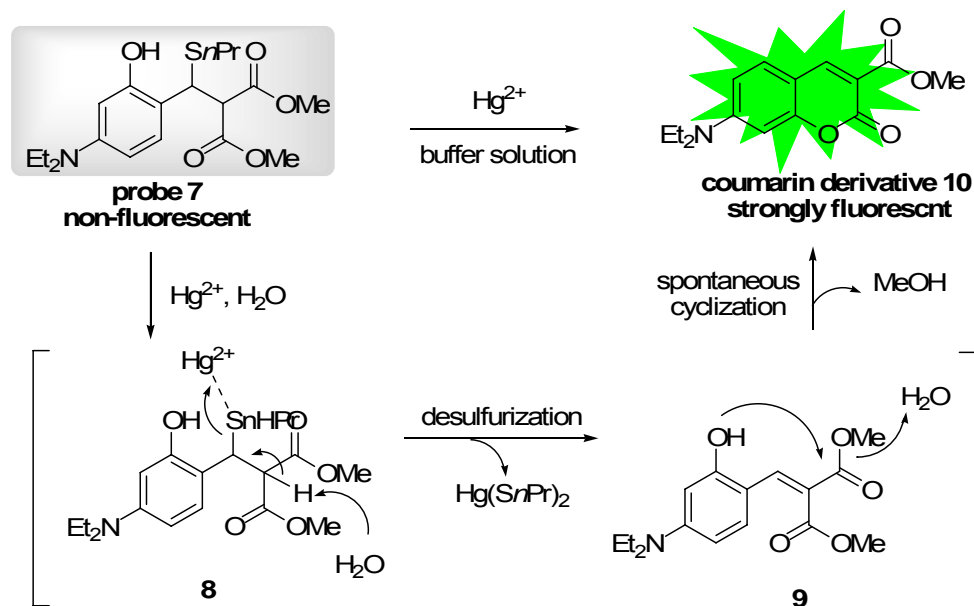
However, **6** failed to act as  $\text{Hg}^{2+}$  sensor because of its poor stability even on TLC.

Self-desulfurization will automatically proceed in the buffer solution and cause the formation of coumarin without the help of mercury ion. The result made us realize that for this cyclic lactone system, the formation of a stable coumarin conjugation is much easier than its de-conjugation by a thiol. Therefore, we came out a possible solution: if we cleave the sulfur-containing lactone and construct an acyclic acid or ester precursor, its flexible structure will greatly improve the stability. At the same time, it still keeps non-fluorescent as a non-conjugated compound. Then the second issue is the generation of fluorescence during  $\text{Hg}^{2+}$ -recognizing process. It is noted that the product of  $\text{Hg}^{2+}$ -promoted desulfurization is like a 2-hydroxy coumarinic ester, if this modified product could undergo a simultaneously cyclization, it will generate strong-fluorescent coumarin as the final solution.

#### **4.3.2.3. New designed model.**

It is well-known that the 2-hydroxy cis-coumarinic acids can undergo facile lactonization to form fluorescent coumarins.<sup>40</sup> Taking advantage of this, we designed molecule **7** containing a sulfur moiety can serve as a “turn-on” chemosensor for  $\text{Hg}^{2+}$  (Figure 4.16). We envisioned the non-conjugated compound **7** should be non-fluorescent. However, in the presence of  $\text{Hg}^{2+}$ , it facilitates desulfurization to generate 2-hydroxycoumarinic ester **9**, which undergoes spontaneous lactonization to give rise to the highly fluorescent coumarin derivative **10**.

**Figure 4.16.** Design of Hg<sup>2+</sup> facilitated facile desulfurization–actonization fluorescent chemodosimeter.



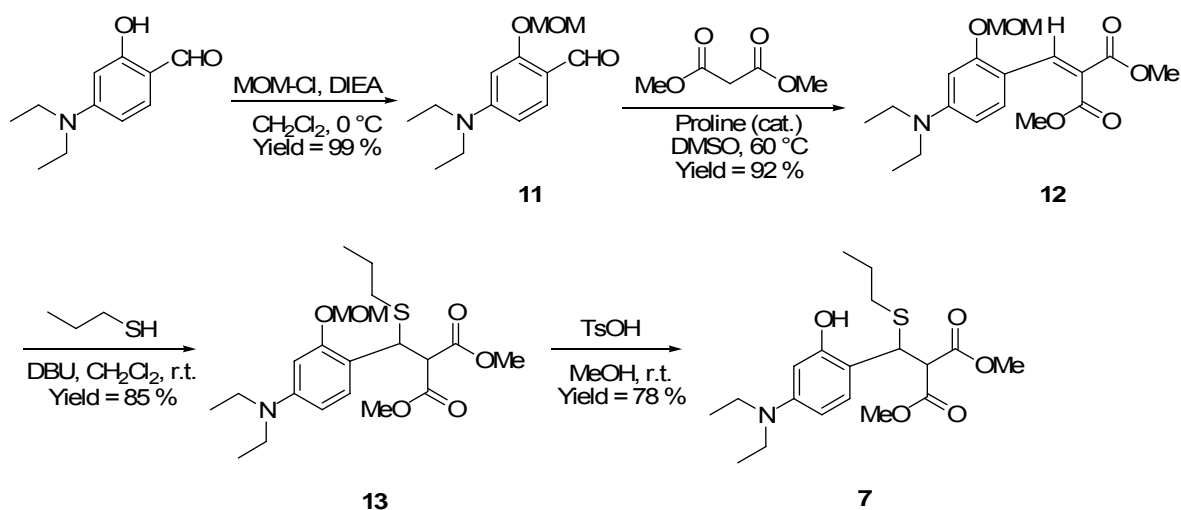
In this design, two critical factors are taken into consideration. A malonate ester moiety rather than a simple ester is incorporated into the system. Such a design can kill two birds with one stone. On the one hand, the malonate enhances the acidity of the hydrogen in **8** so that the elimination process, which is proposed to be a rate-limiting step in the entire process, can be significantly facilitated to generate compound **9**. On the other hand, it eliminates the “*cis*” geometry of the C=C double bond in coumarinic acid necessarily required for the facile lactonization. The resulting non-geometric unsaturated diester is able to process the cyclization without the requirement of geometry. Therefore, the sensor can produce a very fast response towards the analyte Hg<sup>2+</sup>. The second improvement is introducing a diethylamino group into probe **7**. Such a modification can not only improve the water solubility of the probe, but also enhances its quantum yield. Moreover, an important merit of the

approach enables introduction of a variety of functional groups for modulating the properties (e.g. water solubility and fluorescence, etc.) of the fluorescence system. Therefore, it is expected that the designed probe **7** will be a turn-on sensor for  $\text{Hg}^{2+}$ . In the  $\text{Hg}^{2+}$ -free form, it displays non-fluorescence. However, when it reacts with  $\text{Hg}^{2+}$  to yield **10**, strong fluorescence should be observed.

### 4.3.3. Synthesis

Sensor **7** was prepared straightforward in four steps starting from readily available compound **11** (4-(diethylamino)-2-hydroxybenzaldehyde) (Scheme 4.2). Protecting the hydroxy group of **11** with MOM-Cl afforded **12**, which was then subjected to the condensation with dimethyl malonate to obtain unsaturated diester **13**. Michael addition of 1-propanethiol to **13** gave the adduct **14**. Final deprotection of MOM-protected hydroxyl group with TsOH in methanol afforded sensor **7** in good yield.

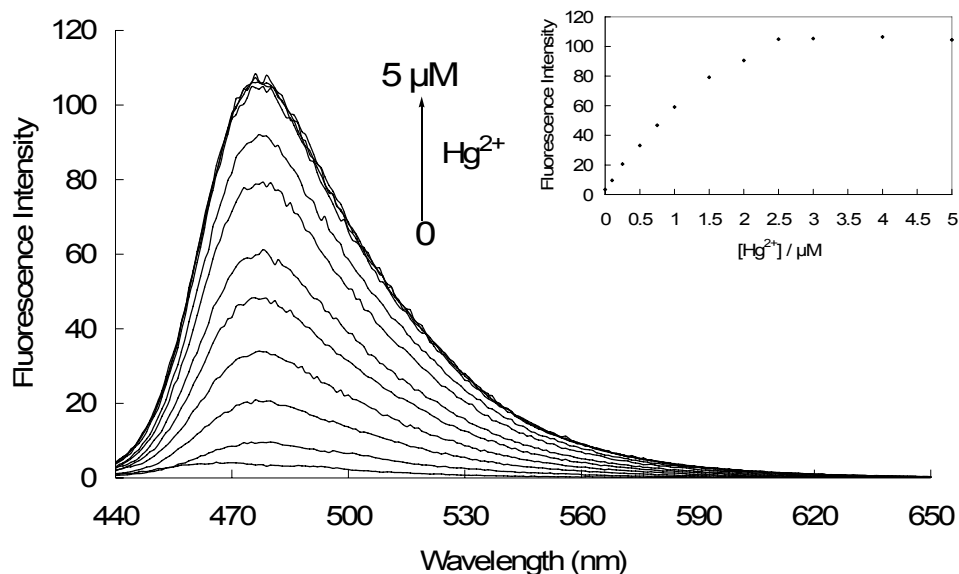
**Scheme 4.2.** Synthesis of sensor **7**.



#### 4.3.4. Results and Discussion.

##### 4.3.4.1. Fluorescent property and response towards $\text{Hg}^{2+}$ .

With sensor **7** in hand, we first examined its fluorescence properties in the absence and presence of  $\text{Hg}^{2+}$  and established the optimal measurement conditions. Notably, compound **7** displayed a good solubility in aqueous solution without addition of an organic solvent. Accordingly, the experiment was performed in an aqueous phosphate buffer (0.05 M, pH 6.0) containing sensor **7** at a concentration of  $5.0 \times 10^{-6}$  M. As expected, sensor **7** exhibited almost non-fluorescence in the absence of  $\text{Hg}^{2+}$  at  $\lambda_{\text{ex}} = 430$  nm. When  $5.0 \times 10^{-6}$  M  $\text{Hg}^{2+}$  was added, the colorless solution became light yellow at once, and a significant increase in fluorescence intensity (>50 folds) was observed rapidly. The expected fluorescent coumarin product **10** was monitored and confirmed by a comparison study with a standard pure compound **10** based on  $^1\text{H}$  NMR analysis. Notably, chemosensor **7** displayed a high sensitivity towards  $\text{Hg}^{2+}$ . It was found that the fluorescence intensity increase displayed a concentration dependent manner. When  $2.5 \times 10^{-6}$  M (0.5 equiv.) of  $\text{Zn}^{2+}$  is added, the fluorescence intensity reached the maximum and almost no more increase was observed for further addition of  $\text{Hg}^{2+}$  (tested up to  $5.0 \times 10^{-6}$  M) (Figure 4.17). A pronounced fluorescent signal change (ca. 1 fold) was observed even when  $\text{Hg}^{2+}$  was as low as  $1 \times 10^{-8}$  M, a range of  $\text{Hg}^{2+}$  concentration close to the maximum contamination level as defined by the United States Environmental Protection Agency (EPA).<sup>41</sup>



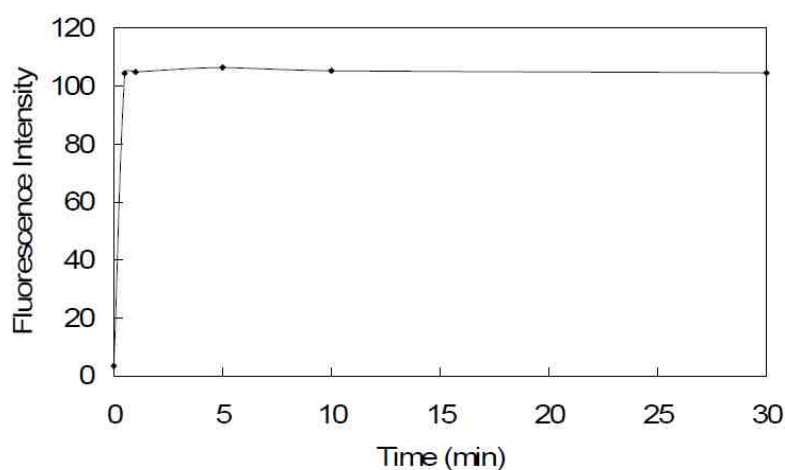
**Figure 4.17.** Fluorescence response ( $\lambda_{\text{ex}} = 430 \text{ nm}$ ) and plot (emission collected at 480 nm) of the  $5 \mu\text{M}$  sensor **7** towards  $\text{Hg}^{2+}$ . Spectra shown are for  $\text{Hg}^{2+}$  concentrations of 0, 0.1, 0.25, 0.5, 0.75, 1.0, 1.5, 2.0, 2.5, 3.0, 4.0 and  $5.0 \mu\text{M}$ , respectively. These data were recorded at 30 seconds after addition of  $\text{Hg}^{2+}$  in a phosphate buffer (0.05 M, pH 6.0) at room temperature.

#### 4.3.4.2. Kinetic analysis.

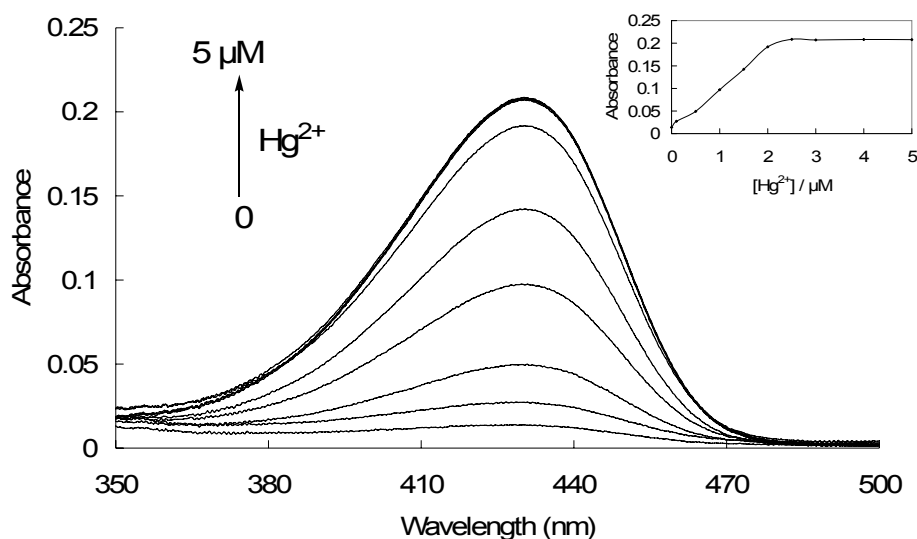
Time-related examination showed sensor **7** showed a fast response toward  $\text{Hg}^{2+}$  completely finished within 30 seconds (Figure 4.18). No further alteration of fluorescence intensity was seen even at longer reaction times (up to 30 min). Moreover, the fluorescence signals kept constantly strong and seldom faded, which exhibited an excellent stability and optical properties of the product.

Stoichiometric titration of  $\text{Hg}^{2+}$  towards sensor **7** ( $5.0 \times 10^{-6} \text{ M}$ ) in UV experiments showed a similar profile like in the fluorescent experiments (Figure 4.19). Since  $\text{Hg}^{2+}$ -free **7** is not a large conjugation, it exhibited no obvious absorption in a range of 380-470 nm. However, upon addition of  $0-2.5 \times 10^{-6} \text{ M}$   $\text{Hg}^{2+}$ , strong absorption bands appeared in this region in a concentration-dependent manner centered at 430 nm, which suggested the formation of fluorescent coumarin **10** ( $\epsilon = 4.1 \times 10^4 \text{ M}^{-1} \text{ cm}^{-1}$ ).

When  $2.5 \times 10^{-6}$  M  $\text{Hg}^{2+}$  (0.5 equiv.) was added, the absorption intensity reached the maximum and almost had no alternation upon further addition of  $\text{Hg}^{2+}$  (up to  $5.0 \times 10^{-6}$  M).



**Figure 4.18.** Reaction time profile of sensor 7 ( $5 \mu\text{M}$ ,  $\lambda_{\text{ex}} = 430 \text{ nm}$ ) towards  $\text{Hg}^{2+}$  ( $2.5 \mu\text{M}$ ) in pH 6.0 phosphate buffer ( $I = 0.05 \text{ M}$ ). Spectra shown are for reaction time of 0, 0.5, 1.0, 5.0, 10.0 and 30.0 minutes. Fluorescence emission data were acquired at 480 nm in at room temperature.

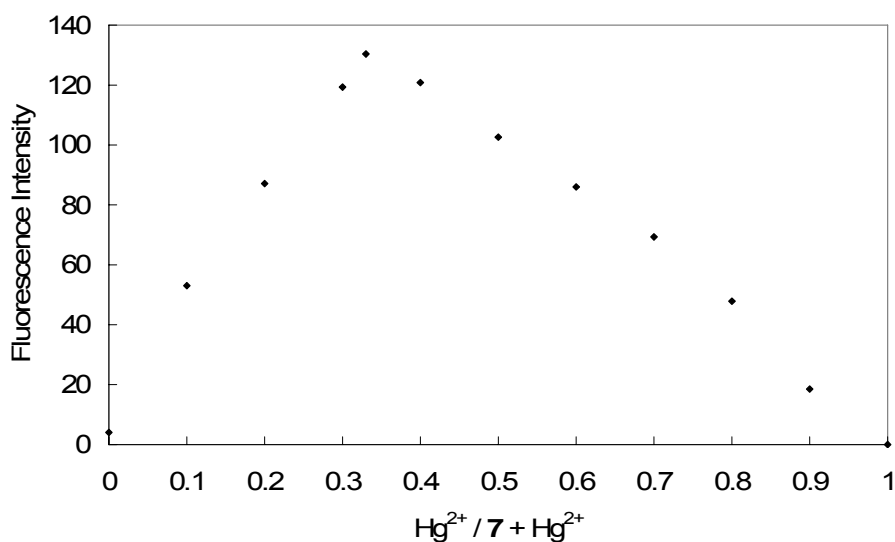


**Figure 4.19.** UV response of the  $5 \mu\text{M}$  sensor 7 towards  $\text{Hg}^{2+}$ . Spectra shown are for  $\text{Hg}^{2+}$  concentrations of 0, 0.1, 0.25, 0.5, 0.75, 1.0, 1.5, 2.0, 2.5, 3.0, 4.0 and  $5.0 \mu\text{M}$ , respectively. These data were recorded at 30 seconds after addition of  $\text{Hg}^{2+}$  in a phosphate buffer ( $0.05 \text{ M}$ , pH 6.0) at room temperature.



Job's plot analysis also exhibited a point of inflection value at 0.33 (Figure 4.20).

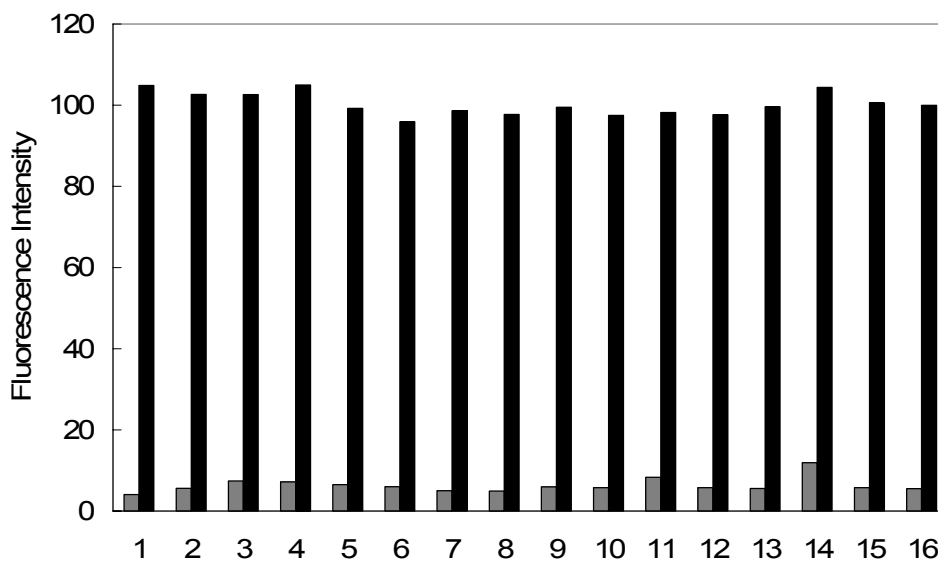
These data revealed that sensor **7** reacted with  $\text{Hg}^{2+}$  in a 1:2 ratio as we expected.



**Figure 4.20.** Job's plot of sensor **7** and  $\text{Hg}^{2+}$ . The total concentration of sensor **7** and  $\text{Hg}^{2+}$  were kept constant  $10 \mu\text{M}$ . Excitation was provided at 430 nm and emission was measured at 480 nm. These data were measured at 30 seconds in pH 6.0 phosphate buffer ( $I = 0.05 \text{ M}$ ) at room temperature.

#### 4.3.4.3. Examination of selectivity

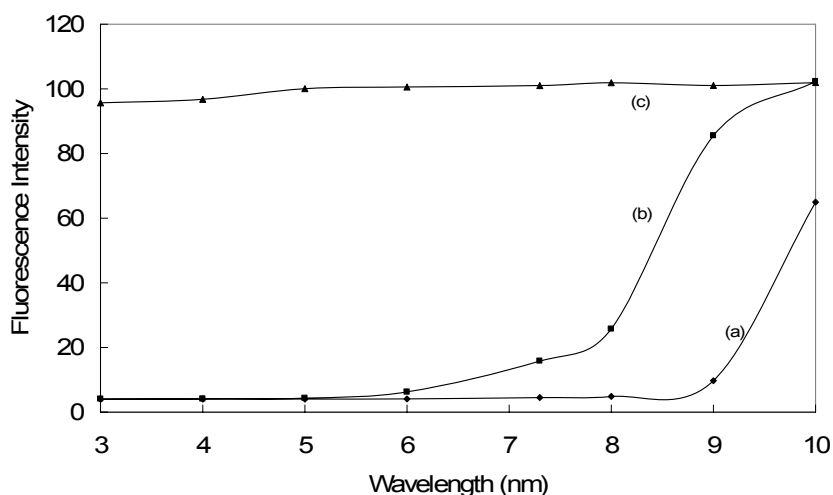
The competition assays were carried out by the subsequent addition of  $\text{Hg}^{2+}$  (0.5 equiv.) to the solution of other metal ions (2-fold excesses). A variety of metal ions are surveyed such as alkali  $\text{Li}^+$ ,  $\text{Na}^+$ , and  $\text{K}^+$ , alkaline-earth  $\text{Mg}^{2+}$ ,  $\text{Ca}^{2+}$  and  $\text{Ba}^{2+}$ , and transition and heavy metal  $\text{Mn}^{2+}$ ,  $\text{Fe}^{2+}$ ,  $\text{Fe}^{3+}$ ,  $\text{Co}^{2+}$ ,  $\text{Ni}^{2+}$ ,  $\text{Cu}^{2+}$ ,  $\text{Zn}^{2+}$ ,  $\text{Cd}^{2+}$ , and  $\text{Pb}^{2+}$  ions. Notably, the addition of these ions did not result in a new emission band to **7**, nor was the fluorescence response associated with the addition of  $\text{Hg}^{2+}$  affected by these ions (Figure 4.21). This indicated that sensor **7** has high specificity toward  $\text{Hg}^{2+}$  without interference by other metal ions.



**Figure 4.21.** Fluorescence response of the 5  $\mu\text{M}$  sensor **7** upon addition of  $\text{Hg}^{2+}$  (5  $\mu\text{M}$ ) and various other metal cations (10  $\mu\text{M}$  each). Gray bar: **7** + metal, black bar: **17** + metal +  $\text{Hg}^{2+}$ . Metal cations: (1) None, (2)  $\text{Li}^+$ , (3)  $\text{Na}^+$ , (4)  $\text{K}^+$ , (5)  $\text{Mn}^{2+}$ , (6)  $\text{Mg}^{2+}$ , (7)  $\text{Ba}^{2+}$ , (8)  $\text{Ca}^{2+}$ , (9)  $\text{Fe}^{2+}$ , (10)  $\text{Fe}^{3+}$ , (11)  $\text{Co}^{2+}$ , (12)  $\text{Ni}^{2+}$ , (13)  $\text{Cu}^{2+}$ , (14)  $\text{Zn}^{2+}$ , (15)  $\text{Cd}^{2+}$ , (16)  $\text{Pb}^{2+}$ . These data were measured at 30 seconds in pH 6.0 phosphate buffer ( $I = 0.05 \text{ M}$ ) at room temperature excited at 430 nm.

#### 4.3.4.4. The effect of pH on the stability and reactivity.

Finally, we evaluated the effect of pH in the buffer solution on sensor **7** (Figure 4.22). When the solution is acidic (pH 3-6), sensor **7** was quite stable and exhibited very sensitive response towards  $\text{Hg}^{2+}$ . Although the reaction proceeded a little bit slower in a lower pH condition, it still completed in less than 1 minute. However, in the basic condition, the self-desulfurization could happen and generated coumarin **10** without assistance of  $\text{Hg}^{2+}$ . Especially when pH was high than 9, spontaneous reaction would happen right after the addition of  $\text{Hg}^{2+}$ . Therefore, sensor **7** can perform well as a  $\text{Hg}^{2+}$  sensor in the acidic condition.



**Figure 4.22.** Effect of pH on the stability of sensor **7** ( $5 \mu\text{M}$ ) and its fluorescence response on  $\text{Hg}^{2+}$ . Excitation was provided at 430 nm and emission was measured in phosphate buffer at 480 nm. (a) right after addition of  $5 \mu\text{M}$  probe into phosphate buffer and stirred 5 seconds; (b) 10 minutes after stirring the probe buffer solution; (c) Addition of  $5 \mu\text{M}$   $\text{Hg}^{2+}$  to the probe solution.

#### 4.3.5. Conclusion

An unprecedented highly selective and sensitive “turn-on” fluorescent chemodosimeter **7** for the detection of  $\text{Hg}^{2+}$  in aqueous media has been developed. The sensor is designed based on a unique  $\text{Hg}^{2+}$  facilitated desulfurization–lactonization cascade reaction by transforming a weakly fluorescent precursor to a highly fluorescent coumarin derivative with a 50-fold increase in fluorescence intensity. Remarkably the responsive speed is very rapid (less than 30 s). The combination of water solubility and positive fluorescence response to the analyte enhance the practical utility of the probe. More significantly, the strategy described here affords a new avenue for the design of novel fluorescence sensors, which constitutes our future endeavors for sensor development.

#### **4.4. Experiment Data**

##### **General Information.**

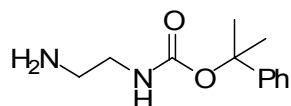
Commercial reagents were used as received, unless otherwise stated. Merck 60 silica gel was used for chromatography, and Whatman silica gel plates with fluorescence F254 were used for thin-layer chromatography (TLC) analysis. <sup>1</sup>H and <sup>13</sup>C NMR spectra were recorded on Bruker Avance 500, and tetramethylsilane (TMS) was used as a reference. Data for <sup>1</sup>H are reported as follows: chemical shift (ppm), and multiplicity (s = singlet, d = doublet, t = triplet, q = quartet, m = multiplet). Data for <sup>13</sup>C NMR are reported as ppm. Mass Spectra were obtained from University of New Mexico Mass Spectral facility.

##### **Spectroscopic materials and methods.**

Millipore water was used to prepare all aqueous solutions. The pH was recorded by a Beckman ΦTM 240 pH meter. UV absorption spectra were recorded on a Shimadzu UV-2410PC UV-Vis spectrophotometer. Fluorescence emission spectra were obtained on a Varian Eclipse fluorescence spectrophotometer.

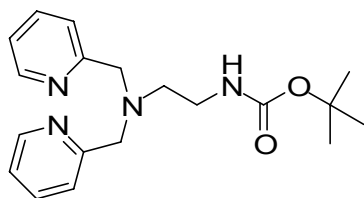
### Synthesis of seneor 1.

Compound **1** was synthesized following the procedures in Scheme 4.1.



### (2-Aminoethyl)carbamic acid tert-butyl ester (**3**).

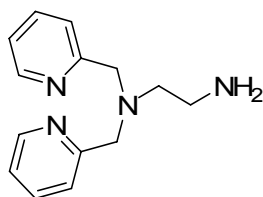
To a solution of ethylenediamine (1.35 mL, 20 mmol) in 10 mL ethanol was added di-*t*-butyl dicarbonate (441 mg, 2 mmol) dropwise at 0 °C. The reaction mixture was warmed up to room temperature and stirred for 24 h under a nitrogen atmosphere, then evaporated in *vacuo*. The residue was dissolved in 20 mL of dichloromethane and washed with aqueous solution of sodium hydroxide. The organic layer was dried with magnesium sulfate, filtered and evaporated in *vacuo* to give the crude product of **3** as colorless oil (315 mg, 91 % yield). <sup>1</sup>H NMR (500 MHz, CDCl<sub>3</sub>): δ 5.23 (s, 1H), 3.09 (d, 2H, *J* = 5.5 Hz), 2.72 (t, 2H, *J* = 6 Hz), 1.47 (s, 2H), 1.36 (s, 9H); <sup>13</sup>C NMR (125 MHz, CDCl<sub>3</sub>): δ 156.4, 79.1, 43.4, 41.9, 28.5.



### *tert*-Butyl 2-(bis(pyridin-2-ylmethyl)amino)ethylcarbamate (**4**).

A mixture of **3** (290 mg, 1.67 mmol), 2-pyridylmethyl chloride hydrochloride (615 mg, 3.67 mmol) and sodium carbonate (467 mg, 7.34 mmol) in 20 mL of ethanol

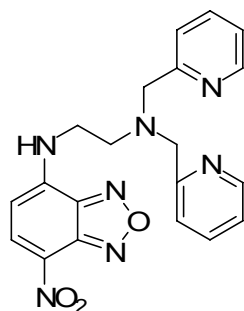
was refluxed for 12 h under a nitrogen atmosphere. Then the solvent was evaporated, the mixture was dissolved in 20 mL of aqueous solution of sodium hydroxide and extracted with dichloromethane (3 × 30 mL). The combined organic layer was dried with magnesium sulfate, filtered and evaporated in *vacuo*. The crude product was purified by silica gel chromatography using triethylamine/methanol/dichloromethane (1:1:100) as the elute to afford **4** as brown oil (400 mg, 70% yield). <sup>1</sup>H NMR (500 MHz, CDCl<sub>3</sub>): δ 8.55 (d, 2H, *J* = 5 Hz), 7.64 (t, 2H, *J* = 7.5 Hz), 7.42 (d, 2H, *J* = 7.5 Hz), 7.16 (dd, 2H, *J*<sub>1</sub> = 5 Hz, *J*<sub>2</sub> = 1.5 Hz), 5.89 (s, 1H), 3.87 (s, 4H), 3.24 (d, 2H, *J* = 5 Hz), 2.70 (t, 2H, *J* = 5.5 Hz), 1.45 (s, 9H); <sup>13</sup>C NMR (125 MHz, CDCl<sub>3</sub>): δ 159.4, 156.3, 149.2, 136.5, 123.2, 122.2, 78.7, 60.3, 53.6, 38.6, 28.6.



***N*-Bis-pyridin-2-ylmethylethane-1,2-diamine (5).**

To 15 mL trifluoroacetic acid was added dropwise a solution of **4** (400 mg, 1.17 mmol) in 10 mL of dichloromethane at 0 °C. The reaction was warmed up to room temperature and stirred 2 h under a nitrogen atmosphere, then evaporated in *vacuo*. The residue was dissolved in an aqueous solution of sodium hydroxide and extracted with dichloromethane (3 × 20 mL). The combined organic layer was dried with magnesium sulfate, filtered and evaporated in *vacuo* to afford **5** as brown oil (280 mg, 99% yield). <sup>1</sup>H NMR (500 MHz, CDCl<sub>3</sub>): δ 8.54 (d, 2H, *J* = 4 Hz), 7.60 (t, 2H, *J* =

7.5 Hz), 7.32 (d, 2H,  $J = 8$  Hz), 7.14 (t, 2H,  $J = 6$  Hz), 4.62 (s, 2H), 3.86 (s, 4H), 2.92 (t, 2H,  $J = 5.5$  Hz), 2.80 (t, 3H,  $J = 5.5$  Hz);  $^{13}\text{C}$  NMR (125 MHz,  $\text{CDCl}_3$ ):  $\delta$  159.6, 149.2, 136.6, 123.1, 122.2, 60.7, 57.0, 39.5.

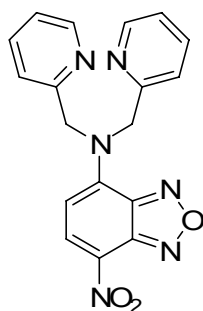


***N*-(2-(Bis(pyridin-2-ylmethyl)amino)ethyl)-7-nitrobenzo[*c*][1,2,5]oxadiazol-4-amine (1).**

To a solution of **5** (243 mg, 1.0 mmol) and triethylamine (169  $\mu\text{L}$ , 1.2 mmol) in 10 mL dichloromethane was added NBD-Cl (245 mg, 1.2 mmol) dropwise at room temperature and stirred overnight, then evaporated in *vacuo*. The residue was dissolved in an aqueous solution of sodium hydroxide and extracted with dichloromethane ( $3 \times 20$  mL). The combined organic layer was dried with magnesium sulfate, filtered and evaporated in *vacuo*. The crude product was purified by silica gel chromatography using triethylamine/methanol/dichloromethane (1:1:60) as elute to afford **1** as brown solid (294 mg, 78% yield).  $^1\text{H}$  NMR (500 MHz,  $\text{CDCl}_3$ ):  $\delta$  10.35 (s, 1H), 8.74 (d, 2H,  $J = 3.5$  Hz), 8.44 (d, 1H,  $J = 8.5$  Hz), 7.60 (t, 2H,  $J = 7.5$  Hz), 7.33 (d, 2H,  $J = 8$  Hz), 7.20 (t, 2H,  $J = 6$  Hz), 6.01 (d, 1H,  $J = 7.5$  Hz), 4.04 (s, 4H), 3.51 (s, 2H), 3.12 (t, 2H,  $J = 5$  Hz);  $^{13}\text{C}$  NMR (125 MHz,  $\text{CDCl}_3$ ):  $\delta$  158.6, 149.5, 145.0, 144.5, 144.4, 137.2, 137.0, 123.1, 122.5, 122.4, 98.1, 59.5, 50.6, 42.5.

## Synthesis of sensor 2.

Compound **2** was synthesized following the procedures in Figure.



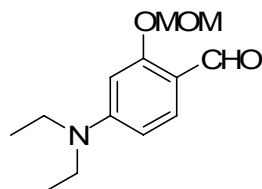
### 7-Nitro-*N,N*-bis(pyridin-2-ylmethyl)benzo[*c*][1,2,5]oxadiazol-4-amine (**2**).

To a solution of di-(2-picolyl)-amine (93  $\mu\text{L}$ , 0.5 mmol) and triethylamine (106  $\mu\text{L}$ , 0.75 mmol) in 10 mL dichloromethane was added NBD-Cl (123 mg, 1.2 mmol) dropwise at room temperature and stirred overnight, then evaporated in *vacuo*. The residue was dissolved in an aqueous solution of sodium hydroxide and extracted with dichloromethane ( $3 \times 20$  mL). The combined organic layer was dried with magnesium sulfate, filtered and evaporated in *vacuo*. The crude product was purified by silica gel chromatography using triethylamine/methanol/dichloromethane (1:1:50) as elute to afford the desired product **2** as brown solid (162 mg, 90% yield).  $^1\text{H}$  NMR (500 MHz,  $\text{CDCl}_3$ ):  $\delta$  8.56 (d, 2H,  $J = 4.5$  Hz), 8.36 (d, 1H,  $J = 9$ Hz), 7.70 (m, 3H), 7.33 (d, 2H,  $J = 8.5$  Hz), 7.24 (dd, 2H,  $J_1 = 5$  Hz,  $J_2 = 2$  Hz), 6.35 (d, 1 H,  $J = 9$  Hz), 5.43 (s, 4H);  $^{13}\text{C}$  NMR (125 MHz,  $\text{CDCl}_3$ ):  $\delta$  155.2, 150.1, 146., 145.0, 144.8, 137.3, 135.5, 123.7, 123.2, 122.0, 103.3, 58.9.



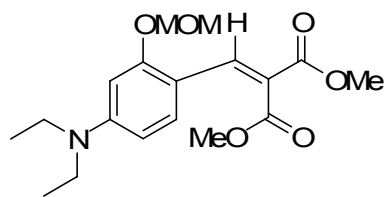
## Synthesis of Probe 7.

Compound **7** was synthesized following the procedures in Scheme 4.2.



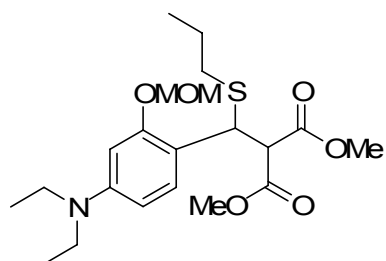
### 4-(Diethylamino)-2-(methoxymethoxy)benzaldehyde (**11**)

To a solution of 4-(diethylamino)-2-hydroxybenzaldehyde (2.03 g, 10 mmol) in 50 mL of anhydrous dichloromethane was added N,N-diisopropylethylamine (5.2 mL, 30 mmol) at room temperature under a nitrogen atmosphere. The solution was cooled to 0 °C and chloromethyl methyl ether (1.5 mL, 20 mmol) was added dropwisely. The reaction mixture was warmed up to room temperature and stirred for 24 h under a nitrogen atmosphere. The reaction solution was washed with water and extracted by dichloromethane (2 × 30 mL). The combined organic layer was dried with magnesium sulfate, filtered and evaporated *in vacuo* to afford **11** as light red solid (2.37 g, 99% yield). <sup>1</sup>H NMR (500 MHz, CDCl<sub>3</sub>): δ 10.16 (s, 1H), 7.72 (d, 1H, *J* = 9.5 Hz), 6.35-6.33 (m, 2H), 5.27 (s, 2H), 3.52 (s, 3H), 3.41 (q, 4H, *J* = 7 Hz), 1.21 (t, 6H, *J* = 7 Hz); <sup>13</sup>C NMR (125 MHz, CDCl<sub>3</sub>): δ 186.9, 162.1, 153.7, 130.2, 114.7, 105.4, 96.0, 94.8, 56.3, 44.8, 12.5.



**Dimethyl 2-[4-(diethylamino)-2-(methoxymethoxy)benzylidene]malonate (12)**

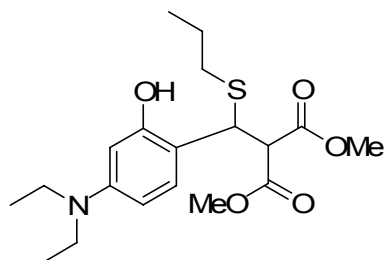
A solution of **11** (2 mmol, 475 mg), dimethyl malonate (350  $\mu$ L, 3 mmol) and proline (46 mg, 0.4 mmol) in 20 mL of DMSO was heated to 60 °C until TLC showed that **11** was completely consumed. Solvents was removed in *vacuo*, the residue was poured into 20 mL of water and extracted by dichloromethane (3  $\times$  20 mL). The combined organic layer was dried with magnesium sulfate, filtered and evaporated in *vacuo*. The crude product was purified by silica gel chromatography to afford **12** as yellow oil (646 mg, 92% yield).  $^1\text{H}$  NMR (500 MHz,  $\text{CDCl}_3$ ):  $\delta$  8.13 (s, 1H), 7.23 (d, 1H,  $J = 9$  Hz), 6.40 (s, 1H), 6.27 (d, 1H,  $J = 9$  Hz), 5.21 (s, 1H), 3.84 (s, 3H), 3.80 (s, 3H), 3.49 (s, 3H), 3.36 (q, 4H,  $J = 7$  Hz), 1.17 (t, 3H,  $J = 7$  Hz);  $^{13}\text{C}$  NMR (125 MHz,  $\text{CDCl}_3$ ):  $\delta$  168.8, 165.9, 158.9, 151.5, 138.3, 130.4, 118.2, 109.9, 105.7, 97.2, 95.0, 56.3, 52.3, 52.1, 44.7, 12.7.



**Dimethyl 2-{[4-(diethylamino)-2-(methoxymethoxy)phenyl](propylthio)methyl} malonate (13):**

To a solution of **12** (40mg, 0.114 mmol), 1-propanethiol (52  $\mu$ L, 0.57 mmol) in

10 mL of dichloromethane was added 1,8-diazabicyclo[5.4.0]undec-7-ene (3.5  $\mu$ L, 0.02 mmol) and stirred 6 h at rt. Solvents were removed under reduced pressure and the crude product was purified directly by silica gel chromatography. (41mg, 85% yield).  $^1\text{H}$  NMR (500 MHz,  $\text{CDCl}_3$ ):  $\delta$  7.04 (d, 1H,  $J = 8.5$  Hz), 6.43 (s 1H), 6.24 (d, 1H,  $J = 8.5$  Hz), 5.20 (s, 2H), 4.67 (d, 1H,  $J = 11.5$  Hz), 4.17 (d, 1H,  $J = 11.5$  Hz), 3.79 (s, 3H), 3.53 (s, 3H), 3.50 (s, 3H), 3.31 (q, 4H,  $J = 7$  Hz), 2.45-2.42 (tm, 2H), 1.58-1.50 (m, 2H), 1.14 (t, 6H,  $J = 7$  Hz), 0.90 (t, 3H,  $J = 7$  Hz);  $^{13}\text{C}$  NMR (125 MHz,  $\text{CDCl}_3$ ):  $\delta$  168.5, 167.7, 156.4, 148.8, 129.6, 115.3, 105.4, 98.8, 95.0, 57.8, 56.2, 52.8, 52.6, 44.6, 43.8, 34.4, 22.9, 13.7, 12.9.

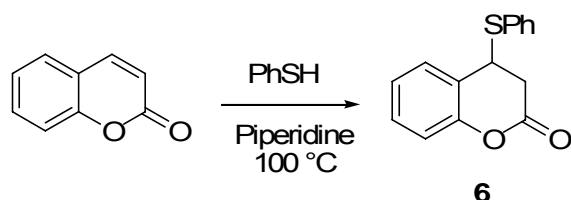


**Dimethyl 2-([4-(diethylamino)-2-hydroxyphenyl](propylthio)methyl)malonate (7):**

A solution of **13** (30 mg, 0.07 mmol) and *p*-toluenesulfonic acid 68 mg, 0.35 mmol) in 3 mL of MeOH was stirred for 2 days at room temperature. Evaporated solvents, the residue was dissolved in 10 mL dichloromethane, washed with 10 mL of aqueous solution of sodium bicarbonate and extracted by dichloromethane (2  $\times$  10 mL). The combined organic layer was dried over magnesium sulfate, filtered and evaporated in *vacuo* and purified by silica gel chromatography (21 mg, 78% yield).

$^1\text{H}$  NMR (500 MHz,  $\text{CDCl}_3$ ):  $\delta$  6.97-6.95 (m, 2H), 6.19-6.17 (m, 2H), 4.56 (d, 1H,  $J = 11$  Hz), 3.97 (d, 1H,  $J = 11$  Hz), 3.80 (s, 3H), 3.53 (s, 3H), 3.30 (q, 4H,  $J = 7$  Hz), 2.44-2.38 (m, 1H), 2.34-2.28 (m, 1H), 1.60-1.48 (m, 2H), 1.14 (t, 6H,  $J = 7$  Hz), 0.90 (t, 3H,  $J = 7.5$  Hz);  $^{13}\text{C}$  NMR (125 MHz,  $\text{CDCl}_3$ ):  $\delta$  168.0, 156.4, 149.4, 131.3, 110.0, 104.8, 101.1, 57.1, 53.0, 52.9, 45.3, 44.5, 33.6, 22.4, 13.5, 12.9; HRMS (ESI): calculated for  $[\text{M}+\text{H}^+]$  384.1845, found 384.1851.

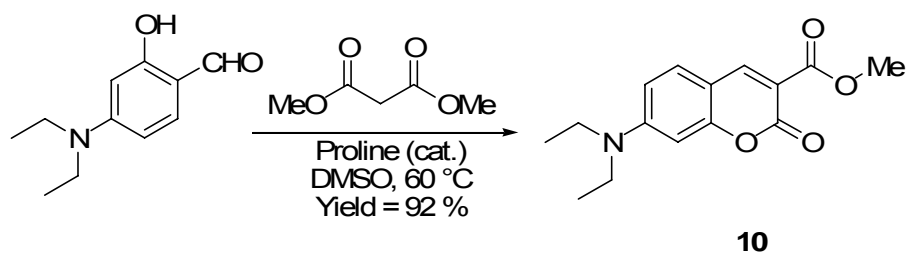
### Synthesis of sensor 6.



A mixture of 0.5 g. of the coumarin under investigation, 0.5 g. of the thiophenol and two drops of freshly distilled piperidine was warmed at 100 °C for three hours, during which all the solid had melted. The cooled reaction mixture was washed with cold hexane (*ca.* 40 ml.) several times and the resulting solid crystallized from the mixture solvent of hexane and dichloromethane to afford **6** in 70 % yield.  $^1\text{H}$  NMR (500 MHz,  $\text{CDCl}_3$ ):  $\delta$  7.44-7.43 (m, 2H), 7.36-7.30 (m, 4H), 7.19 (d, 1H,  $J = 7.5$  Hz), 7.09 (dd, 2H,  $J_1 = 7.5$  Hz,  $J_2 = 3$  Hz), 4.50 (t,  $J = 4$  Hz), 3.01-3.00 (m, 2H).

### Synthesis of coumarin derivative 10.

Compound **10** was synthesized following the procedure in the scheme below.



A solution of 4-(diethylamino)-2-hydroxybenzaldehyde (2 mmol, 475 mg), dimethyl malonate (350  $\mu$ L, 3 mmol) and proline (46 mg, 0.4 mmol) in 20 mL of DMSO was heated to 60  $^{\circ}$ C until TLC showed that 4-(diethylamino)-2-hydroxybenzaldehyde was completely consumed. Solvents were removed in *vacuo*, the residue was poured into 20 mL of water and extracted by dichloromethane (3  $\times$  20 mL). The combined organic layer was dried with magnesium sulfate, filtered and evaporated in *vacuo*. The crude product was purified by silica gel chromatography to afford **10** as yellow oil (646 mg, 92% yield).  $^1\text{H}$  NMR (500 MHz,  $\text{CDCl}_3$ ):  $\delta$  8.45 (s, 1H), 7.36 (d, 1H,  $J = 9.0$  Hz), 6.61 (dd, 1H,  $J_1 = 9.0$  Hz,  $J_2 = 2.5$  Hz), 6.46 (d, 1H,  $J = 2.5$  Hz), 3.91 (s, 3H), 3.45 (q, 4H,  $J = 7$  Hz), 1.24 (t, 6H,  $J = 7$  Hz);  $^{13}\text{C}$  NMR (125 MHz,  $\text{CDCl}_3$ ):  $\delta$  165.2, 158.7, 158.5, 153.1, 149.8, 131.3, 109.8, 108.7, 107.9, 96.8, 52.5, 45.3, 12.6.

#### 4.5. References

1. (a) Vallee, B. L. and Falchuk, K. H. *Physiol. Rev.* **1993**, *73*, 79. (b) de Silva, J. J. R. F. and Williams, R. J. P. in *The Biological Chemistry of Elements: The Inorganic Chemistry of Life*, Oxford University Press, New York, **2001**. (c) Williams, R. J. P. and de Silva, J. J. R. F. *Coord. Chem. Rev.* **2000**, *200*, 247.
2. Bush, A. I. *Trends Neurosci.* **2003**, *26*, 207.
3. Sorensen, M. B.; Stoltenberg, M.; Juhl, S.; Danscher, G.; and Ernst, E.; *Prostate.* **1997**, *31*, 125.
4. Chausmer, A. B. *J. Am. Coll. Nutr.* **1998**, *17*, 109.
5. (a) Kimura, E.; and Aoki, S. *BioMetals* **2001**, *14*, 191. (b) Fahrni, C. J. and O'Halloran, T. V. *J. Am. Chem. Soc.* **1999**, *121*, 11448. (c) Nasir, M. S.; Fahrni, C. J.; Suhy, D. A.; Kolodsick, K. J.; Singer, C. P. and O'Halloran, T. V. *J. Biol. Inorg. Chem.* **1999**, *4*, 775. (d) Shults, M. D.; Pearce, D. A. and Imperiali, B. *J. Am. Chem. Soc.* **2003**, *125*, 10591. (e) Royzen, M.; Durandin, A.; Young, V. G. Jr.; Geacintov, N. E. and Canary, J. W. *J. Am. Chem. Soc.* **2006**, *128*, 3854. (f) Liu, Y.; Zhang, N.; Chen, Y. and Wang, L. H. *Org. Lett.* **2007**, *9*, 315.
6. (a) Ajayaghosh, A.; Carol, P. and Sreejith, S. *J. Am. Chem. Soc.* **2005**, *127*, 14962. (b) Peng, X.; Xu, Y.; Sun, S.; Wu, Y. and Fan, J. *Org. Biomol. Chem.* **2007**, *5*, 226.
7. (a) Koike, T.; Watanabe, T.; Aoki, S.; Kimura, E. and Shiro, M. *J. Am. Chem. Soc.* **1996**, *118*, 12696. (b) Thompson, R. B.; Maliwal, B. P.; Feliccia, V. L.; Fierke, C. A. and McCall, K. *Anal. Chem.* **1998**, *70*, 4717. (c) Prodi, L.; Bolletta, F.; Montalti, M. and Zaccheroni, N. *Eur. J. Inorg. Chem.* **1999**, 455.

8. Zapata, F.; Caballero, A.; Espinosa, A.; Tarraga, A. and Molina, P. *Org. Lett.* **2007**, *9*, 2385.
9. (a) Godwin, H. A. and Berg, J. M. *J. Am. Chem. Soc.* **1996**, *118*, 6514. (b) Elbaum, D.; Nair, S. K.; Patchan, M. W.; Thompson, R. B. and Christianson, D. W. *J. Am. Chem. Soc.* **1996**, *118*, 8381. (c) Burdette, S. C.; Walkup, G. K.; Spingler, B.; Tsien, R. Y. and Lippard, S. J. *J. Am. Chem. Soc.* **2001**, *123*, 7831. (d) Hirano, T.; Kikuchi, K.; Urano, Y. and Nagano, T. *J. Am. Chem. Soc.* **2002**, *124*, 6555. (e) Burdette, S. C.; Frederickson, C. J.; Bu, W. and Lippard, S. J. *J. Am. Chem. Soc.* **2003**, *125*, 1778. (f) Woodrooffe, C. C. and Lippard, S. J. *J. Am. Chem. Soc.* **2003**, *125*, 11458.
10. (a) Akkaya, E. U.; Huston, M. E. and Czarnik, A.W. *J. Am. Chem. Soc.* **1990**, *112*, 3590. (b) Hennrich, G.; Sonnenschein, H. and Resch-Genger, U. *J. Am. Chem. Soc.* **1999**, *121*, 5073.
11. (a) Maruyama, S.; Kikuchi, K.; Hirano, T.; Urano, Y. and Nagano, T. *J. Am. Chem. Soc.* **2002**, *124*, 10650. (b) Henary, M. M. and Fahrni, C. J. *J. Phys. Chem. A*, **2002**, *106*, 5210. (c) Ohshima, A.; Mototake, A. and Arai, T. *Tetrahedron Lett.* **2004**, *45*, 9377. (d) Taki, M.; Wolford, J. L. and O'Halloran, T. V. *J. Am. Chem. Soc.* **2004**, *126*, 712.
12. Xu, Z.; Qian, X.; Cui, J. and Zhang, R. *Tetrahedron* **2006**, *62*, 10117.
13. Kiyose, K.; Kojima, H.; Urano, Y. and Nagano, T. *J. Am. Chem. Soc.* **2006**, *128*, 6548.
14. Frederickson, C. J.; Kasarskis, E. J.; Ringo, D. and Frederickson, R. E. *J.*

*Neurosci. Methods.* **1987**, *20*, 91.

15. (a) Fahrni, C. J. and O'Halloran, T.V. *J. Am. Chem. Sci.* **1999**, *121*, 11448 (b) Zalewski, P. D.; Forbes I. J. and Betts, W. H. *Biochem. J.*, **1993** 296, 403.
16. (a) Zalewski, P. D.; Forbes, I. J. and Betts, W. H. *Biochem. J.* **1993**, 296, 403. (b) Mahadevan, I. B.; Kimber, M. C.; Lincoln, S. F.; Tiekink, E. R. T.; Ward, A. D.; Forbes, I. J. and Zalewski, P. D. *AUST. J. Chem.* **1996**, *49*, 561. (c) Tsien, R. Y. *Nature* **1981**, *290*, 527.
17. (a) Arslan, P.; Di Virgilio, F.; Meltrame, M.; Tsien, R. Y. and Pozzan, T. J. *Biol. Chem.* **1985**, *260*, 2719. (b) Zalewski, P. D.; Forbes, I. J.; Seamark, R. F.; Borlinghaus, R.; Betts, W. H.; Lincoln, S. F. and Ward, A. D. *Chem. Biol.* **1994**, *1*, 153.
18. (a) Walkup, G. K.; Burdette, S. C.; Lippard, S. J.; Tsien, R. Y. *J. Am. Chem. Soc.* **2000**, *122*, 5644. (b) Burdette, S. C.; Walkup, G. K.; Spingler, B.; Tsien, R. Y.; Lippard, S. J. *J. Am. Chem. Soc.* **2001**, *123*, 7831. (c) Chang, C. J.; Nolan, E. M.; Jaworski, J.; Burdette, S. C.; Sheng, M.; Lippard, S. J. *Chem. Biol.* **2004**, *11*, 203–210. (d) Woodroffe, C. C.; Masalha, R.; Barnes, K. R.; Frederickson, C. J.; Lippard, S. J. *Chem. Biol.* **2004**, *11*, 1659. (e) Burdette, S. C.; Frederickson, C. J.; Bu, W.; Lippard, S. J. *J. Am. Chem. Soc.* **2003**, *125*, 1778. (f) Nolan, E. M.; Burdette, S. C.; Harvey, J. H.; Hilderbrand, S. A.; Lippard, S. J. *Inorg. Chem.* **2004**, *43*, 2624. (g) Chang, C. J.; Nolan, E. M.; Jaworski, J.; Okamoto, K. I.; Hayashi, Y.; Sheng, M.; Lippard, S. J. *Inorg. Chem.* **2004**, *43*, 6774. (h) Goldsmith, C. R.; Lippard, S. J. *Inorg. Chem.* **2006**, *45*, 555. (i) Nolan, E. M.;



- Jaworski, J.; Racine, M. E.; Sheng, M.; Lippard, S. J. *Inorg. Chem.* **2006**, *45*, 9748.
19. *Handbook of Fluorescent Probes and Research Products*, Haugland, R. P. (ed.) *Molecular Probes, Inc.*, Eugene, OR, **2002**.
20. (a) de Silva, A. P.; Gunaratne, H. Q. N.; Gunnlaugsson, T.; Uhuxley, A. J. M.; McCoy, C. P.; Rademacher J. T. and Rice, T. E. *Chem. Rev.* **1997**, *97*, 1515. (b) Scheller, F. W.; Schubert F. and Fedrowitz, J. *Frontiers in Biosensorics I. Fundamental Aspects*, Birkhauser Verlag, Berlin. **1997**. (c) Scheller, F. W.; Schubert F. and Fedrowitz, J. *Frontiers in Biosensorics II. Practical Applications*, Birkhauser Verlag, Berlin **1997**. (d) Wang, W.; Gao S. and Wang, B. *Curr. Org. Chem.* **2002**, *6*, 1285.
21. (a) Clarkson, T. W. *Environ. Health Perspect.* **1993**, *100*, 31. (b) Renzoni, A.; Zino, F. and Franchi, E. *Environ. Res.* **1998**, *77*, 68. (c) Malm, O. *Envir. Res.* **1998**, *77*, 73.
22. (a) Davidson, P. W.; Myers, G. J.; Cox, C.; Axtell, C.; Shamlaye, C.; Sloane-Reeves, J.; Cernichiari, E.; Needham, L.; Choi, A.; Wang, Y.; Berlin, M. and Clarkson, T. W. *J. Am. Med. Assoc.* **1998**, *280*, 701; (b) Tchounwou, P. B.; Ayensu, W. K.; Ninashvili, N. and Sutton, D. *Environ. Toxicol.* **2003**, *18*, 149; (c) Clarkson, T. W.; Magos, L. and Myers, G. J. *N. Engl. J. Med.* **2003**, *349*, 1731.
23. Mason, R. P.; Morel, F. M. M.; Hemond, H. F. *Water, Air, Soil Pollut.* **1995**, *80*, 775.
24. Celso, V.; Lean, D. R. S.; Scott, S. L. *Sci. Total Environ.* **2006**, *368*, 126.

25. Nendza, M.; Herbst, T.; Kussatz, C.; Gies, A. *Chemosphere* **1997**, *35*, 1875.
26. Renzoni, A.; Zino, F.; Franchi, E. *Environ. Res., Sect. A* **1998**, *77*, 68.
27. (a) Mason, R. P.; Reinfelder, J. R.; Morel, F. M. M. *Water, Air, Soil Pollut.* **1995**, *80*, 915. (b) Harris, H. H.; Pickering, I. J.; George, G. N. *Science* **2003**, *301*, 1203. (c) Kraepiel, A. M. L.; Keller, K.; Chin, H. B.; Malcolm, E. G.; Morel, F. M. M. *Environ. Sci. Technol.* **2003**, *37*, 5551. (d) Burger, J.; Gochfeld, M. *Environ. Res.* **2004**, *96*, 239. (e) Kuwabara, J. S.; Arai, Y.; Topping, B. R.; Pickering, I. J.; George, G. N. *Environ. Sci. Technol.* **2007**, *41*, 2745.
28. (a) Boening, D. W. *Chemosphere* **2000**, *40*, 1335. (b) Johnson, D. W.; Lindberg, S. E. *Water, Air, Soil Pollut.* **1995**, *80*, 1069.
29. (a) Forman, J.; Moline, J.; Cernichiari, E.; Sayegh, S.; Torres, J. C.; Landrigan, M. M.; Hudson, J.; Adel, H. N.; Landrigan, P. J. *Environ. Health Perspect.* **2000**, *108*, 575. (b) Silbergeld, E. K.; Silva, I. A.; Nyland, J. F. *Toxicol. Appl. Pharmacol.* **2005**, *207*, S282. (c) Newby, C. A.; Riley, D. M.; Leal-Almeraz, T. O. *Ethn. Health* **2006**, *11*, 287. (d) Drexler, H.; Schaller, K.-H. *Environ. Res., Sect. A* **1998**, *77*, 124. (e) Factor-Litvak, P.; Hasselgren, G.; Jacobs, D.; Begg, M.; Kline, J.; Geier, J.; Mervish, N.; Schoenholtz, S.; Graziano, J. *Environ. Health Perspect.* **2003**, *111*, 719. (f) Dye, B. A.; Schober, S. E.; Dillon, C. F.; Jones, R. L.; Fryar, C.; McDowell, M.; Sinks, T. H. *Occup. Environ. Med.* **2005**, *62*, 368. (g) Magos, L. *J. Appl. Toxicol.* **2001**, *21*, 1. (h) Pichichero, M. E.; Cernichiari, E.; Lopreiato, J.; Treanor, J. *Lancet* **2002**, *360*, 1737.
30. (a) Clarkson, T. W.; Magos, L.; Myers, G. J. *New Engl. J. Med.* **2003**, *349*, 1731.

- (b) Clarkson, T. W.; Magos, L. *Crit. Rev. Toxicol.* **2006**, *36*, 609. (c) Magos, L.; Clarkson, T. W. *Ann. Clin. Biochem.* **2006**, *43*, 257.
31. (a) McKeown-Eyssen, G. E.; Ruedy, J.; Neims, A. *Am. J. Epidemiol.* **1983**, *118*, 470. (b) Davidson, P. W.; Myers, G. J.; Cox, C.; Shamlaye, C. F.; Marsh, D. O.; Tanner, M. A.; Berlin, M.; Sloane-Reeves, J.; Cernichiari, E.; Choisy, O.; Choi, A.; Clarkson, T. W. *Neurotoxicol.* **1995**, *16*, 677. (c) Grandjean, P.; Weihe, P.; White, R. F.; Debes, F. *Environ. Res. Sec. A.* **1998**, *77*, 165. (d) Bolger, P. M.; Schwetz, B. A. *New Eng. J. Med.* **2002**, *347*, 1735. (e) Counter, S. A.; Buchanan, L. H. *Toxicol. Appl. Pharmacol.* **2004**, *198*, 209.
32. (a) Kaur, P.; Aschner, M.; Syversen, T. *Neurotoxicol.* **2006**, *27*, 492. (b) Milaeva, E. R. *J. Inorg. Biochem.* **2006**, *100*, 905. (c) Shanker, G.; Mutkus, L. A.; Walker, S. J.; Aschner, M. *Mol. Brain Res.* **2002**, *106*, 1. (d) Zalups, R. K.; Ahmad, S. *J. Am. Soc. Nephrol.* **2004**, *15*, 2023. (f) Zalups, R. K.; Lash, L. H. *Toxicol. Appl. Pharmacol.* **2006**, *214*, 88.
33. Recent reviews of sensors for detection of mercury ions, see: (a) Nolan, E. M. and Lippard, S. J. *J. Chem. Rev.* **2008**, *108*, 3443 and Selected examples of small molecule-based fluorescent sensors, see: (b) Hennrich, G.; Sonnenschein, H. and Resch-Genger, U. *J. Am. Chem. Soc.* **1999**, *121*, 5073. (c) Prodi, L.; Bargossi, C.; Montalti, M.; Zaccheroni, N.; Su, N.; Bradshaw, J. S.; Izatt, R. M. and Savage, P. B. *J. Am. Chem. Soc.* **2000**, *122*, 6769. (d) Guo, X.; Qian, X. and Jia, L. *J. Am. Chem. Soc.* **2004**, *126*, 2272. (e) Moon, S. Y.; Cha, N. R.; Kim, Y. H. and Chang, S. K. *J. Org. Chem.* **2004**, *69*, 181. (f) Caballero, A.; Martinez, R. Loveras, V.;

Ratera, I.; Vidal-Gancedo, J.; Wurst, K.; Tarraga, A.; Molina, P. and Veciana, J. *J. Am. Chem. Soc.* **2005**, *127*, 15666. (g) Moon, S.Y.; Youn, N. J.; Park, S. M. and Chang, S. K. *J. Org. Chem.* **2005**, *70*, 2394. (h) Nolan, E. M. and Lippard, S. J. *J. Mater. Chem.* **2005**, *15*, 2778. (i) Kim, S. H.; Kim, J. S.; Park, S. M. and Chang, S. K. *Org. Lett.* **2006**, *8*, 371. (j) Nolan, E. M.; Racine, M. E. and Lippard, S. J. *Inorg. Chem.* **2006**, *45*, 2742. (k) Wang, J.; Qian, X. and Cui, J. *J. Org. Chem.* **2006**, *71*, 4308. (l) Wang, J. and Qian, X. *Org. Lett.* **2006**, *8*, 3721. (m) Meng, X. M.; Liu, L.; Hu, H. Y.; Zhu, M. Z.; Wang, M.; Shi, X. J. and Guo, Q. X. *Tetrahedron Lett.* **2006**, *47*, 7961. (n) J. Wang and X. Qian, *Chem. Commun.*, 2006, 109. (o) Coskun, A. and Akkaya, E. U. *J. Am. Chem. Soc.* **2006**, *128*, 14474. (p) D. Wu, W. Huang, C. Duan, Z. Lin and Q. Meng, *Inorg. Chem.*, **2007**, *46*, 1538. (q) Ho, M. L.; Chen, K. Y.; Wu, L. C.; Shen, J. Y.; Lee, G. H.; Ko, M. J.; Wang, C. C.; Lee, J. F. and Chou, P.T. *Chem. Commun.* **2008**, 2438.

34. Fluorescence sensors based on Hg<sup>2+</sup> coordination with sulfur moieties, see: (a) Rurack, K.; Kollmannsberger, M.; Resch-Genger, U. and Daub, J. *J. Am. Chem. Soc.* **2000**, *122*, 968. (b) Sakamoto, H.; Ishikawa, J.; Nakao, S. and Wada, H. *Chem. Commun.* **2000**, 2395. (c) Descalzo, A. B.; Martı'nez-Ma'n'ez, R.; Radeglia, R.; Rurack, K. and Soto, J. *J. Am. Chem. Soc.* **2003**, *125*, 3418. (d) Nolan, E. M. and Lippard, S. J. *J. Am. Chem. Soc.* **2003**, *125*, 14270. (e) Mello, J. V. and Finney, N. S. *J. Am. Chem. Soc.* **2005**, *127*, 10124. (f) Tatay, S.; Gavina, P.; Coronado, E. and Palomares, E. *Org. Lett.* **2006**, *8*, 3857. (g) Nolan, E. M. and Lippard, S. J. *J. Am. Chem. Soc.* **2007**, *129*, 5910. (h) Yoon, S.; Miller, E. W.; He,

- Q.; Do, P. H. and Chang, C. J., *Angew. Chem., Int. Ed.* **2007**, *46*, 6658. (i) Wang, H. and Chan, W. H. *Tetrahedron.* **2007**, *63*, 8825.
35. Hg<sup>2+</sup> facilitated dosimeters, see: (a) Chae, M. Y. and Czarnik, A. W. *J. Am. Chem. Soc.* **1992**, *114*, 9704. (b) Hennrich, G.; Sonnenschein, H. and Resch-Genger, U. *J. Am. Chem. Soc.* **1999**, *121*, 5073. (c) Dickerson, T. J.; Reed, N. N.; Laclair J. J. and Janda, K. D. *J. Am. Chem. Soc.* **2004**, *126*, 16582. (d) Liu, B. and Tian, H. *Chem. Commun.* **2005**, 3156. (e) Ros-Lis, J. V.; Marcos, M. D.; Marti'nez-Ma'n'ez, R.; Rurack, K. and Soto, J. *Angew. Chem., Int. Ed.* **2005**, *44*, 4405. (f) Yang, Y.K.; Yook, K. J. and Tae, J. *J. Am. Chem. Soc.* **2005**, *127*, 16760. (g) Zhang, G.; Zhang, D.; Yin, S.; Yang, X.; Shuai Z. and Zhu, D. *Chem. Commun.* **2005**, 2161. (h) Song, K. C.; Kim, J. S.; Park, S. M.; Chung, K. C.; Ahn, S. and Chang, S. K. *Org. Lett.* **2006**, *8*, 3413. (i) Zheng, H.; Qian, Z. H.; Xu, L.; Yuan, F. F.; Lan L.D. and Xu, J. G. *Org. Lett.* **2006**, *8*, 859. (j) Zhu, X. J.; Fu, S. T.; Wong, W. K.; Guo, J. P. and Wong, W. Y. *Angew. Chem., Int. Ed.* **2006**, *45*, 3150. (k) Wu, Z.; Zhang, Y.; Ma, J. S. and Yang, G. *Inorg. Chem.* **2006**, *45*, 3140. (l) Zhao, Y.; Lin, Z.; He, C.; Wu, H. and Duan, C. *Inorg. Chem.* **2006**, *45*, 10013. (m) Wu, J. S.; Hwang, I. C.; Kim, K. S. and Kim, J. S. *Org. Lett.* **2007**, *9*, 907. (n) Lee, M. H.; Cho, B. K.; Yoon, J. and Kim, J. S. *Org. Lett.* **2007**, *9*, 4515. (o) Chen, X.; Nam, S. W.; Jou, M. J.; Kim, Y.; Kim, S. J.; Park, S. and Yoon, J. *Org. Lett.* **2008**, *10*, 5235. (p) Shi, W. and Ma, H. *Chem. Commun.* **2008**, 1856. (q) Zhan, X. Q.; Qian, Z. H.; Zheng, H.; Su, B. Y.; Lan, Z. and Xu, J. G. *Chem. Commun.* **2008**, 1859. (r) Zhang, X.; Xiao, Y. and Qian, X. *Angew. Chem., Int. Ed.* **2008**, *47*, 8025.

36. Materials-based Hg<sup>2+</sup> fluorescence sensors, see: (a) Murkovic, I. and Wolfbeis, O. *Sens. Actuators, B*, **1997**, *39*, 246. (b) Fan, L. J.; Zhang, Y. and Jones, W. E. *Macromolecules*, **2005**, *38*, 2844. (c) Kim, I. B. and Bunz, U. H. F. *J. Am. Chem. Soc.* **2006**, *128*, 2818. (d) Liu, X.; Tang, Y.; Wang, L.; Zhang, J.; Song, S.; Fan, C. And Wang, S. *Adv. Mater.* **2007**, *19*, 1471. (e) Zhao, Y. and Zhong, Z. *J. Am. Chem. Soc.* **2006**, *128*, 9988.
37. Biomecucles-based Hg<sup>2+</sup> fluorescence sensors, see: (a) Chen, P. and He, C. *J. Am. Chem. Soc.* **2004**, *126*, 728. (b) Ono, A. and Togashi, H. *Angew. Chem., Int. Ed.* **2004**, *43*, 4300. (c) Matsushita, M.; Meijler, M. M.; Wirsching, P.; Lerner R. A. and Janda, K. D. *Org. Lett.* **2005**, *7*, 4943. (d) Zhao, Y. and Zhong, Z. *J. Am. Chem. Soc.* **2006**, *128*, 9988. (e) Wegner, S. V.; Okesli, A.; Chen P. and He, C. *J. Am. Chem. Soc.* **2007**, *129*, 3474. (f) Lee, J. S.; Han, M. S. and Mirkin, C. A. *Angew. Chem., Int. Ed.* **2007**, *46*, 4093. (g) Darbha, G. K.; Ray A. and Ray, P. C. *ACS Nano*, **2007**, *1*, 208. (h) Wieckowska, D. Li, A. and Willner, I. *Angew. Chem., Int. Ed.* **2008**, *47*, 3927. (i) Liu, C. W.; Hsieh, Y. T.; Huang, C. C.; Lin, Z. H. and Chang, H. T. *Chem. Commun.* **2008**, 2242. (j) Xue, X.; Wang, F. and Liu, X. *J. Am. Chem. Soc.* **2008**, *130*, 3244. (k) Ono A. and Togashi, H. *Angew. Chem., Int. Ed.* **2004**, *43*, 4300. (l) Chiang, C. K.; Huang, C. C.; Liu C. W. and Chang, H. T. *Anal. Chem.* **2008**, *80*, 3716. (m) Wang, Z.; Lee, J. H. and Lu, Y. *Chem. Commun.* **2008**, 6005.
38. A review of rhodamine fluorescent sensors based on ring-opening strategies; see: Kim, H. N.; Lee, M. H.; Kim, H. J.; Kim, J. S. and Yoon, J. *Chem. Soc. Rev.* **2008**,

1465.

39. Mustafa, A.; Kamel, M.; Alama, M. A.; Harhash A. H. E. S. and Harssan A. E. A.  
*A. J. Am. Chem. Soc.* **1956**, 78, 5011.
40. (a) Hershfield, R. and Schmir, G. L. *J. Am. Chem. Soc.* **1975**, 95, 7459; (b) Wang,  
B.; Zhang, H. and Wang, W. *Bioorg. Med. Chem. Lett.* **1996**, 6, 945.
41. Mercury Update: Impact on Fish Advisories: EPA Fact Sheet EPA-823-F-01-011;  
EPA, Office of Water: Washington, DC, 2001: The maximum contamination  
concentration of mercury in drinking water is 2 ppb (10 nM).